On the morphology of RIVERS ON VOLCANO SLOPES

August 1990

C.J. Sloff

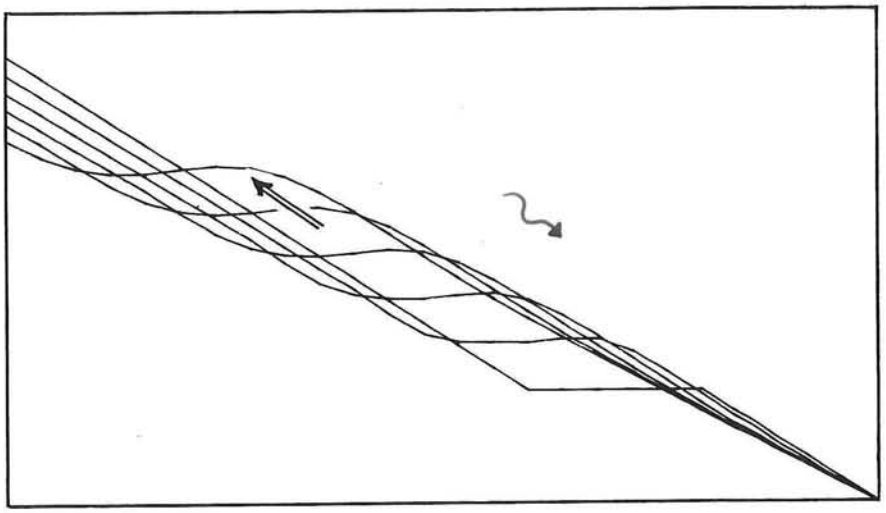

TU Delft
Delft University of Technology

Faculty of Civil Engineering
Hydraulic and Geotechnical Engineering Division
Hydraulic Engineering Group

On the morphology of

RIVERS ON VOLCANO SLOPES

by

C. J. Sloff

August 1990

Acknowledgements

Prof. Dr. M. de Vries is gratefully acknowledged for his encouraging guidance and his inspiring support in the river morphology.

I wish to thank Mr. E. Mosselman for his careful and painstacking review of the manuscript.

Further I would like to express my gratitude to Dr. Z. B. Wang, Prof. Dr. G. Stelling and Mr. G. J. Klaassen for their valuable comments.

Finally I wish to thank the staff members of the civil engineering department of the ITS-University (Surabaya, Indonesia) for their cooperation and support during my stay in Indonesia.

Abstract

The rivers on the slopes of the Kelud volcano in Indonesia are marked by steep slopes and fine sediment. Therefore often supercritical flow and large sediment transports occur.

In this exploratory study a mathematical model has been developed for this type of rivers. The properties of this model are examined with an analysis of the characteristics and with numerical computations. The results show rapid bed variations propagating upstream, which agrees with observations in the rivers on the Kelud volcano.

Contents

Chapter 1

Introduction

A main concern in mountainous and volcanic areas is the increased erosion and sedimentation in the mountain rivers. The type of rivers on volcanic slopes in Indonesia is marked by steep slopes and fine loose sediment. This often implies supercritical flow and large sediment transport. The destructive force of this flow and the excessive deposition of the sediment in the downstream reaches are the cause of catastrophes, like inundation. Prevention from these catastrophes by mechanical means is referred to as "sabo engineering" or "sediment and erosion control".

The main objective in this exploratory study is the development of a mathematical model for these volcanic rivers. This objective originated from the demand for simulation of the time-depended morphological processes due to sabo works.

General basic equations are derived for unsteady flow with high sediment concentrations which can be applied to volcanic rivers with bed slopes less than approximately 10%. The general equations are simplified and investigated with four different approaches.

- A model for steady non-uniform flow on a fixed bed has been developed. The numerical computations of this type of flow and of hydraulic jumps illustrate the variations in water depth and flow velocity near sabo works.
- Basic equations for unsteady flow without the influence of high concentrations is treated for comparison, to investigate the influence of the concentration on the river flow (e.g. by considering the characteristic celerities).
- The highly concentrated unsteady flow is first approached and analysed with the concentration expressed

in terms of transport formulas without adaptation time and length of the suspended sediment.

- A second approach for the sediment-laden unsteady flow is considered with the concentration expressed in terms of the suspended load. The adaptation length and time scale of the suspended transport process are included and again the characteristic celerities are examined.

For the analysis of the system of unsteady sediment-laden flow equations (second approach) numerical computations (computer program SABOFLOW) are considered. Finally the conclusions that have been drawn from this study, are discussed.

Chapter 2

Sediment and erosion control, or sabo-engineering.

2.1 Introduction

Since time immemorial humanity is plagued by natural disasters. The occurrence and the scale of these disasters can usually not be determined. Therefore it is very difficult to prevent damage to man and his properties.

Dealing with the sediment disasters is within the scope of river engineering. These disasters occur in mountainous and volcanic areas. Landslides, avalanches, volcanic eruptions and increased erosion can load the mountain rivers with a concentrated superabundance of sediment, adding up to a destructive flow.

Transported downstream, this material accumulates in the bed of the lower reaches of the river, where the bottom slope decreases, and it can cause inundation of the surrounding land. Many cases are known where houses and fields are buried in the sediment layer covering this land after the flood, and where many people died because of the unexpected occurrence of the disaster.

All mechanical efforts that have been taken to prevent these catastrophes are called "*sabo engineering*" or "*sediment and erosion control engineering*". This field of study is very extensive and still a lot of research has to be done.

In this chapter the discussions of sabo engineering will be restricted to a description of this subject and to considerations of mountain rivers and river works to prevent

propagation of excessive sediment in the river (*torrent control*). In section 2.5 the occurrence of head losses in river bends is considered as a tool for sabo engineering. Conclusions are given for the computability of the energy dissipation and the changes in flow and morphology.

2.2 Description of sediment and erosion control or sabo engineering.

In order to summarize all the topics that deal with the prevention of sediment disasters, the terms *sabo engineering* or *erosion and sediment control* are used. In fact, the japanese technical term "*sabo*" has in original sense been used for land conservation (particularly forest land conservation in mountainous regions). This also includes the necessarily non-physical countermeasures such as administrative regulation of forestry management and land use plan.

The simple well-sounded word *sabo* nowadays has become an international technical term in its original Japanese meaning. However, the term "erosion and sediment control engineering" is also used in this meaning, but it denotes to a greater extent the mechanical aspect of the sediment disaster prevention instead of a vegetative way of land conservation.

Limiting the considerations to the technical land conservative measures, sabo engineering incorporates measures against accelerated devastation of land, slope failure or landslides, unstable river channels, excessive sedimentation in reservoirs and in river beds, and so on. The constructions that are built for these purposes, like dams, are therefore called "*sabo works*".

One of the important issues of sabo engineering is the

research on the behaviour of the water and sediment mixture in, and the properties of, mountain rivers. This will be discussed in the following section.

2.3 Properties of mountain river flow

2.3.1 Subdivision of a mountain river

Sabo engineering includes the measures to prevent excessive sediment from entering the rivers. Nature, however, cannot completely be conquered (e.g. volcanic eruptions) and sediment can still flow into the rivers. Therefore it is necessary to stem and to control the abundance of material in the river course before it can cause any damage to life and property. Such countermeasures require knowledge about the properties of the rivers involved.

In general a mountain river can be divided into three parts (Parcy, 1982) (see fig. 2.1)

1- The upper part of the watershed or catchment area is the greatest source of the sediment load and the collecting area for the water supply. Small torrents with steep slopes flow together in this area where landslides, avalanches and debris flow can develop. Erosion can increase dramatically in case of deforestation.

2- The middle course is often a narrow non-alluvial gorge with armoured bed and eroding banks. The torrents from the catchment area have flown together into a concentrated water and sediment flow. In volcanic areas, however, this part of the river often will flow in deposits from former eruptions (loose graded material) so that the concentrated flow causes deepening of the bed. Bottomslopes in the middle reach are less than those in the upper part of the catchment area, yet still substantially steep.

3- The alluvial fan (fan-shaped) or alluvial (or debris) cone (cone-shaped) is the lower reach of the river where the bottom slope is relatively small. Decrease of the flow velocity causes sedimentation. The river can fan out and continuously change its course after erosion of the river banks or if its bed has been silted up. Accreted material forms the alluvial cone or fan.
Downstream, the river flows into the main receiving river, in a lake or in the sea.

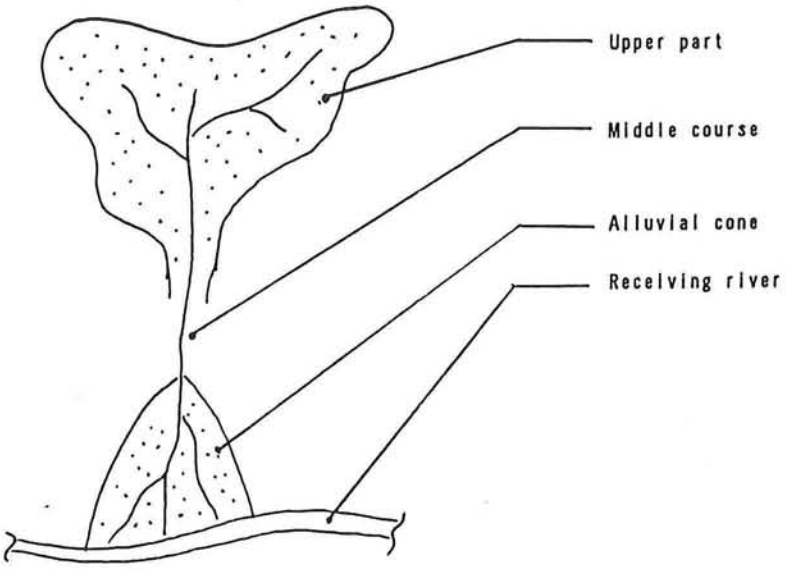

fig. 2. 1 Mountain River

Each of these three river reaches has its own properties besides the properties of the overall mountain river. The following discussion is divided into four sub-sections to discuss the whole river and its three reaches separately.

2. 3. 2 Overall mountain river

In the overall mountain river the discharge shows large fluctuations. Peak floods in general have a large kinetic energy and a considerable drag and lift force on the river bed and bank material. In this high velocity flow, both bed load transport and suspended load transport can occur together. The high sediment transport rates imply that the influence of the concentration of the transported material cannot be neglected in the morphological computations.

Common formulas to predict the sediment transport cannot be applied or have to be adapted to mountain river conditions. Much research is being carried out to find a general applicable transport formula to predict the transport. Usually these formulas are a function of the local hydraulic conditions and do not include the adaptation proces of the sediment transport in the case of suspended load.

The sediments can also be transported as a sediment gravity flow (Debris flow or mud flow, see section 2.3.3) depending on the morphology (the bed slope), the quantity of sediment (concentration), and the quality of the sediment (grain size distribution).

Another problem is that the attack of the supercritical flow on the constructions in the river (such as sabo works) is seriously large. Damage to dams and bank protection is a very common fact.

Armouring of the upper layer of the river bed often occurs but this armoured layer can be destroyed during floods, and be rebuilt during lower discharges.

The waterflow in the upstream reaches is supercritical as a result of the steep slopes. This means that the disturbances in the water flow (e.g. from structures in the stream) can only propagate in downstream direction. However, in the lower reaches, or near structures (backwater effect), the

waterflow can jump to subcritical depth. Then the kinetic energy of the flow decreases considerably.

A decrease of mean grain size and a decrease of gradation of grainsizes over the river length is partly caused by the gradually decrease of the bottom slope, and thus a gradually decrease of flow velocity, in the river. The decrease of mean grain size over the river length can also be caused by abrasion of the grains during transport. Investigations of Parker (1989) showed that this abrasion is essentially negligible for quartz. However, it can be important in the case of other kinds of sediment (e.g. volanic material).

More details on the different reaches are discussed in the following subsections. Nevertheless, these reaches make up one river basin and are therefore dependant on each other.

2.3.3 Flow in the catchment area

Sediment and water are mainly supplied in the catchment area or watershed. This area with its steep slopes is liable to severe erosion. Avalanches, landslides and volcanic ash can cause *debris flow*. Debris flow is a highly destructive viscous flowing flood made up of debris (stones, sand, trees and so on) or volcanic material, mixed with water. Debris flow can occur if slopes are larger than 15% to 20%.

Debris flow can come to a halt if slopes decrease and the water concentration has not been increased before that time. The debris can block the river (form a *debris-jam*) and cause the river to change its direction. A breaking debris-jam can result in a new destructive shock-floodwave of water and debris.

The *torrential* flow in this part of the mountain river

is substantially influenced by the roughness of the river bed, because of the fact that the dimensions of the bed material are of the same order of size as the waterdepth. This implies a large turbulence of the flow.

Sabo works in this area are for example (see section 2.4) small *checkdams* (constructions to induce sedimentation of excessive sediment in order to prevent it from rushing down), *slope drainage* (to stop or prevent landslides), *debris flow breakers* (construction to break the debris flow to destroy its devastating force) and so on.

The small torrents in the watershed run together and make up one larger river with concentrated flow. Then at this point the river has reached the toe of the watershed and it continues as the *middle course*.

2.3.4 Flow in the middle reach

The middle reach is subjected to a highly concentrated and thus erosive flow. It is consequently almost not alluvial. Large rocks in the riverbed form a strong armoured layer (small particles have been washed out). That also implies a substantial influence of the roughness of the bed on the flow. Nevertheless, in case of a river in volcanic deposits, the erosion of the riverbed can often continue because of the thick layer of relatively fine material on the riverbed. The morphology in such a river is therefore different.

Sabo works (see section 2.4) in this middle reach are *consolidation dams*, *checkdams* and *sand-pockets* (constructions to induce deposition of excessive sediment in the riverflow and to stabilize the riverbed), *debris flow breakers* (constructions to break the debris flow to prevent it from rushing down), *groundsills* (constructions to fix the riverbed at a

certain point to prevent deepening) and *riverbank protection* (undercutting of sloping banks can cause the bank to collapse into the river).

2.3.5 Flow in the lower reach

In the lower reaches the slope can decrease to such an extent that *subcritical* flow can occur. Accretion of the excessive sediment in this alluvial cone or fan causes an increase of the bedlevels. Deposits are spread over the area as a result of the bed displacement caused by streambank cutting and the silting up of the riverbed.

Sediment in the alluvial cone or fan is usually rather uniform and of a small grainsize, this in contrary to the upstream reaches.

Sabo works in the alluvial cone (or fan) are *riverbank protection* (to stabilize the riverchannel), *checkdams, consolidation dams, groundsills* (threshold shaped submerged stabilization dams), and so on.

In the following section, various sabo works and their properties are discussed. This discussion is restricted to constructions in the river course. Structures to stabilize mountain-slopes or to prevent the erosion of these slopes are not relevant in this scope.

2.4 An outline of sabo works

2.4.1 Subdivision of sabo works

In order to prevent damage to common goods in a river basin it is necessary to fix the rivercourse and to bring a halt to substantial erosion and sedimentation in the river. This must be accomplished by the *sabo works*.

Construction and location of the sabo works are based on the characteristics of the mountain river flow as discussed in the preceding section. To achieve a clear discussion of the sabo works, a subdivision is made, based on the appearance of the different structures.

Before making this subdivision the functions of the sabo dams have to be given to support the description of various sabo works. These functions in torrent control can be classified as follows (Armanini 1989):

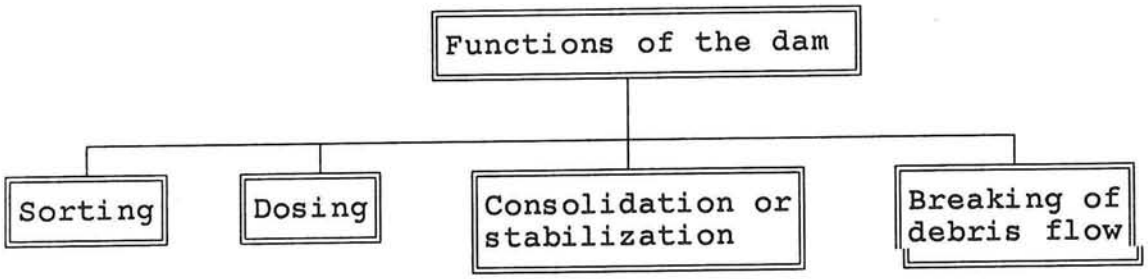

In which *sorting* denotes that sediment is only retained during high floods, while *dosing* implies retention of only bigger-size particles. In sabo engineering the term *consolidation* is used to denote the stabilization of the rivercourse by elevating and fixing the riverbed.

According to their appearance the sabo works are distinguished into the following three groups :

1- *Closed structures* that are developed to check the runoff of all the excessive sediment directly.

2- *Open structures* to check the runoff of a part of the excessive sediment directly.

3- *Structures to fix the rivercourse*, to prevent substantial sedimentation and to prevent riverbank collapse (consolidation or stabilization structures).

In the following subsections, these three groups of sabo works are discussed by means of some frequently used structures (Armanini 1989, United Nations FAO 1981). As stated before, this consideration is not comprehensive but is restricted to the rivercourse.

2.4.2 Direct check of all excessive sediment

This category includes all the *closed checkdams* (or correction dams, see fig. 2.2). These empty-type checkdams are mainly located (usually stepwise in series) in the upper reaches (watershed and middle course) to catch the surplus of sediment in case of sediment overload. This overload is always induced by a floodwave.

The effect of these structures is based on the creation of a small detention reservoir upstream of the dam. Supercritical flow turns into subcritical flow through which the flow velocity decreases considerably causing accumulation of the transported sediment. The transition of super- to subcritical flow takes place via a hydraulic jump. This is a wave-shaped static turbulent irregularity (see section 3.3.5).

The effect of the dam is only guaranteed temporarily.

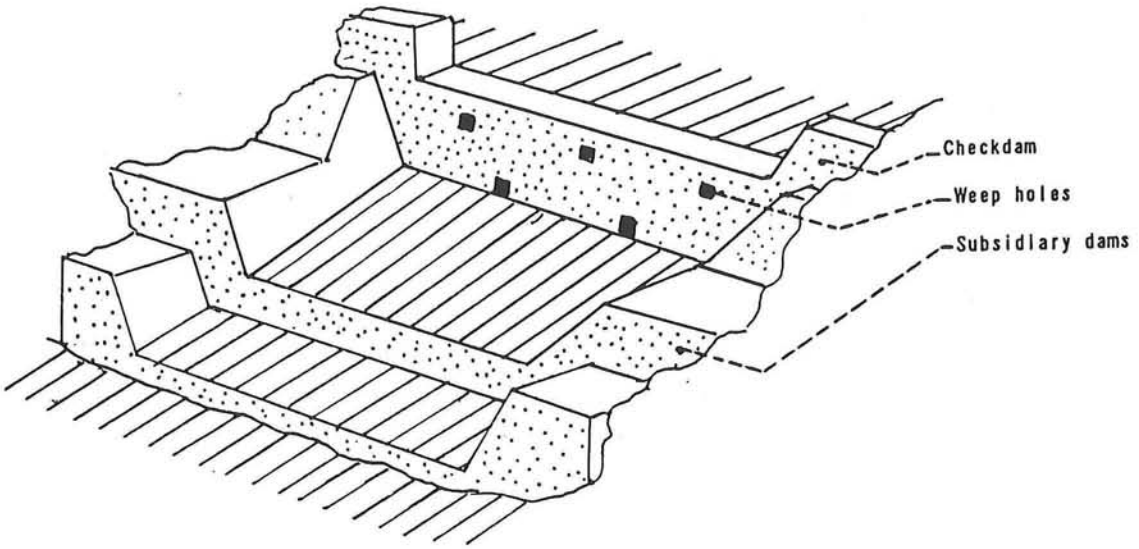

fig. 2.2 Closed checkdam with sub dams

Excavating of accreted material is necessary after a flood has filled up the upstream artificial "reservoir". Therefore the deposited sediment is drained (by means of small holes in the dam, called weep-holes, see fig. 2.2), at least to some extent, thus permitting quick access to excavators.
This excavation, however, is often not put into practice. This implies that the checkdam functions as a kind of "consolidation dam" (discussed in subsection 2.4.4).

Design of the foundation depth of checkdams depends on the downstream erosion. Local scour and overall degradation of the river downstream of the dam, as a result of the turbulence of the overfalling water and the decreased sediment supply (since sediment is trapped upstream of the dam), denotes a considerable deepening of the riverbed. To protect the downstream toe of the dam often an auxiliary dam or sub(-sidiary) dam is constructed as shown in fig. (2.2). The energy from the drop is dissipated in the stilling basin enclosed by the main dam and the sub dam. The foundation of the dam has to be

designed below the scour level to accomplish stability of the structure.

Severe attack of the crest and of the wings of the dam requires a protective layer of strong material. Formerly natural materials (available on the construction site) were used to built the structure because of the difficulties to transport other materials to the site. Nowadays, modern equipment is being developed sufficiently to overcome these problems. Presently all checkdams are constructed with reinforced concrete.

The size of the different checkdams varies considerably. Heights of these dams range from 2 to 10 meters.

On the slopes of active volcanoes in Indonesia, many *sand pockets* have been constructed (in the lower and middle reaches) to detain sediment from *lahar flow* (hot volcanic mud flow). A large artificial reservoir for accumulation is created by enclosing a wide part of the flood plain with dikes (see fig. 2. 3).

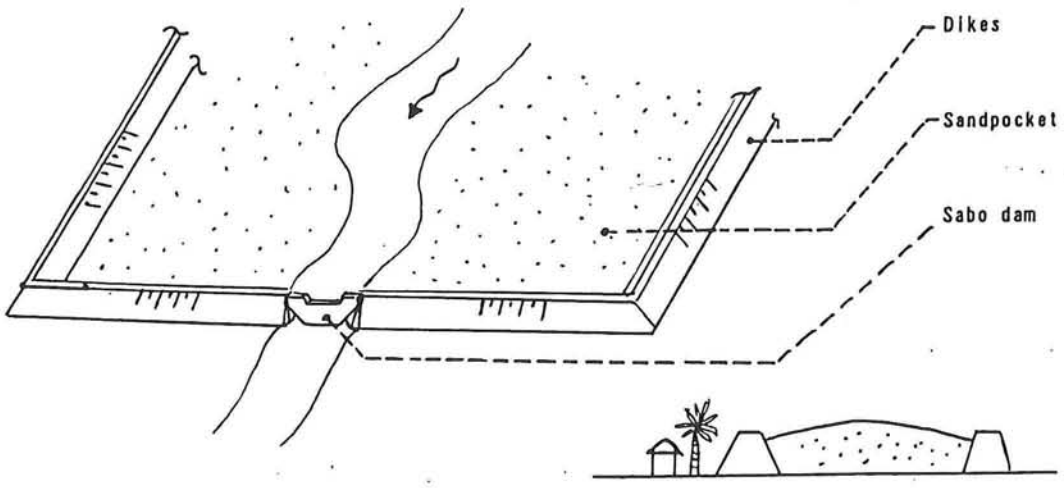

fig. 2. 3 Sand pocket

2.4.3 Direct check of a part of the sediment

A recent trend is the construction of dams that are not completely closed. The main type of up-to-date dam can be classified into four groups. In the following the seperate groups are discussed.

Empty dam with big drain hole or narrow slit:

This type of dam is used for dosing, i.e accumulation of sediment during high floods by means of backwater effect (hydraulic jump and subcritical flow) and gradually washing out of the (fine) sediment later (through the slit) with minor floods. The required capacity, to retain large bedload at high floods, is then longer maintained.

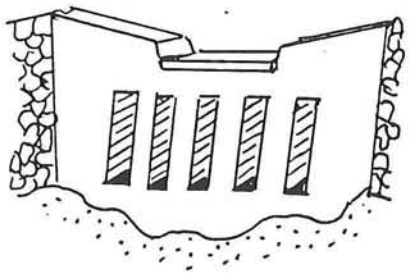

fig. 2.4 Checkdam with large conduits

Open dam (wire dam, iron-basket dam, grating dam, debris breaker etc.)

To break debris flow (section 2.3.3) and to retain bigger debris that can cause damage downstream. These structures are usually built in the upper reaches upstream of other types of dams. They must be designed strong, capable to resist the impact of the debris flow (usually protected with thick iron plates).

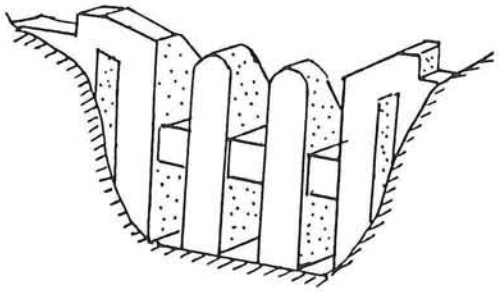

fig. 2. 5 Debris Breaker

Open-crown-dam for dosing (slit dam, slit dam with grating)

Equally to the empty dam with narrow slit, the slit dam is capable of selective outflow of sediment. Slit dams in series are used to retard and trap large boulders. Minor floods flow undisturbed (eroding) through the dam carrying the amount of sediment that can be managed by the downstream torrent.

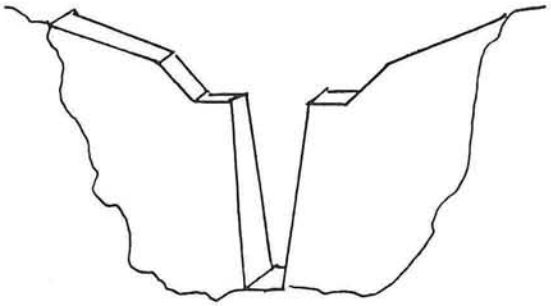

fig. 2. 6 Slit dam

Closed-crown dam for sorting (beam dam, screen dam)

The purpose of the beam dam with wide horizontal openings is mostly filtering or selecting both bed load and logs. They are usually used in torrents with debris flow. Sometimes the beam dams tend to be clogged by logs and other vegetal

parts, which have to be removed.

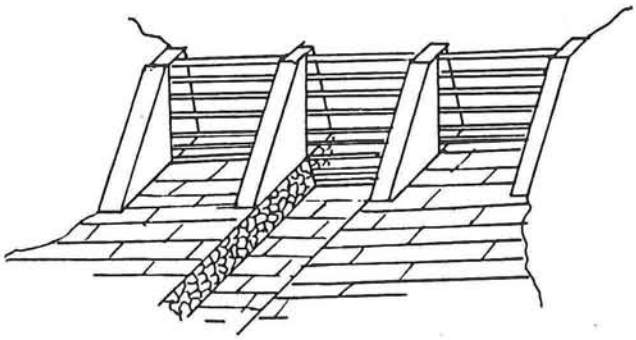

fig. 2.7 Beam Dam

For all types of dams above the openings of the dam can be protected from obstruction (by logs and other plant material) by a declining steel screen placed upstream of the dam. This only works during subcritical flow (backwater): The plant material floats and is pushed to the top, letting the lowest part of the screen free and water flowing through.

Equally to closed checkdams the local scour can be decreased by means of subdams (subsidiary dams).

2.4.4 Works to fix the river course

Consolidation which denotes the mere fixation of the torrent profile allows a better stability on the previously eroded side slopes by elevating the riverbed. Consolidation checkdams still continue to be the most important structures and represent by far the most common tool for torrent control

Consolidation dams are wall-type checkdams. The deposition space is usually filled in a very short time causing a modification of the slope of the profile up to the point when

the landing line is parallel to the original bed. The diminished slope and widened profile cause additional detention of material and prevention of torrent erosion (both bed and riverbanks).

Groundsills (submerged sills in the riverbed) are used to fix the riverbed for a certain point, to prevent further erosion of the bed.

For channels in the lower reaches the cross section can be fixed using revetments. Protecting the banks prevents the channel to change its course. Decreasing the width, by means of training walls or groynes etc., prevents sedimentation.

2.5 Head losses in bends

A bend in a channel flow causes a local variation in the velocity distribution, together with a depth alteration and a development of secondary flow. The separation of the stream lines at the inner wall of the bend and the generation of secondary flow cause increased head losses. The determination of these losses have been subject of investigation for many authors (Müller 1943, Shukry 1950, Naudascher 1987, Henderson 1959, Chow 1959). In this section a description of, and the conclusions on head losses in mountain river bends are given. Also the associated bed level variations are considered. The flow is assumed to be supercritical ($Fr>1$).

The head losses in a open channel bend have been mainly analyzed empirically. The total energy loss due to curve resistance can be expressed in terms of the velocity head:

$$H_f = \xi_b \frac{u^2}{2g}$$

where u is the mean velocity in the section and ξ_b is the coefficient of curve resistance.

A large number of independent variables influences the magnitude of ξ_b:

Fr (Froude Number); a/B (depth/width); r_c/B (radius of curve/width); Re (Reynolds Number); θ(total angle of deflection).

Comparing the coefficients of curve resistance of various investigators (Henderson, 1959) indicated a substantial difference in their values, dependent on the approach conditions. Therefore the use of one of these empirical coefficients can give head losses which may be three or four times too large. In practice the ξ_b is determined from data of the river.

According to Müller (1943) the energy line and flow profile in a uniform curved channel, and the bed variations caused by these profiles, can be shown as in fig (2.8).

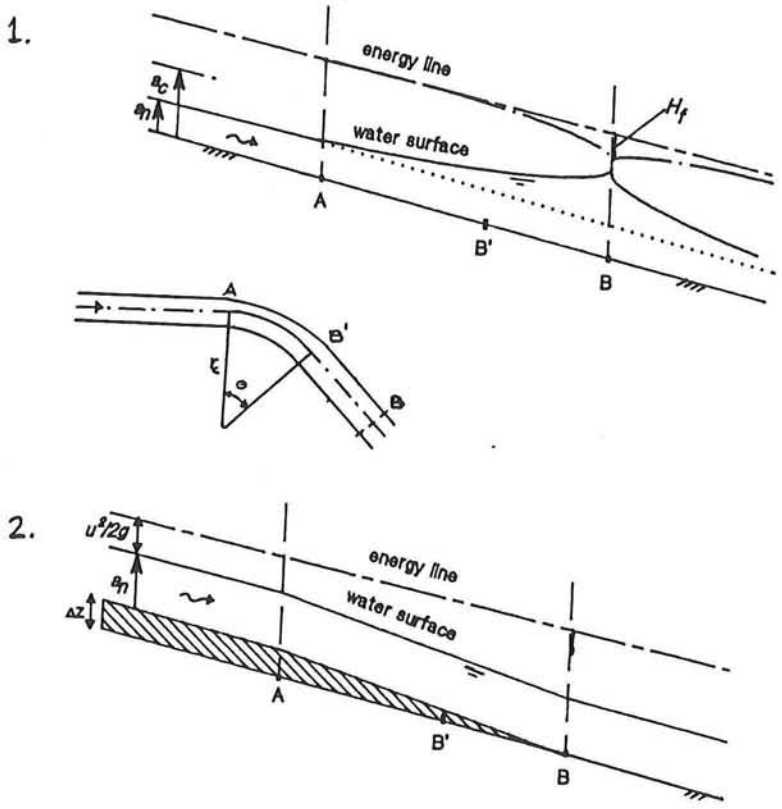

fig 2.8 Head Losses in Bends

Case 1 illustrates supercritical flow in the curved channel. It can be seen that the energy line is dropped by H_l at *B*, corresponding to the amount of energy dissipated in the curve and the downstream channel *B′ B*. The water surface is raised from *A* to *B* (a hydraulic jump will be produced if the water

surface rises above the critical-depth line).

Case 2 illustrates the equilibrium situation which is formed as a result of the flow in "case 1" and also applies to subcritical flow in bends. Sedimentation of the upstream reach occurs.

The energy losses in bends in supercritical flow are partially caused by the generation of *cross waves* by the turning effect of the curved channel walls. It has been investigated whether the coefficient of curve resistance can be derived from the head losses due to these cross waves.

The phenomena are described by Ven te Chow (1959), Täubert (1971), and others. The outer wall which turns inward to the flow, will produce an oblique hydraulic jump and a corresponding positive disturbance line or positive wave front. The inner wall, which turns away from the flow will develop an oblique expansion wave and a negative disturbance line or negative wave front. Both types of waves will be reflected back and forth between the walls and will interfere with each other, resulting in a disturbance pattern of cross waves (alternating maximum and minimum depths on both outer and inner wall, hence a fluctuating depth along the walls will occur).

Determination of the *cross wave pattern* and the energy losses (Täubert, 1971) is too complicated and cannot easily be included in a morphological model for mountain rivers. The irregularity of a natural river (no smoothly curved walls), and the smallness of the head losses due to cross waves, decreases the reliability of the results from computations.

Because of the lack of agreement for the various values of the coefficient of curve resistance in the literature, and because of the unreliability and the extent of cross wave computations, the applicability of head loss computations in a morphological model presents difficulties. For this reason the

head losses are included in the friction losses determined by the Chezy roughness coefficient.

Chapter 3

One dimensional modelling of mountain river flow

3.1 Introduction

The human interference (sabo engineering) in mountain rivers can alter sedimentation and erosion. For the prediction of these morphological processes mathematical models are developed.

The unsteady flows in mountain rivers are categorized as unsteady shallow-water flow. They can be treated as one dimensional (1-D) as far as the horizontal variations of the transverse profile are negligibly small (fixed banks).

In this chapter a one-dimensional mathematical model is discussed for the simulation of mountain river flow and morphology. For reasons of stability and simplicity of the computations, the validity of the model is restricted by the following assumptions (see section 3.2):

- Bed slopes are assumed to be smaller than approximately 10%.
- The mountain river is assumed to flow in deposits from volcanic or alluvial origin of relative fine material. The dimensions of the sediment are very small compared to the depth of flow.

These assumptions imply that the model can be applied for rivers in the middle and lower reaches.

In section 3.2, a general approach for the derivation of a set of basic flow equations is outlined, which should be helpful in understanding the subsequent mathematical and phy-

sical analyses of the equations.

In the following sections four final forms of the equations are summarized for varied approximations and applications.

The non-uniform flow is treated in section 3.3, assuming steady flow on a fixed bed (without sediment transport). Surface profiles and hydraulic jumps are considered to gain insight into properties of mountain river flow. Hydraulic jumps are the discontinuities in the steady non-uniform flow.

Next the equations for unsteady flow with mobile bed are discussed in three distinctive forms:

- With low sediment concentration (section 3.4), which can be used to investigate the influence of sediment on the properties of sediment-laden flow.
- First approach: with large sediment concentrations (section 3.5), determined by the sediment transport capacity from sediment transport formulas (Adaptation of suspended sediment distribution over the vertical is not included).
- Second approach: with large sediment concentrations (section 3.6), determined by the amount of suspended material. This requires an additional basic equation for the adaptation of the sediment concentration to the local hydraulic conditions.

For each type of flow physical and mathematical properties are analyzed using the characteristic celerities of disturbances in the system.

3.2 General basic equations

In this section, the basic equations of unsteady flow are derived for shallow water conditions. The shallow-water theory is applied when the pressure distribution in the ver-

tical can be assumed hydrostatic. The physical process of the morphological problem is schematised in a one-dimensional model. The flow velocity u, waterdepth a, sediment transport s and the bedlevel z are averaged over the cross section. The set of assumptions needed to arrive at the final form of the equations is as follows (Chintu Lai 1986, Mahmood & Yevjevich 1975):

(a) The shallow water theory applies (vertical acceleration of a fluid particle is very small compared with the acceleration of gravity g and hence can be neglected).

(b) Only shear stresses due to horizontal velocity components are significant.

(c) The frictional resistance coefficient for unsteady flow is the same as that for steady flow, and hence it can be approximated from the Chézy equation.

(d) The bed material is supposed to be uniform along the river section.

(e) The river banks are fixed. Thus the erodibility of the banks is assumed to be much smaller than that of the bed.

(f) The Chézy roughness coefficient is assumed constant throughout the reach under consideration.

(g) The channel is prismatic and wide (hydraulic radius R = waterdepth a).

(h) Bed slopes are assumed to be smaller than approximately 10%, to prevent the *Froude number* exceeding a certain value for which stability of the (supercritical) flow cannot be maintained. According to Mayer (1957) instability can be classified into *rollwaves* (transverse ridges of high velocity with quiescent regions between the crests) and *slug flows* (surges of turbulent ridges with wave crests separated by highly agitated regions). It is hard to take this instability into account.

(i) The dimensions of the bed material are small compared to the water depth, to prevent the bottom resistance from causing instability as described in assumption (h).

The general procedure for the derivation of a set of basic equations is to begin from the equations of continuity and motion for water and sediment (Jansen, 1979). The equation of motion is derived from Newton's second law of conservation of momentum, and the continuity equations are derived from conservation of mass, all for a certain control volume. The derivation is outlined in appendix (1).

The basic equations for sediment-laden flow on a steep mobile bed as derived, then become:

Equation of motion

$$\frac{\partial u}{\partial t} + u\frac{\partial u}{\partial x} + g\cos(\zeta)\left(\frac{\partial z_w}{\partial x} - i_b\right) + \frac{1}{2}g\cos(\zeta)\frac{a}{\rho_m}\frac{\partial \rho_m}{\partial x} + \frac{gu^2}{C^2 a}\cos(\zeta) = 0 \qquad (3.1)$$

Continuity equation for mass

$$\frac{\partial a}{\partial t} + a\frac{\partial u}{\partial x} + u\frac{\partial a}{\partial x} + \frac{a}{\rho_m}\frac{\partial \rho_m}{\partial t} + \frac{ua}{\rho_m}\frac{\partial \rho_m}{\partial x} = 0 \qquad (3.2)$$

Continuity equation for sediment volume

$$\alpha\frac{\partial z_b}{\partial t} + \frac{\partial \phi a}{\partial t} + \frac{\partial \phi a u}{\partial x} = 0 \qquad (3.3)$$

Relation concentration and density

$$\rho_m = (1-\phi)\rho + \phi\rho_s$$

$$\rho_m = \rho\left(1 + \frac{\alpha \Delta s}{au}\right) \qquad (3.4)$$

In which: a = waterdepth

i_b = $\tan\zeta$ = bed slope

s = sediment transport = $f(u)$

u = flow velocity
z_b = bed level
z_w = water level (= z_b+a)
ϕ = averaged concentration of sediment
ζ = angle of river bed
ρ_m = density of the water/sediment mixture
ρ = density of water (≈ 1000 kg/m^3)
ρ_s = density of sediment particles
Δ = relative density = $(\rho_s - \rho)/\rho_s$

These equations can be adapted and simplified for various applications. In the following sections a few forms of basic equations are discussed that are used in the investigations. For all these models the assumption (h) (small bed-slopes) yields that the cosinus and sinus terms in the basic equations can be approximated by:

$$\sin(\zeta) \approx 0 \quad \text{and} \quad \cos(\zeta) \approx 1$$

3.3 Steady non-uniform flow on a fixed bed

3.3.1 Simplified basic equations

When the depth of flow in an open channel flow varies spatially with the longitudinal distance, the flow is termed non-uniform. Such situations occur both upstream and downstream of control sections, such as dams.

In general all solutions which have been developed for steady non-uniform depend on the following assumptions:

1- The discharge is assumed to be constant in time, which implies *steady flow.* The terms with $\partial/\partial t$ in the basic equations (3.1) to (3.2) are equal to zero.

2- Sediment transport is considered relatively small ($s/q \ll 1$) so that the influence of the sediment concentra-

tion on the water flow can be neglected. Concentration ϕ, all derivatives of ρ_m and $\partial z/\partial t$ are equal to zero.

3- The slope of the channel is small, which denotes that $\cos(\zeta) \approx 0$ and $\sin(\zeta) \approx i_b$.

Starting from the assumptions the basic equations become:

Momentum equation

$$u\frac{\partial u}{\partial x} + g\frac{\partial a}{\partial x} - gi_b + \frac{gu^2}{C^2 a} = 0 \qquad (3.3.1)$$

Continuity equation

$$a\frac{\partial u}{\partial x} + u\frac{\partial a}{\partial x} - \frac{\partial q}{\partial x} = 0 \qquad (3.3.2)$$

In which q = discharge per unit of width (constant in x direction).

Combining these two equations yields the *dynamic gradually varied flow equation.*

$$\frac{\partial a}{\partial x} = \frac{i_b - \frac{q^2}{C^2 a^3}}{1 - \frac{q^2}{ga^3}} = f(a) \qquad (3.3.3)$$

The solution of this equation can be found by means of both analytical and numerical integration. In section (3.3.3) and (3.3.4) some integration methods are considered.

3.3.2 Classification of flow profiles

It is necessary to distinguish different types of flow for ease of survey and for comprehensibility of the results from gradually varied flow computations. The conditions of the flow determine this classification.

In a given channel, the normal depth line a_n and the critical depth line a_c are fixed, and divide the channel into three sections (Ven Te Chow 1959, Carlier 1972):

- *Region 1*: The space above the upper line.
- *Region 2*: The space between the two lines.
- *Region 3*: The space below the lower line.

Thus the flow profiles may be classified into thirteen different types according to the nature of the channel slope and the zone in which the flow surface lies.

These types are designated as *H2, H3; M1, M2, M3; C1, C2, C3; S1, S2, S3; and A2, A3;* where the letter is descriptive of the slope: *H* for horizontal, *M* for mild (subcritical), *C* for critical, *S* for steep (supercritical), and *A* for adverse slope and where the numeral represents the region number.

The full representation of this classification is given in appendix (2).

3.3.3 Method of direct integration: the Bresse function

Eq. (3.3.3) may be written as:

$$\frac{\partial a}{\partial x} = i_b \frac{a^3 - a_c^3}{a^3 - a_n^3} = i_b \left(\frac{1 - \frac{q^2}{C^2 a^3 i_b}}{1 - \frac{q^2}{g a^3}} \right) \qquad (3.3.4)$$

This equation is valid in the special case of a rectangular channel with the conveyance expressed in terms of the Chézy equation, C = constant.

Integration of the eq. (3.3.4) leads to the result :

$$x_2 - x_1 = \frac{a_n}{i_b} [(\eta_2 - \eta_1) - \beta(\psi(\eta_2) - \psi(\eta_1))] \qquad (3.3.5)$$

where $\psi(\eta)$ is known as the *Bresse function*, and is equal to

$$\psi(\eta) = \int \frac{d\eta}{1 - \eta^3} =$$

$$= \frac{1}{6} \ln \left(\frac{\eta^2 + \eta + 1}{(\eta - 1)^2} \right) - \frac{1}{\sqrt{3}} \operatorname{arccot} \left(\frac{2\eta + 1}{\sqrt{3}} \right) \qquad (3.3.6)$$

in which $\eta = a / a_n$

$\beta = 1 - (a_c / a_n)^3$

A more simple analytical solution is possible if i_b=0. The Bresse function is not valid in that case because of division by zero. Then eq. (3.3.3) yields:

$$\frac{\partial a}{\partial x} = - \frac{q^2 / C^2}{a^3 - (q^2 / g)} \qquad (3.3.7)$$

Integration of this equation yields:

$$x_2 = x_1 - \frac{C^2}{g^2}\left(\frac{a_2^4}{4} - a_c^3 a_2 - \frac{a_1^4}{4} + a_c^3 a_1\right) \qquad (3.3.8)$$

In which x_1 is the known value on a location upstream (in case of supercritical flow) or downstream (in case of subcritical flow) of the desired unknown distance x_2.

An analytical method can be used besides a numerical method to verify the numerical results.

3.3.4 Methods of numerical integration

The gradually varied flow equation is a first order non-linear differential equation:

$$da/dx = f(a,x) \qquad (3.3.9)$$

Two chosen numerical integration methods are described to solve the gradually varied flow equation. At the end of this section the choice of these methods is considered. For all these numerical methods it is important that calculations must proceed in upstream direction in subcritical flows and in downstream direction in supercritical flow.

The Simpson rule

This method is suitable in prismatic channels and can be applied to solve the gradually varied flow differential equation if eq. (3.3.9) is independent of the distance x :

$$da/dx = f(a) \qquad (3.3.10)$$

In general it is preferable to rewrite the equation as follows:

$$dx/da = g(a) \qquad (3.3.11)$$

The solution of this equation now is an integral that can be solved by means of the *trapezoidal rule* or the *Simpson rule*.

This enables us to calculate x-values, starting at an initial waterdepth a_1 (at one end of the channel), calculating in (small) depth steps until the final depth a_2 (at the other end of the channel) is reached.

Because the Simpson rule gives more accurate solutions than the trapezoidal rule and therefore needs a smaller number of computation steps, it is more efficient to use the Simpson rule to compute surface profiles.

The *multi-segment Simpson rule* can be represented (Almering, 1984) as:

$$\begin{aligned} x_2 - x_1 = {} & \frac{1}{3} h[\, g(a_1) + 4g(a_1+h) + g(a_1+2h) \,] + \\ & + \frac{1}{3} h[\, g(a_1+2h) + 4g(a_1+3h) + g(a_1+4h) \,] + \\ & + \ldots + \frac{1}{3} h[\, g(a_2-2h) + 4g(a_2-h) + g(a_2) \,] \end{aligned} \qquad (3.3.12)$$

or represented as:

$$x_2 - x_1 = x[a_1+2h] + x[a_1+4h] + x[a_1+6h] + \ldots + x[a_2] \qquad (3.3.13)$$

Notice that an even number of segments must be utilized to implement the method.

An error estimation for the multiple-segment Simpson's Rule is obtained by first computing with a stepsize h and secondly with a stepsize $\frac{1}{2} \cdot h$. Then the following estimate can be found (Almering, 1984):

$$Error = I - I_3 \approx 1/15 \cdot (I_3 - I_2) \qquad (3.3.14)$$

where I = exact value

I_2 = value computed with a stepsize h

I_3 = value computed with a stepsize $\frac{1}{2} \cdot h$

Notice that this method can only be applied when the bottom

slope and friction coefficient remain constant along the channel axis.

Runge-Kutta method

Another method that can be applied for the integration of eq. (3.3.10) is the *Runge-Kutta method*. It is used to calculate the waterdepth as a function of the distance x (the Simpson rule is used to compute $x=f(a)$). For the hydraulic Jump computations (discussed in a following section) this method had to be used to avoid long space steps of flow profiles near the normal depth line.

The Runge-Kutta method can be compared with many other numerical explicit (predictor-corrector) integration methods. It is also possible to compute with varying bottom slopes and C values (assumed that their continuous variation in x direction can be described by a certain function $g(x)$).

Using $da/dx = f(a,x)$ (3.3.15)

The *standard fourth order Runge-Kutta method (SRK)* becomes:

$$a_{i+1} = a_i + \frac{1}{6}(K1+2K2+2K3+K4) \qquad (3.3.16)$$

where h = space step in x-direction

$K1 = h \cdot f(a_i, x_i)$

$K2 = h \cdot f(a_i+\frac{1}{2}K1, x_i+\frac{1}{2}h)$

$K3 = h \cdot f(a_i+\frac{1}{2}K2, x_i+\frac{1}{2}h)$

$K4 = h \cdot f(a_i+K3, x_i+h)$

The *SRK* is a predictor-corrector method based on the Simpson Rule. It has a relatively high accuracy and a more efficient use of the available memory of the computer.

The principle of error estimation is equal to that of the Simpson's Rule and the Heun Method (not discussed here).

$$Error \approx (1/15)*(a_{½h} - a_h) \qquad (3.3.17)$$

Stability of the Runge-Kutta Method requires a certain maximum step size. Condition for stability of *SRK* is

$$h_i < 2.8/|\mu_i|$$
$$\mu_i = df(a_i, x_i)/da \qquad (3.3.18)$$

Note that the maximum step size that is required for stability can vary for different parts of the flow profile (μ_i is a function of a_i). In general the step size for that part of the curve that is close to the critical depth has to be smaller then elsewhere. It is advisable to use a variable step size during the computations.

Comments on the chosen methods

Besides the two methods described here, there are some other methods that can be applied to solve the equation. Accuracy and stability conditions differ for each method. Implicit methods can be used to prevent instability in case of large step size (*Crank-Nicholson*).

When the flow is non-steady then time dependent equations have to be used. The basic equations of the water movement can be solved numerically with an explicit or implicit method. Application of methods in non-steady flow can be found in the literature.

3.3.5 Hydraulic jump computation

A hydraulic jump occurs when a supercritical flow meets a subcritical flow. The supercritical flow jumps up to meet its alternate (downstream subcritical) depth. A precise mathematical model to describe this phenomenon has not yet been determined. Many empirical formulas, however, have been developed to compute for instance the location of the jump and

the energy losses.

In general one can distinguish between jumps in horizontal and jumps in sloping channels. The approach of the jump computations is partially different for both kinds of jumps, as is explained later in this chapter. *Adverse* bottom slopes, however, are not discussed because of their rare appearance and the lack of experimental data on these jumps.

In appendix (2) a classification is given of hydraulic jumps on a horizontal bottom. Classification of the jumps is important for surveyability and distinction of various possible jumps.

Sequent depths in a horizontal channel

The water level upstream of the jump is called the *initial level* y_1, and the one downstream of it is called the *sequent depth* y_2. In a rectangular channel with a horizontal bed the sequent depth follows from the solution of the momentum equation (Chow, 1959):

$$\frac{y_2}{y_1} = \frac{1}{2}\left[\sqrt{1+8Fr_1^2} - 1\right] \qquad (3.3.19)$$

It must be emphasized that y_2 is the result of the downstream control; i.e., if the downstream control produces the depth y_2, then a jump forms.

Length of the jump in a horizontal channel

The length of the jump (L_j) is an important parameter in the computation method. This length may be defined as the distance measured from the front face of the jump to a point on the surface immediately downstream from the roller. It cannot be determined easily by theory but the results of

several experimental investigations have yielded that :
$L_j / y_2 = f(Fr_1)$ (Chow, 1959, p398).

Sequent depths and length of the jump on a sloping floor

Relating to constructions in mountain rivers it is important to consider hydraulic jumps in horizontal channels as well as in sloping channels.

In the analysis of hydraulic jumps in sloping channels, it is essential to consider the weight of the water enclosed in the jump (influence of the gravity component). In horizontal channels the effect of this weight is negligible. Thus, the momentum equations for jumps on a horizontal bed cannot be applied straightforwardly to jumps on a sloping bed. However, the momentum principle can be used to derive an equation analogous to eq. (3.3.19). This derived equation contains an empirical function that has to be determined experimentally. Based on a laboratory study by the U.S. Bureau of Reclamation (1955), the following sequent depth variation can be noted:

$$\frac{y_t}{y_2} \approx 0.42 + 0.58 \exp(4.7\, i_b) \qquad (3.3.20)$$

In which y_t = sequent depth (tailwater depth)
y_2 = equivalent sequent depth in a horizontal floor jump (corresponding to y_2 in eq. (3.3.19))

It appears that the sloping-bed jump requires more tailwater depth y_t than the corresponding horizontal-bed jump. Further, the results are not valid for negative bottomslopes, as it was stated already in the begin of this section.

The length of the jump L_j on a sloping bed is longer than the corresponding L_j of a jump on a horizontal bed. Similarly

to the horizontal bed, the relative length of the jump L_j/Y_2 may also be shown as a function of Fr_1 and ib and represented by curves based on experimental data of the Bureau of Reclamation USBR (Ven Te Chow, 1959, p428). Elevatorski's (1959) analysis of the USBR data indicates that the jump length can be expressed as (Subramanya, 1982):

$$L_j = m_s \cdot (Y_t - Y_1) \qquad (3.3.21)$$

in which $m_s \approx \dfrac{6.9}{5.42 \sinh(\tan\zeta) + 1}$

ζ = angle of the bottom slope in degrees

Eq. (3.3.21) is based on a wide range of values for Fr_1.

Location of the jump on a sloping floor

The location of the hydraulic jump can now be estimated using the upstream and downstream surface profiles, the sequent depths belonging to the supercritical profile equation (3.3.20) and the length of the jump eq. (3.3.21). Theoretically speaking the jump occurs where the sequent depth curve (collective curve of depths Y_t conjugate to the corresponding depths Y_1 of the supercritical surface profile), intersects with the subcritical surface profile (downstream). This theoretical condition is generally used to locate the position of the jump on extensive longitudinal profiles.

For a closer estimation of the location of the jump, the length of the jump has to be considered also. The procedure for locating the jump is described in appendix (2). This procedure gives direct determination of the end points of a jump and the method is general and can therefore be applied in a wide variety of jump situations.

3.4 Unsteady flow with low sediment concentrations

3.4.1 Basic Equations

When the discharge varies in time the flow is called unsteady. When the sediment transport is assumed to be relatively small ($s/q \ll 1$), then the influence of concentration on the equations of motion and continuity can be neglected with respect to the discharge ($\phi=0$).

The variations of sediment storage in equation (3.3) are now only dependent on the rate of accumulated bed-load material along the river axis (see appendix (1)).

The basic equations (3.1) to (3.3) can be rewritten as

$$\frac{\partial u}{\partial t} + u\frac{\partial u}{\partial x} + g\frac{\partial a}{\partial x} + g\frac{\partial z}{\partial x} = -\frac{gu^2}{C^2 a} \qquad (3.5)$$

$$\frac{\partial a}{\partial t} + a\frac{\partial u}{\partial x} + u\frac{\partial a}{\partial x} = 0 \qquad (3.6)$$

$$\frac{\partial z_b}{\partial t} + \frac{\partial s_b}{\partial x} = 0 \qquad (3.7)$$

In which $s_b = \alpha\phi a u = f(u)$ (3.8)

(Assumed is that $\cos(\zeta) \approx 0$ and $\sin(\zeta) \approx i_b$)

The properties of this system of equations are investigated by many authors (e.g. Jansen 1979, de Vries 1959). Comparing their analysis with the analysis of the equations for sediment-laden flow (sections 3.6 and 3.7) enables us to come to certain conclusions on the influence of sediment concentrations on the river flow. For this objective the

characteristic celerities of the system are treated in the following subsection.

3.4.2 Characteristic celerities

Because of the close relationship between physical and mathematical properties, the method of characteristics is a basic concept and tool in analyzing the complex system of basic equations. With this method it is possible to draw pertinent and easily understandable physical interpretations from the mathematical expressions.

In this section the charcteristic celerities of small disturbances are treated as a tool for determination of the rapidity of changes in the flow and morphology, and for imposing the boundary conditions.

In appendix (1) the general matrix approach is used to derive celerities. The same approach yields for the basic equations (3.5) to (3.8) (see Jansen 1979 and de Vries 1959) that the three celerities, defined as $c = dx/dt$, follow from the cubic equation

$$- c^3 + 2uc^2 + (ga - u^2 + gf_u)c - ugf_u = 0 \qquad (3.9)$$

in which $f_u = \frac{ds}{du}$

Inserting dimensionless parameters φ, Fr, ψ in this equation yields

$$\varphi^3 - 2\varphi^2 + (1 - Fr^{-2} - \psi Fr^{-2})\varphi + \psi Fr^{-2} = 0 \qquad (3.10)$$

in which $\varphi = c/u$ = relative celerity

$Fr = u/(ga)^{\frac{1}{2}}$ = Froude Number

$\psi = f_u/a$ = dimensionless transport parameter

The general goniometrical solution of this cubic equation

gives for the real celerities

$$\varphi_1 = \frac{2}{\sqrt{3}}\sqrt{q}\,\cos\left(\frac{\alpha_\varphi}{3}\right) + \frac{2}{3} \qquad (3.11)$$

$$\varphi_2 = -\frac{2}{\sqrt{3}}\sqrt{q}\,\cos\left(\frac{\pi-\alpha_\varphi}{3}\right) + \frac{2}{3} \qquad (3.12)$$

$$\varphi_3 = -\frac{2}{\sqrt{3}}\sqrt{q}\,\cos\left(\frac{\pi+\alpha_\varphi}{3}\right) + \frac{2}{3} \qquad (3.13)$$

in which $q = \frac{1}{3} + Fr^{-2} + \psi Fr^{-2}$

$$r = -\frac{2}{27} + \frac{2}{3}Fr^{-2} - \frac{1}{3}\psi Fr^{-2}$$

$$\alpha_\varphi = \arccos\left[\left(\frac{3}{q}\right)^{3/2}\frac{r}{2}\right]$$

In the following sections these celerities will be used to consider the influence of the concentration terms in the basic equations , e. g. on the momentum and mass balance.

3. 5 Unsteady flow large sediment concentrations: first approach

3. 5. 1 Basic equations

The flow is called unsteady when the discharge varies in time. The general basic equations for the mountain river flow (section 3. 2) can be rewritten if the concentration rate of the flow is due to high sediment transport. For the derivation

of the new basic equations the concentration of sediment in the flow is predicted with a sediment transport formula which relates the transport to the local hydraulic conditions. The adaptation of the sediment transport, which applies to the suspended transport, is not included.

The derivation of the equations is described in appendix (1). The basic equations for unsteady flow with high transport rates are:

$$\frac{\partial u}{\partial t} + u\left[1+\frac{1}{2}Fr^{-2}V_c\cos(\zeta)\left(\frac{u}{s}f_u-1\right)\right]\frac{\partial u}{\partial x} + g\cos(\zeta)\frac{\partial z_b}{\partial x} + \\ + g\cos(\zeta)\left[1-\frac{1}{2}V_c\right]\frac{\partial a}{\partial x} + \frac{gu^2}{C^2a}\cos(\zeta) - g\sin(\zeta) = 0 \qquad (3.14)$$

$$\left[\frac{\alpha\Delta}{au}\left(uf_u-s\right)\right]\frac{\partial u}{\partial t} + u\left[1+\alpha\Delta\frac{f_u}{a}\right]\frac{\partial u}{\partial x} + \frac{u}{a}\frac{\partial a}{\partial t} + \\ + \frac{u^2}{a}\frac{\partial a}{\partial x} = 0 \qquad (3.15)$$

$$\frac{\partial z}{\partial t} + \frac{a}{u}\left[\frac{uf_u-s}{au}\right]\frac{\partial u}{\partial t} + f_u\frac{\partial u}{\partial x} = 0 \qquad (3.16)$$

In which $f_u = \frac{\partial s}{\partial u}$ and $s = f(u)$

$$Fr = \frac{u}{\sqrt{ga}} \quad \text{and} \quad V_c = \frac{\alpha\Delta s}{ua+\alpha\Delta s}$$

3.5.2 Characteristic celerities

Corresponding to the analysis given in section 3.4 the

characteristic celerities of the system are derived for this type of flow equations and compared with the celerities of the flow with low sediment concentrations (from section 3.5.2). In appendix (1) the cubic equation is derived that describes the celerities:

$$c^3 + \left[-uR_A + \frac{ga}{u}\cos(\zeta)R_G - u + \frac{ga}{u}R_BR_C\right]c^2 + \qquad (3.17)$$
$$+ \left[u^2R_A - ga(R_DR_B + \cos(\zeta)R_G) - g\cos(\zeta)f_u\right]c + guf_u\cos(\zeta) = 0$$

In which

$$R_A = 1 + \frac{1}{2}Fr^{-2}V_c\left(\frac{u}{s}f_u - 1\right)\cos(\zeta)$$

$$R_B = \cos(\zeta)\left[1 - \frac{V_c}{2}\right]$$

$$R_C = \frac{\alpha\Delta}{ua}(uf_u - s)$$

$$R_D = 1 + \alpha\Delta\frac{f_u}{a}$$

$$(R_E = 1)$$

$$(R_F = 1)$$

$$R_G = \frac{uf_u - s}{ua}$$

$$V_c = \frac{\alpha\Delta s}{ua + \alpha\Delta s}$$

In appendix (1) it is also shown (graphically) that for certain flow velocities (or Froude Numbers) the celerities can differ from those for equations without the influence of concentration. Therefore the sediment transport has been predicted using the Engelund Hanssen Formula or the Meyer

Peter Müller formula. For small Froude numbers the celerities agree reasonably with these celerities for the low sediment concentration equations (section 3.5.2).

In the following section a second approach of the approximation of sediment concentrations in the basic equations is considered. Therefore the suspended load is seperated from the total sediment load.

3.6 Unsteady flow with large sediment concentrations: second approach

3.6.1 Basic equations

Comparably to the derivation of basic equations for flow with large concentrations in the previous section, the concentration of sediment is determined by the sediment transport rate. The following assumptions apply:

- The influence of sediment on the water movement is supposed to be dependent on the concentration of suspended load only. This assumption holds for the fact that bedload transport in volcano rivers is small compared to the suspended load transport, and therefore does not appreciably contribute to the concentration distribution averaged over the vertical.
- The adaptation of the suspended load concentration distribution (over the vertical) to the local hydraulic conditions is described with an additional basic equation for the depth-integrated suspended load concentration (Galapatti, 1983). Only the adaptation of the concentration can cause the degradation processes downstream of a sediment detention dam and is therefore important in the volcano river model.
- The van Rijn sediment tranport formulas (for bedload and

suspended load, van Rijn 1984) are applied for the model. This choice is based on the fact that appreciable results can be achieved for high velocity flow and fine sediment (van Rijn, 1986) compared to the methods of Engelund Hansen, Meyer Peter Müller and others.

The derivation of the equations is briefly described in appendix (1). The following system of basic equations is derived:

$$\frac{\partial u}{\partial t} + u\frac{\partial u}{\partial x} + g\cos(\zeta)\frac{\partial a}{\partial x} + \frac{1}{2}R_1 g\cos(\zeta)\frac{\partial Cs}{\partial x} + g\cos(\zeta)\frac{\partial z_b}{\partial x} - g\sin(\zeta) + \frac{gu^2}{C^2 a}\cos(\zeta) = 0 \qquad (3.18)$$

$$\frac{\partial a}{\partial t} + u\frac{\partial a}{\partial x} + a\frac{\partial u}{\partial x} + R_1\left(\frac{\partial Cs}{\partial t} + u\frac{\partial Cs}{\partial x}\right) = 0 \qquad (3.19)$$

$$\alpha\frac{\partial z}{\partial t} + \alpha f_u\frac{\partial u}{\partial x} + \frac{R_1}{\Delta}\left(\frac{\partial Cs}{\partial t} + u\frac{\partial Cs}{\partial x}\right) = 0 \qquad (3.20)$$

$$T_a\frac{\partial Cs}{\partial t} + L_a\frac{\partial Cs}{\partial x} + Cs - Cse = 0 \qquad (3.21)$$

In which Cs = Concentration of suspended material

R_1 = $(a\Delta)/(1+\Delta Cs)$

Cse = s_s/ua (s_s=suspended load rate from van Rijn)

= equilibrium concentration (capacity)

and

$$L_a \approx uT_a$$

$$U = \frac{u_*}{u}$$

$$T_a \approx \frac{\tau a}{W_s}$$

$$x_\tau = \frac{W_s/u_*}{1+2(W_s/u_*)^2}$$

$$\tau = \exp[\ (4.287-22.453U)x_\tau^3 + (24.827U-6.412)x_\tau^2 + (3.2U-1.568)x_\tau\ ]$$

These coefficients have been derived for the van Rijn (1987) diffusion coefficient and the van Rijn (1987) transport formula (see appendix 1). In the following subsection the characteristic celerities of the system are determined to investigate the properties of the equations.

3.6.2 Characteristic celerities

In appendix (1) the characteristic celerities for the system are determined, as a tool for determination of the rapidity of changes in the flow and morphology and for imposing the boundary conditions. The quartic equation that represents the four celerities of the system is (for $L_a=uT_a$):

$$c^4 - 3uc^3 + [3u^2 - gf_u\cos(\zeta) - ga\cos(\zeta)]c^2 + [2guf_u\cos(\zeta) + gau\cos(\zeta) - u^3]c - gu^2f_u\cos(\zeta) = 0 \qquad (3.22)$$

which can be rewritten as

$$(c-u)\left(c^3 - 2uc^2 + \left[u^2 - gacos(\zeta) - gf_u cos(\zeta)\right]c + guf_u cos(\zeta)\right) = 0$$

If the celerities are compared with the celerities for flow with low sediment concentrations (section 3.5.2) then the following conclusions can be drawn (if bed slopes are negligible $\cos(\zeta) \approx 1$):

- The celerities for water movement and bed levels are equal for both systems.
- The celerity originating from the concentration of suspended load is equal to ratio of the adaptation length to the adaptation time, which is approximately equal to the flow velocity. This can be explained considering that the depth integrated suspended sediment equation can be rewritten as the derative of *Cs* moving with a velocity *u* in *x*-direction:

$$\frac{DCs}{Dt} = \frac{Cse - Cs}{T_a}$$

  This equals the equation for the characteristic celerity.
- All celerities except that of the bed levels are positive in *x*-direction. The boundary conditions have to be imposed at the upstream boundary. However, the bed-level boundary has to be taken at the downstream end of the channel section. Boundary conditions are discussed in section 4.2.3.
- The model appeared to be well applicable for mountain river flow (if the assumptions in section 3.2 apply). A numerical model for the solution of the basic equations is described in chapter 4.

3.7 Discussion and conclusions

Three basic equations have been derived for steep

rivers. The density of the sediment/water mixture ρ_m represents the influence of the sediment transport on the flow and the morphology. For reasons of flow instability, the bed slopes have been assumed to be smaller than 10% and have been neglected in the final reduced equations.

The three general basic equations have been reduced for different assumptions. The "gradually varied flow" equations are derived for steady non-uniform flow on a fixed bed without sediment transport. The application of this model is very limited in natural rivers, but it gives a good insight into the properties of the flow for various situations.

If the sediment concentration (represented by the density of the water/sediment mixture ρ_m) is neglected in the basic equations, then a system of equations remains as described in section 3.4.

Finally the equations have been reduced including the concentration of transported sediment. Firstly, the concentration has been expressed by a sediment transport formula, and secondly by the concentration of suspended load including the adaptation of the sediment to the flow.

The celerities of the first set of equations were determined using the Engelund Hansen (EH) and the Meyer Peter Müller (MPM) transport formula. However, the possibility of extrapolating the EH-formula to the large flow velocities is doubtful, and the MPM-formula only describes bed-load transport.

The celerities for the second method, which includes the adaptation of the concentration of suspended sediment, agreed with those originating from the basic equations for the flow without the influence of sediment concentration. This phenomenon does not imply , however, that the sediment concentration is negligible. The influence of the

concentration follows from the applications in section 4.3. The fourth equation that describes the adjustment process of the concentration caused an additional celerity equal to the ratio of adaptation length to adaptation time, which is approximately equal to the flow velocity.

Chapter 4

Numerical modelling of the mountain river flow

4.1 Computer model for gradually varied flow: STUWK.

The solution of the gradually varied flow equations (steady flow on a fixed bed, possibly with a hydraulic jump) as described in section 3.3 (and appendix 2) is incorporated in a computer model called STUWK. Since the application of the model is restricted to prismatic channels with constant roughness and bed slope the results of STUWK primarily have an instructive character to increase the understanding in the variations of flow caused by disturbances in the river. The occurrence of backwater curves on a moving bed is generally accompanied by erosion or sedimentation (equation 3.7). Hence, insight in the flow variations also indicates the variation of bed levels.

A description of the program and some applications are presented in appendix 2. The method of computation can be chosen by the user. For any given input (bed slope, Chezy value, discharge) the surface profiles are then determined. If the upstream boundary implies supercritical flow and the downstream boundary subcritical flow then a hydraulic jump is computed.

The results are presented on the screen both numerically and graphically. The program also includes analytical solution of the basic equations for reasons of verification of the numerical values.

4.2 Model for unsteady flow with a high suspended load rate, SABOFLOW

4.2.1 Formation of algebraic equations using the Preissmann implicit scheme

The system of basic equations is given in section (3.7.1). The equation for motion (3.18), for continuity of mass (3.19), for continuity of sediment volume (3.20) and for the depth integrated suspended load concentration (3.21), are rewritten into algebraic equations which can be solved numerically. Therefore the variables and their deratives are discretized by a difference scheme.

Finite difference method

An implicit finite difference method is chosen to overcome the limitations imposed on Δt in using the explicit scheme. All the explicit schemes are restricted in computational timestep by the Courant condition (CFL-Condition, Courant 1928)

$$c\frac{\Delta t}{\Delta x} \leq 1$$

where c is the maximum celerity of the system, and since $c_{max}=O(u)$ for large Froude Numbers (see section 3.6.2) the CFL-condition yields: $\Delta t_{max}=O(\Delta x/u)$. The stepsize for implicit methods is mainly dependent on the required accuracy. For acceptable results Stelling (1990) recommends a Courant Condition of

$$c\frac{\Delta t}{\Delta x} < 10$$

The Preissmann (SOGREAH) implicit method (Preissmann, 1961) has been chosen because it is simple in its basic computational grid-point structure. Other implicit schemes for open channels exist but their applicability for this model has not been evaluated.

Formation of algebraic equations

Figure (4.1) and equations (4.1) to (4.3) show the actual discretization of dependent variables and their deratives in a centerpoint, according to Preissmann (1961):

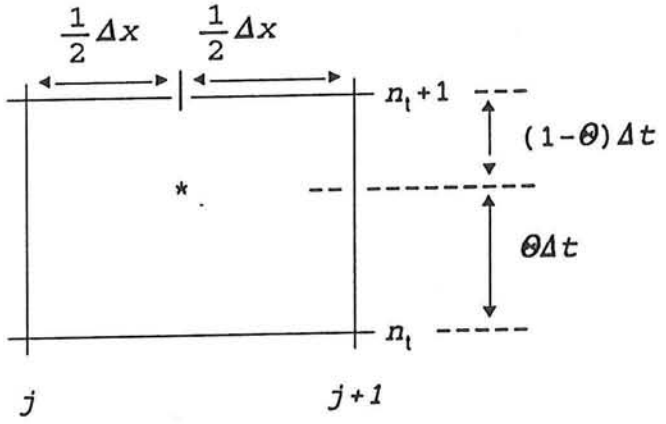

figure 4.1 Preissmann box-scheme

$$f(x,t) = \frac{\theta}{2}\left[f_{j+1}^{n_t+1} + f_j^{n_t+1}\right] + \frac{(1-\theta)}{2}\left[f_{j+1}^{n_t} + f_j^{n_t}\right] \qquad (4.1)$$

$$\frac{\partial f}{\partial x} = \frac{\theta}{\Delta x}\left[f_{j+1}^{n_t+1} - f_j^{n_t+1}\right] + \frac{(1-\theta)}{\Delta x}\left[f_{j+1}^{n_t} - f_j^{n_t}\right] \qquad (4.2)$$

$$\frac{\partial f}{\partial t} = \frac{f_{j+1}^{n_t+1} - f_{j+1}^{n_t} + f_j^{n_t+1} - f_j^{n_t}}{2\Delta t} \qquad (4.3)$$

where θ is a time weighting coefficient ($0.5<\theta<1$).

The algebraic equations are formed by replacing the variables and their deratives in eq. (3.18) to (3.21) by the Preissmann finite differences. For each segment (box-scheme) now four finite difference equations can be written. In a

channel reach with n_x segments, a system of $4*n_x$ equations is formed (with $4(n_x+1)$ unknown variables). In the following section three numerical methods are described to solve the system of equations.

Remark For all methods the flow is assumed to be supercritical. The transition of the supercritical flow to subcritical flow (hydraulic jump) could not be incorporated. For unsteady flow the location of the jump is variable but cannot be decoupled from the bedlevels near the jump which beforehand cannot be described by any mathematical relation. For the numerical computation of the morphology of the subcritical flow section as well as the supercritical section, bed levels have to be known at the location of the jump. These values cannot beforehand be determined.

4.2.2 Summary of numerical methods

In this section three methods are described that are examined on their applicability for the model as derived. First the Newton iteration method is described which is generally used to solve systems of non-linear equations. The second method decouples the flow and sediment concentration from the bed levels. An iteration process is developed that first computes the depth, velocity and concentration which can be used to compute the bed levels (explicit). The flow parameters can be corrected for the new bed levels etc. etc.. A third method applies to the basic equations after partially linearizing them on the lower (known) time level. The linear system represented as a matrix can be solved using the Gauss elimination method.

Newton's iteration method

The Newton iteration method or Modified Newton Raphson method is treated in appendix (3). The four equations are expressed in their non-linear form for all space steps with known values at the current time level and unknowns at the advanced time level. Together with boundary conditions this gives $4 \cdot (n_x+1)$ non-linear equations. The Newton's method incorporates an iteration (which includes a Gauss elimination for solving a matrix) until the condition of convergence is reached.

Evaluation

To incorporate the procedure as described in appendix (3), it is necessary to deduce the Jacobian matrix for the Preissmann representation of the equations. Especially the differentials of the chosen Van Rijn transport formula appear to be very extensive and highly non-linear.

Dependent on the number of x steps, the number of computations to determine the Jacobian and to solve the matrix increases substantially. With that also the computation time becomes long, since the process mainly depends on the rapidity of convergence of the iteration. After trial the following conclusions can be given:

- The stability of the computations cannot be guaranteed for any specific step size. The choice of starting values, the condition for the iteration to end, and the errors in boundary and initial conditions cannot be properly imposed or predicted.
- The method as described requires a large number of computational operations. If a certain ratio R_t is defined as

$$R_t = \frac{computation\ time\ for\ one\ timestep\ dt}{physical\ timestep\ dt_{real}}$$

then R_t appeared to be much bigger for this method than for less accurate but more simple computation methods described in the following.

Predictor-corrector iteration method

This method is treated in appendix (3) as an alternative for the solution of the mountain river flow equations. This method contains the computation process where the water depth, velocity and concentration (at the advanced time level) are determined for bed levels at the current time level. Next the bed levels at the advanced time level are determined using the flow parameters from the preceding step in an explicit representation of equation (3.20).

After trials the following conclusions can be given:

- For small time/space steps (e.g. 5 s and 1 m) and small riversections (e.g. 50 m) the computations appeared to be converging. However, for more realistic applications (volcanic rivers) the process became instable. Growing fluctuations of bedlevel and flow occurred and the computations did not converge.
- The gain of computation time compared to the Newton iteration method was small, because the small steps that are required for stability caused a large number of computations.

Matrix solution method for linearized equations with predictor for flow variables

This method turned out to be the most successful in solving the basic equations. The full method is outlined in appendix (3). Summarizing:

- The basic equations are discretized according to Preissmann. All components are linearized by taking them at the current time level ($t=t_0$) and by using the predictor method. Only the deratives then include unknown values at the advanced time level ($t=t_0+dt$).
- The velocities, depths and concentrations in the linearized components are first estimated on the advanced time level as the solution of unsteady flow equations on a fixed bed with low sediment transport. Concentration C_s is equal to C_{se}. These new values are used to predict the corresponding variables in the linearized components.
- The sediment concentration equation (3.21) can be solved independently of the unknown a, u, z values. Computing from the upstream boundary stepwise in downstream direction, since the celerity of concentration is positive for the assumption of supercritical flow (section 3.6.2).
- The three remaining equations (concentrations substituted) for each box ($dt*dx$) form a system of $3 \cdot n_x$ which can be presented, after substitution of boundary conditions (section 4.2.3) as a banded matrix (bandwidth 9). This matrix is solved using the Gauss elimination method (LU decomposition method) for which the matrix is first transformed for the positive x-direction and then solved in the opposite direction (double sweep method).

Conclusions regarding this method are:

- This method appeared to be stable for about $dx<100$m and about $dt<100$s (dependent on the magnitude of the variations in flow and bed over a space/time-step). For larger steps the linearization of coefficients does not hold. Besides, an additional error is generated from the decrease of numerical accuracy for larger steps for the implicit schemes. A precise condition for the maximum step sizes can only be determined by trial and error. Numerical oscillations (e.g. near wave fronts) must

decrease in time.

- The ratio R_t (see Newton's method) is smaller than that of the other methods described in this section (e.g. $R_t < \frac{1}{2}$)

For reasons of stability and computation time this method is chosen for modelling the mountain river flow (computer model *SABOFLOW* sect. 4.2.4). However, it might still be possible to develop even better solution methods, similar to the present method with linearized equations.

4.2.3 Boundary conditions and initial condition

For solution of the morphological model four boundary conditions and one initial condition (t=0) are required. In this section the conditions are described as they are used in the model.

Boundary conditions

From section 3.6.2 it followed that for supercritical flow the characteristic celerities of the velocity u, depth a, and concentration Cs are positive (in x-direction) and negative for the bed level z. This implies that a, u, Cs (or $q=u \cdot a$) can only be influenced by changes upstream so that the boundary conditions for these variables have to be imposed at the upstream boundary:

$x=0$: a, q, Cs *values for* $t=0$ *to* t_{end}

If any sediment detention dam is located at $x=0$ then $Cs < Cse$.

For similar reasons the bed level condition has to be imposed at the downstream boundary:

$x=x_n$: z *values for* $t=0$ *to* t_{end}

This bed level is again dependent on unknown downstream conditions. Therefore the bedlevel is assumed to be fixed, e.g.

at a dam where the boundary is the crest of the dam.
To prevent the generation of a hydraulic jump upstream of the structure, the bed upstream of the structure must nearly be filled up and it must have a slope larger than critical.

Initial condition

The solution of the Preissmann algebraic equations for the first time step ($t=dt$) requires all values of a, u, Cs, z at the initial time level ($t=0$). For many volcanic rivers in tropical areas, practically, this condition is a dry bed with zero discharge. However, this zero initial condition causes infiltration during the first period of the flood. This infiltration has not been included in the basic equations, hence it cannot be incorporated in the model (cf. Schropp and Fontijn, 1989). To avoid this problem a small discharge is assumed so that the computations can start.

Although the initial values can be determined from the Q-h relations along the river axis or from measurements, it appeared more convenient and appropriate to determine these values from the boundary conditions and the bottom levels at $t=0$ by a single sweep computation for usteady flow over a fixed bed. This applies to the almost equilibrium situation which exists for a small steady discharge during a short timestep. The concentration of suspended load is then equal to the transport capacity which can be determined with the Van Rijn sediment transport formula.

The equations and the solution for the computation of the initial condition are described in appendix (3).

4.2.4 Computer program SABOFLOW

In section 4.2.2 the numerical method to solve the equations for mountain flow with high suspended load transport is considered. The computer program that is developed to predict the flow and morphology is called "SABOFLOW"

First the structure of the program is described. Secondly the limitations, imposed for reasons of simplicity, are considered.

Execution of the computations proceeds as follows:

- SABOFLOW creates an input file of data inserted by the user. For that file the computations are executed, during which the results are written to an output file. Computations are terminated if the Froude number becomes one or less.
- SABOPLOT is the supporting program that processes the results from the output file and plots them on the screen. Bedlevels are plotted for a reference level defined by a straight line from $z[0,0]$ to $z[n_x,0]$ at the time level t=0 (initial bed reference).

In appendix 3 the flow charts for both programs are given.

The programs are composed of several units that can be overlaid for more efficient use of the memory available (units are not loaded into the memory unless they are needed).

The programming language is Turbo Pascal and if available an extended memory and a coprocessor are used.

For reasons of simplicity the program is limited in its applicability and in the size of the computations. The main limitations are:

- The program can only be used for mountain river problems for which the assumptions, on which the model is based, apply (e.g. supercritical flow without a hydraulic jump).
- The downstream bed level is assumed to be fixed (e.g.

the crest of a dam).

- The maximum number of space steps is two hundred.
- The step sizes (time and space) are determined by the numerical method (section 4.2.2). Space steps smaller than 50 m and time steps smaller than 50 s give appreciable results.
- The model does not include varying space steps.

Applications of the computer model are described in section 4.3. These applications give an impression of the problems that can be solved using the model and the differences of the solutions for flow with and without influence of suspended load concentration as applied in SABOFLOW.

4.3 Applications of the model for mountain river flow

The computer program SABOFLOW is applied to compute several cases. Some of them are described in appendix 3. Conclusions regarding these cases are discussed in this section. Finally the computations of the morphology for the Kali Thermas Lama is described, a river on the slopes of the Kelud volcano in Indonesia.

General applications

The application of the program to some general cases is described in appendix 3. These computations give an impression of the physical properties of the model.

- Equilibrium situation: Occurs if the depth is equal to the normal depth (no flow profiles) and the concentration is equal to the capacity *Cse* (following from the Van Rijn transport formula). Steady flow is assumed.

- Flow over a small shoal: If again the same conditions as

for the equilibrium situation are applied, then the shoal appears to move in upstream direction (both for flow with and without the influence of sediment concentration and for both cases with the same velocity). This phenomenon agrees with the negative celerity of the bed disturbances as found in section 3.6.2. The local increase of the bed level is accompanied with a local increase of water depth and a local decrease of flow velocity and sediment concentration. The height of the shoal appeared to be increasing in time and downstream of the shoal a scour hole occurred. However, for flow without influence of concentration (section 3.4) the height decreased and sedimentation occurred downstream. The increase of height and the scour is caused by the adaption of the suspended concentration to the flow variations. At the upstream face of the shoal sedimentation occurs which continues after the velocity increases over the top of the shoal (erosion), until the concentration has been adapted to that new condition. The mimimum of the phase of the concentration variations is located downstream of the top of the shoal (shifted phases). The gradient of the concentration at the top of the shoal ,causes net sedimentation. A similar process holds for the lower eroding face of the shoal. Erosion continues downstream until the concentration has been adapted.

- Flow over a small trench: If a similar computation as for the small shoal is executed for the trench, then comparable results are found (celerity upstream, increasing depth of the trench during the process, diminished water depth, increased flow velocity, and sedimentation downstream). This process is also due to the adaptation of suspended load concentration to the flow conditions.

Following from these cases it appeared that the con-

centration of suspended material does not affect the celerities (cf. section 3.6.1), but it appears to influence the adaptation of the erosion and sedimentation processes to the flow conditions.

Kali Thermas Lama in Indonesia

To test the program in its final stage a test-case has been chosen for a mountain river on the slopes of the Mount Kelud in East-Java before its eruption in February 1990.

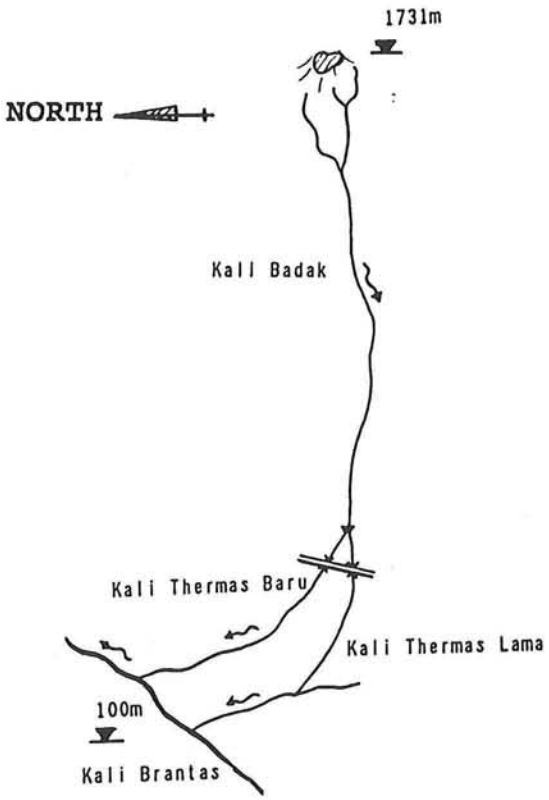

fig. 4.2 Kali Badak/Kali Thermas Lama

The upstream part of this river is called the Kali Badak. About 20 km downstream there is a bifurcation. Because of the Sumbersari dam (a consolidation dam to induce deposition of excessive sediment) at that point, there is no influence of both river branches on the Kali Badak upstream of this dam and these branches cannot influence each other. For that reason it is possible to consider the left riverbranch only: the Kali Thermas Lama. About 20 km more downstream this river flows into the Kali Brantas. The Kali Badak and Thermas Lama are dry during ten months per year. Because the slopes of the Kelud cosists of fine loose volcanic material, some sabo-works have been built in the rivers to protect the downstream overpopulated areas against sediment disasters (lahar flow and inundation of accumulated river sections). The sabo-works in the test-case river are e.g. checkdams, groundsills, and river-bank revetments (see chapter 2).

Problems in the Kali Badak and Thermas Lama occurred when the first checkdams were built upstream. Increased erosion of the downstream riverbed near the dam and accumulation in the downstream reaches were the results of the disturbed equilibrium in the river. Also later built dams did not solve the problems. The higher reach of the Kali Thermas Lama near the bridge for the road to Kediri became clogged up with relatively fine sediment. The riverbed level had reached the level of the surrounding fields. A river like that is usually called a ceiling river. This part of the river has to be excavated before the annual floods.

The computations have been executed for the river part between upstream the Karanggondang bridge and downstream the Tawangrejo bridge. The propagation of material accumulated near the downstream boundary, in upstream direction is investigated to explain the severe sedimentation near the Karanggondang bridge and the upstream river section. Further the degradation downstream of the Sumbersari dam is considered.

The data available on the Kali Thermas Lama in the main research centre were very limited. Available data were:

- Bottom levels of the whole river bed in 1985 and 1987 from the "Proyek Penanggulangan Bercana Alam Akibat Letusan Gunung Kelud").

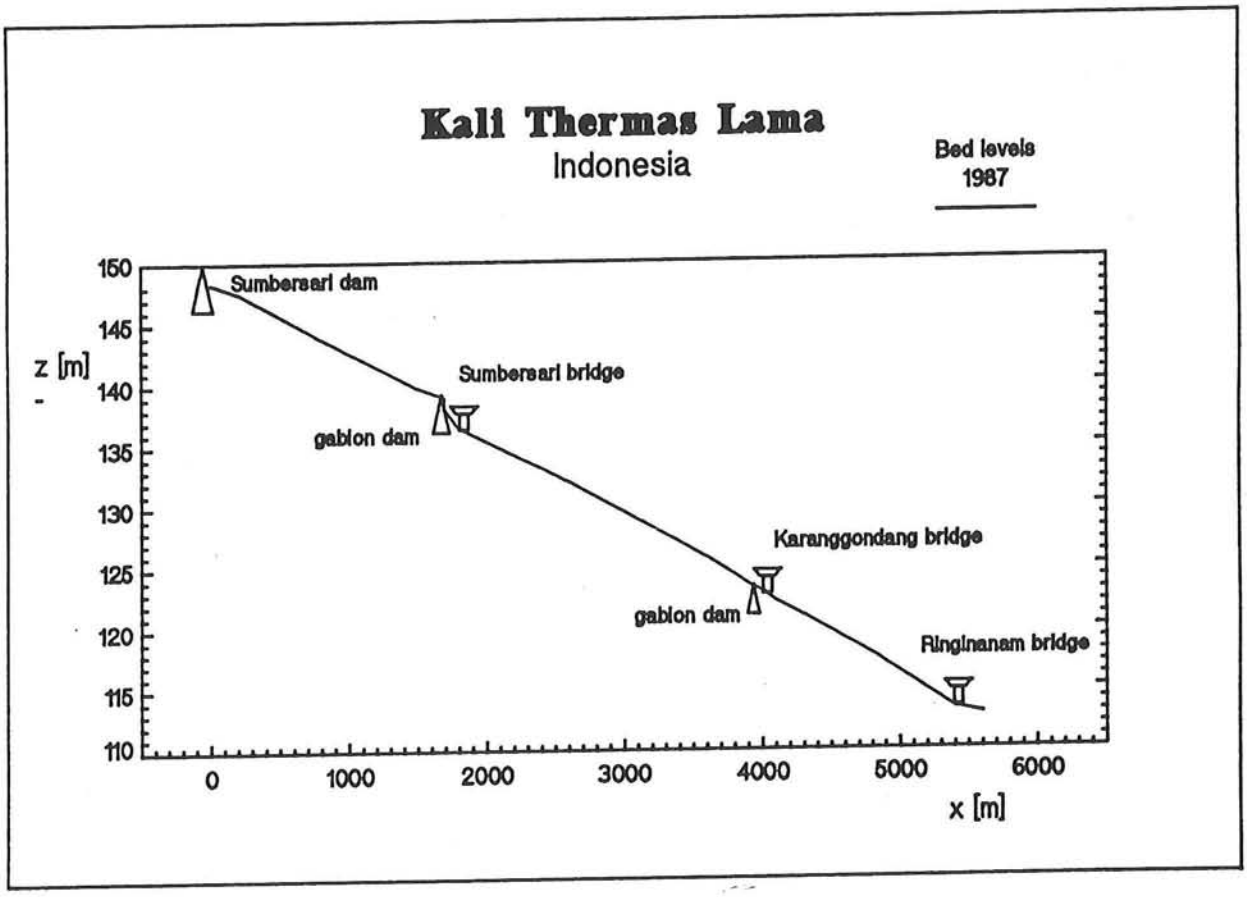

fig. 4.3 Bed levels Kali Thermas Lama 1987

- Grain size distribution of the bed material of the Kali Thermas Lama near the Karanggondang bridge following from a seaving analysis for six samples dried at 20° C.

d_{16} = 165 µm
d_{35} = 239 µm
d_{50} = 302 µm
d_{84} = 555 µm

d_{90} = 664 μm

and d_m = 367 μm with σ_m = 52 μm

d_g = 302 μm with σ_g = 56 μm

These grainsizes show that the bed material is fine sand and therefore the sediment transport is expected to be high.

- Density of the bed material of the Kali Thermas Lama near the Karanggondang bridge was determined for twelve samples using a pyknometer.

  ρ_s = 2907 kg/m^3

  with a standard deviation σ_ρ= 170 kg/m^3
- Average width of the rivers: about 30 m
- Data on representative discharges during a maximum flood (banjir) for the Kali Thermas Lama (q_{max} = 4.2 m^2/s)
- The Chézy roughness coefficient in the river is assumed to be approximately 50 m$^{\frac{1}{2}}$/s (including head losses in the bends).

First the bed level variation has been computed, downstream of the Karanggondang bridge, during a schematized flood wave. The main objective was to investigate the river-bed stabilization if a downstream elavation is imposed. The computation is presented in appendix 3. The results show that the elavation propagates in upstream direction and that in a short time period (several hours) the bed level at the upstream boundary is raised already.

The conclusion from this computation is that the the severe accumulation of sediment near the Karanggondang bridge is mainly caused by the downstream raise of the bed level. This raise starts where the flow jumps to subcritical flow. The hydraulic jump is probably located approximately 1300 or 1400 m downstream near the Ringinanam bridge (flow obstruction by the bridge) or several kilometers more downstream (slope becomes less than critical).

A second case is considered which describes the degradation of the river bed in the most upstream part of the Kali Thermas Lama (downstream of the Sumbersari dam). The Sumbersari dam is an approximately 3 meter high consolidation dam. Upstream sediment is detained so that the concentration at the boundary is less than equilibrium. Local scour is not included in the model. The water depth is assumed to be equal to the normal depth. The computations (appendix 3) show that for a short time period appreciable degradation occurs. The degradation of the bed will continue until the equilibrium concentration satisfies the sediment supply.

Chapter 5

Conclusions, discussion and recommendations

A one dimensional model has been developed that can be applied for various cases of degradation and sedimentation in volcanic rivers. The influence of the sediment transport on the flow is expressed in terms of the suspended load. An important limitation is that a hydraulic jump cannot be included in the computations. Therefore sedimentation upstream of a sabo dam or at a mildly sloping channel section, cannot be predicted using the model.

The following conclusions have been drawn from this study:

- The upstream propagation of small bed disturbances agrees with the negative characteristic celerity of the equations. The influence of the suspended load concentration appears in the growth of bed irregulerities. This is caused by the redistribution process of the concentration in case of net erosion or sedimentation.
- Degradation occurs from the upstream boundary, expanding downstream if suspended sediment is detained at the boundary (cf. check dam).
- Numerical computations and analysis of the characteristics show a fast progress of the erosion and sedimentation processes, and a fast propagation of flow alterations. Hence, accurate numerical computations require small space and time steps.
- In spite of the schematic character of the model, the trend of the results agrees with observations in the Kali Badak and Kali Thermas Lama in Indonesia. Therefore the main objective of this study (develop a mathematical model for volcanic river flow) has been reached satisfactorily.

A more complete model for volcano rivers requires to include the hydraulic jump. Therefore more study is necessary to a moving jump on a moving bed.

Also local scour downstream of a sabo dam needs to be considered if a model is applied to determine the foundation depth of such a dam (bed level lowering by degradation and scour).

Further topics of investigation in future studies can be:

* Stability and accuracy of the numerical method or development of alternative methods.
* Variable cross sections and flood plains (bank erosion).
* Non-uniform bed material (grain sorting).
* Energy losses in bends.
* Suspended sediment concentration near a structure and sediment transport formulas.

References

Almering, J. H. J. (1984) Analyse. Delftse uitgevers maatschappij, Delft.

Armanini, A., Dellagiacoma, F., Ferrari, L. (1989) From the checkdam to the development of functional check dams for a most effective torrent control, Proc. Int. Workshop on Fluvial Hydraulics of mountain regions, Trent, Italy.

Carlier, M (1972) Hydraulique générale et applique, Eyrolles, Paris

Chintu Lai (1986) Numerical modelling of unsteady open-channel flow, Advances in hydroscience, vol 14, Orlando.

Chow, Ven Te (1959) Open channel hydraulics, McGraw-Hill, New York.

Courant, R., Friedrichs, K., and Lewy, H. (1928) Über die partieller Differenzen Glichungen der Mathematischen Physik, Math. Ann. 100.

Elevatorski, E. A. (1959) Hydraulic energy dissipators, McGraw-Hill, New York.

Engelund, F., Hansen, E. (1967) A monograph on sediment transport in alluvial streams, Teknisk Forlag.

Galappatti, R. (1983) A depth integrated model for suspended transport, Communications on hydraulics, Delft University of Technology, Delft.

Henderson, F. M. (1966) Open channel flow, McMillan, New York.

Jansen, P. Ph. (1979) Principles of river engineering, Pitman, London.

Mahmood, K. and Yevjevich, V. (1975) Unsteady flow in open channels, Vol. 1, Water Resources Publications, Colorado.

Mayer, P. G. H. (1957) A study of roll waves and slug flows in inclined open channels, Ph. D. Thesis, Cornell Univ. Ithaca, New York.

Meyer-Peter, E. and Müller, R. (1948) Formulas for bed-load transport, Proc. IAHR, Stockholm, Vol. 2, paper 2, pp 39-64.

Müller, R. (1943) Theoretische Grundlagen der Fluß- und Wildbachverbauungen, Eidgenössische Technische Hochschule, Zürich, Mitteilungen der Versuchsanstalt für Wasserbau und Erdbau, No. 4.

Naudascher, E. N. (1987) Hydraulik der Gerinne und Gerinnebauwerke, Spring Verlag, Vienna, 1987.

Parcy, P. and others (1982) Taschenbuch der Wasserwirtschaft, Verlag Paul Parcy, Hamburg, 1982.

Parker, G. (1989) Downstream variation of grain size in gravel rivers: abrasion versus selective sorting, Proc. Int. Workshop on fluvial hydraulics of mountain regions, Trent, Italy.

Preissmann, A. (1961) Propagation des intumescences dans les canaux et rivières, Proc. 1st Congres de l'Assoc. Francaise de Calcul Grenoble, France.

Rijn, L. C. van (1984) Sediment transport, part 1: bed-load transport, Journal of Hydraulic Engineering, Vol. 110, No. 10.

Rijn, L. C. van (1984) Sediment transport, part 2: Suspended-load transport, Journal of Hydraulic Engineering, Vol. 110, No. 10.

Rijn, L. C. van (1986) Sand transport at high velocities, Report M2127, A, B, Delft Hydraulics, Delft.

Rijn, L. C. van (1987) Mathematical modelling of morphological processes in the case of suspended-sediment transport, Thesis, Delft University of Technology, Delft.

Ribberink, J. S. (1986) Introduction to the depth-integrated model for suspended transport (Galapatti, 1983), Delft University of Technology, Dept. of Civil Eng., Report No. 6-86.

Schropp, M. and Fontijn H. L. (1989) Flow profiles for steady spatially varied flow - an explorative analysis, Journal of hydraulic research, vol. 27, no. 1.

Shukry, A. (1950) Flow around bends in an open flume, Transactions, American Society of Civil Engineers, Vol. 115.

Stelling, G. S. (1990) Personal communications.

Subramanya, K. (1982) Flow in open channels, McGraw-Hill, New Delphi.

Täubert, U. (1971) Der Abfluß in schußrinnen-Verengungen, Der Bauingenieur, Jg. 46, Heft 11.

United Nations, FAO. (1981) Torrent control terminology, FAO conservation guide No. 6, Rome.

U. S. Bureau of Reclamation (1955) Research studies on stilling basins, energy dissipators, and associated appurtenances, Hydraulic laboratory report No. Hyd-399.

Vries, M. de (1959) Transients in bed-load transport (basic considerations), Delft Hydraulics Laboratory, Report R3.

Wang, Z. B. (1990) Personal communications.

Main symbols

symbol	definition	dimension
a	depth of water	[L]
a_c	critical depth	[L]
a_n	normal depth	[L]
B	width	[L]
c	characteristic celerity	$[LT^{-1}]$
C	Chézy coefficient	$[L^{0.5}T^{-1}]$
Cs	concentration of suspended load	[-]
Cse	equilibrium concentration	[-]
d	grain size	[L]
d_{50}	median particle size	[L]
d_{90}	90% particle size	[L]
Fr	Froude number $u/\sqrt{(ga)}$	[-]
F	force	$[MLT^{-2}]$
f_u	derative of transport $\partial s_b/\partial u$	[L]
g	acceleration of gravity	$[LT^{-2}]$
H	energy level	[L]
i_b	bed slope	[-]
L_a	Adaptation length	[L]
L_j	length of hydraulic jump	[L]
p	pressure	$[ML^{-1}T^{-2}]$
q	discharge per unit of width	$[L^2T^{-1}]$
R	hydraulic radius	[L]
Re	Reynolds number	[-]
s	total transport per unit of width	$[L^2T^{-1}]$
s_b	bed-load transport	$[L^2T^{-1}]$
s_s	suspended-load transport	$[L^2T^{-1}]$
t	time	[T]
Δt	time step	[T]
T_a	adaptation time	[T]
u	flow velocity	$[LT^{-1}]$
u_*	bed shear velocity	$[LT^{-1}]$
W_s	fall velocity	$[LT^{-1}]$
x	ordinate in flow direction	[L]

Δx	space step	[L]
y_1	initial depth (hydraulic jump)	[L]
y_2	sequent depth horizontal bottom	[L]
y_t	sequent depth sloping bottom	[L]
z	vertical ordinate	[L]
	bed level (general)	[L]
z_b	bed level	[L]
z_w	water level	[L]
α	porosity factor	[-]
Δ	relative density	[-]
ε_s	sediment-diffusion coefficient	[-]
ζ	angle of river bed	[-]
θ	weighting coefficient	[-]
κ	constant of van Karman	[-]
ν	kinematic viscosity coefficient	$[L^2T^{-1}]$
ξ_b	coefficient of curve resistance	[-]
ρ	density of water	$[ML^{-3}]$
ρ_s	density of sediment	$[ML^{-3}]$
ρ_m	density of sediment/water mixture	$[ML^{-3}]$
τ	bed shear stress	$[ML^{-1}T^{-2}]$
ϕ	averaged sediment concentration	[-]
φ	dimensionless celerity (c/u)	[-]
ψ	dimensionless transport parameter	[-]

Appendix 1

Basic derivations

The procedure of the derivation of the basic equations is described in section 3.2. Three equations are derived to describe the mountain river flow and its morphology. First the equation of motion is treated, next the continuity equations.

A *control volume* is defined which is one unit of width in the horizontal direction normal to the flow, and the position x is at the upstream side of the element. The volume is of finite height *a*. The dimension in the *x*-direction, *dx*, will be taken to zero.

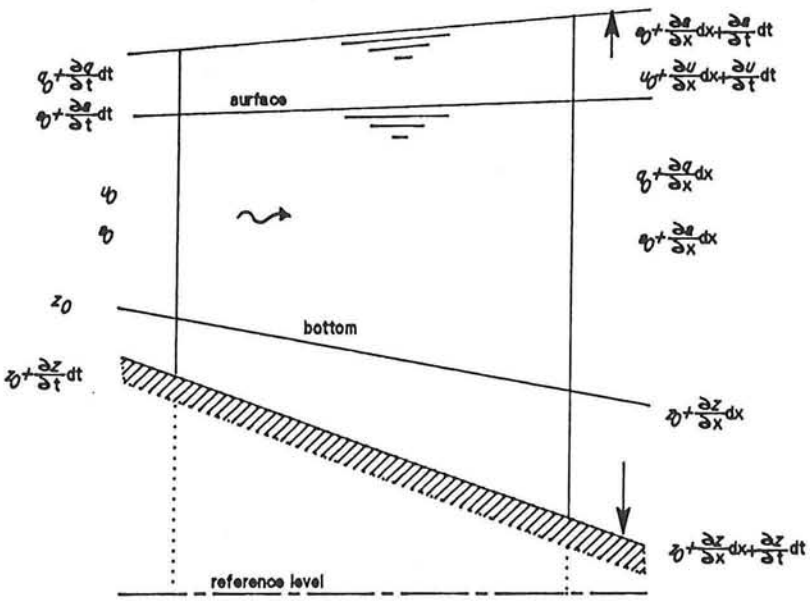

fig. 1 control volume and variables

1. Equation of motion

Conservation of momentum states:

The net rate of momentum entering the element + the sum of the forces acting on the element = the rate of accumulation of momentum.

* Rate of momentum

The rate of flow of momentum in a fluid is the product of the flux and the velocity. Hence

time=t

Momentum flux entering: $\rho_m u^2 a$

Momentum flux leaving : $\rho_m u^2 a + \frac{\partial \rho_m u^2 a}{\partial x} dx$

yields net momentum flux entering: $- \frac{\partial \rho_m u^2 a}{\partial x} dx$

time=t+dt

Momentum flux entering: $\rho_m u^2 a + \frac{\partial \rho_m u^2 a}{\partial t} dt$

Momentum flux leaving : $\rho_m u^2 a + \frac{\partial \rho_m u^2 a}{\partial x} dx + + \frac{\partial}{\partial t} \left(\frac{\partial \rho_m u^2 a}{\partial x} \right) dxdt + \frac{\partial \rho_m u^2 a}{\partial t} dt$

Net momentum entering: $- \frac{\partial \rho_m u^2 a}{\partial x} dx - \frac{\partial}{\partial t} \left(\frac{\partial \rho_m u^2 a}{\partial x} \right) dxdt$

Averaging the net momentum flux over the time interval dt yields

$$- \frac{\partial \rho_m u^2 a}{\partial x} dx - \frac{1}{2} \frac{\partial}{\partial t} \left(\frac{\partial \rho_m u^2 a}{\partial x} \right) dxdt \qquad \text{(I)}$$

The accumulation of the momentum in the control volume during the time interval dt is

$$\frac{\partial \rho_m ua}{\partial t} dx + \frac{1}{2} \frac{\partial}{\partial t} \left(\frac{\partial \rho_m ua}{\partial x} \right) dx^2 \qquad \text{(II)}$$

Three types of forces are considered: gravity, pressure and frictional resistance. All of these must be resolved in the *x*-direction.

*** Force due to gravity** (weight component along the channel)

time=t - Net weight of water/sediment control volume

$$G_t = \frac{1}{2} g \sin(\zeta) dx \left[2\rho_m a + \frac{\partial \rho_m a}{\partial x} dx \right] -$$

$$- g \sin(\zeta) dx \left[\rho_m a + \frac{1}{2} \frac{\partial \rho_m a}{\partial x} dx \right]$$

time=t+dt - Net weight of control volume

$$G_{t+dt} = g \sin(\zeta) dx \left[\rho_m a + \frac{1}{2} \frac{\partial \rho_m a}{\partial x} dx + \frac{1}{2} \frac{\partial}{\partial t} \left(\frac{\partial \rho_m a}{\partial x} \right) dxdt + \frac{\partial \rho_m a}{\partial t} dt \right]$$

Averaging the net weight of the control volume over the time interval *dt* gives

$$\overline{G} = g \sin(\zeta) dx \left[\rho_m a + \frac{1}{2} \frac{\partial \rho_m a}{\partial x} dx + \frac{1}{4} \frac{\partial}{\partial t} \left(\frac{\partial \rho_m a}{\partial x} \right) dxdt + \right.$$

$$\left. + \frac{1}{2} \frac{\partial \rho_m a}{\partial t} dt \right] \qquad \text{(III)}$$

*** Force due to pressure differences**

The pressure at a depth *z* gives:

$$p(z) = -\rho_m g \cos(\zeta) (z_w - z)$$

The pressure force on a vertical section of unit width in water of depth a is $F_p = \int_{z_b}^{z_w} p\,dz$

in which z_w is the water level and z_b is the bed level.

time=t Net pressure force on the control volume is

$$F_{Pt} = -\int_{z_b}^{z_w} \frac{\partial p}{\partial x}\,dx\,dz$$

time=t+dt Net pressure force on the control volume is

$$F_{Pt+dt} = -\int_{z_b}^{z_w} \left[\frac{\partial p}{\partial x}\,dx + \frac{\partial}{\partial t}\left(\frac{\partial p}{\partial x}\right) dx\,dt \right] dz$$

Averaging the net pressure force over the time interval dt yields

$$\overline{F_p} = -\int_{z_b}^{z_w} \left[\frac{\partial p}{\partial x}\,dx + \frac{1}{2}\,\frac{\partial}{\partial t}\left(\frac{\partial p}{\partial x}\right) dx\,dt \right] dz$$

or

$$\overline{F_p} = -\frac{1}{2}\,g\cos(\zeta)\,a^2\,\frac{\partial \rho_m}{\partial x}\,dx - g\cos(\zeta)\,\rho_m a\,\frac{\partial z_w}{\partial x}\,dx + - \int_{z_b}^{z_w} \left[\frac{1}{2}\,\frac{\partial}{\partial t}\left(\frac{\partial p}{\partial x}\right) dx\,dt \right] dz \qquad \text{(IV)}$$

* Force due to bottom friction

The frictional resistance is manifested by means of a shear stress along the bottom of a channel. One of the empirical equations for open channel resistance (viz. the Chézy

equation) is used to express the friction resistance.

time=t The shear stress on the control volume is

$$\tau_t = \frac{g\cos(\zeta)}{2C^2} dx\left[2\rho_m u^2 + \frac{\partial \rho_m u^2}{\partial x} dx\right]$$

time=t+dt The shear stress on the control volume is

$$\tau_{t+dt} = \frac{g\cos(\zeta)}{2C^2} dx\,[\,2\rho_m u^2 + 2\frac{\partial \rho_m u^2}{\partial t} dt + \frac{\partial \rho_m u^2}{\partial x} dx +$$

$$+ \frac{\partial}{\partial t}\left(\frac{\partial \rho_m u^2}{\partial x}\right) dxdt\,]$$

Averaging the shearstress over the time interval dt gives

$$\bar{\tau} = \frac{g\cos(\zeta)}{4C^2} dx\,[\,4\rho_m u^2 + 2\frac{\partial \rho_m u^2}{\partial t} dt + 2\frac{\partial \rho_m u^2}{\partial x} dx + \qquad \text{(V)}$$

$$+ \frac{\partial}{\partial t}\left(\frac{\partial \rho_m u^2}{\partial x}\right) dxdt\,]$$

* Resulting momentum equation

Combining these averaged elements into a single equation for conservation of momentum (I + III + IV + V - II = 0) considering the following:

- Take dx and dt to zero.
- Divide by $\rho_m a dx$.
- $\sin(\zeta) = i_b \cos(\zeta)$

$$\frac{\partial u}{\partial t} + \frac{u}{a}\frac{\partial a}{\partial t} + 2u\frac{\partial u}{\partial x} + \frac{u^2}{a}\frac{\partial a}{\partial x} +$$

$$+ \frac{u}{\rho_m}\frac{\partial \rho_m}{\partial t} + \left(\frac{u}{\rho_m} + \frac{1}{2}\frac{ga}{\rho_m}\cos(\zeta)\right)\frac{\partial \rho_m}{\partial x} + \qquad \text{(A1)}$$

$$+ g\cos(\zeta)\left(\frac{\partial z_w}{\partial x} - i_b\right) + \frac{gu^2}{C^2 a}\cos(\zeta) = 0$$

2. Continuity equation for mass

Conservation of mass for the control volume states:

The net rate of mass flow into the volume = rate of change of storage in the volume.

* Mass storage

time=t Mass of the control volume

$$\frac{1}{2}dx\left[2\rho_m a + \frac{\partial \rho_m a}{\partial x}dx\right] = \rho_m a dx + \frac{1}{2}\frac{\partial \rho_m a}{\partial x}dx^2$$

time=t+dt Mass of the control volume

$$\rho_m a dx + \frac{\partial \rho_m a}{\partial t}dxdt + \frac{1}{2}\frac{\partial}{\partial t}\left(\frac{\partial \rho_m a}{\partial x}\right)dx^2 dt + \frac{1}{2}\frac{\partial \rho_m a}{\partial x}dx^2$$

The change of mass over time interval dt then becomes

$$\frac{\partial \rho_m a}{\partial t}dxdt + \frac{1}{2}\frac{\partial}{\partial t}\left(\frac{\partial \rho_m a}{\partial x}\right)dx^2 dt \qquad \text{(I)}$$

* Mass inflow

time=t The flow of mass into the control volume over a time interval dt at the conditions of time t is

$$-\frac{\partial \rho_m u a}{\partial x}dxdt$$

time=t+dt The mass inflow over interval dt at the conditions of time $t+dt$ is

$$-\frac{\partial \rho_m u a}{\partial x}dxdt - \frac{\partial}{\partial t}\left(\frac{\partial \rho_m u a}{\partial x}\right)dxdt^2$$

Averaging the mass inflow for the conditions of time t and $t+dt$ gives

$$- \frac{\partial \rho_m ua}{\partial x} dxdt - \frac{1}{2} \frac{\partial}{\partial t}\left(\frac{\partial \rho_m ua}{\partial x} \right) dxdt^2 \qquad \text{(II)}$$

*** Mass Balance**

The continuity equation or mass balance thus is (if terms I=II and the dimensions dx and dt are taken to zero)

$$\frac{\partial a}{\partial t} + \frac{a}{\rho_m} \frac{\partial \rho_m}{\partial t} + a \frac{\partial u}{\partial x} + u \frac{\partial a}{\partial x} + \frac{ua}{\rho_m} \frac{\partial \rho_m}{\partial x} = 0 \qquad \text{(A2)}$$

3. Continuity equation for sediment volume

Conservation of the volume of sediment in the control volume states:

> The net transport of sediment into the volume = the net variation of storage of sediment in the volume.

*** Rate of sediment transport**

The rate of sediment transport is the product of the concentration, the depth and the flow velocity

time=t Net transport of sediment into the volume over an interval dt for the conditions at time t is

$$- \frac{\partial \phi au}{\partial x} dxdt$$

time=t+dt Net transport into volume over dt for the conditions at time $t+dt$ is

$$- \frac{\partial \phi au}{\partial x} dxdt - \frac{\partial}{\partial t}\left(\frac{\partial \phi au}{\partial x} \right) dxdt^2$$

Averaging this transport for time=t and $t+dt$ gives:

$$- \frac{\partial \phi a u}{\partial x} dxdt - \frac{1}{2} \frac{\partial}{\partial t}\left(\frac{\partial \phi a u}{\partial x}\right) dxdt^2 \qquad \text{(I)}$$

* Sediment storage

Variations of sediment storage in the volume are caused by variations of the concentration and the change of the amount of bed material stored in the bottom with a porosity α.

time=t The volume of sediment is

$$\alpha z dx + \frac{1}{2} \alpha \frac{\partial z}{\partial x} dxdt + \phi a dx + \frac{1}{2} \frac{\partial \phi a}{\partial x} dx^2$$

time=t+dt The volume of sediment is

$$\alpha z dx + \alpha \frac{\partial z}{\partial t} dxdt + \frac{1}{2} \alpha \frac{\partial z}{\partial x} dx^2 + \frac{1}{2} \alpha \frac{\partial}{\partial t}\left(\frac{\partial z}{\partial x}\right) dx^2 dt +$$
$$+ \phi a dx + \frac{\partial \phi a}{\partial t} dxdt + \frac{1}{2} \frac{\partial}{\partial t}\left(\frac{\partial \phi a}{\partial x}\right) dx^2 dt + \frac{1}{2} \frac{\partial \phi a}{\partial x} dx^2$$

The net variation of sediment storage over time interval dt is

$$\alpha \frac{\partial z}{\partial t} dxdt + \frac{1}{2} \alpha \frac{\partial}{\partial t}\left(\frac{\partial z}{\partial x}\right) dx^2 dt + \frac{\partial \phi a}{\partial t} dxdt +$$
$$+ \frac{1}{2} \frac{\partial}{\partial t}\left(\frac{\partial \phi a}{\partial x}\right) dx^2 dt \qquad \text{(II)}$$

* Sediment balance

The net transport and net variation of sediment storage (I=II) gives the continuity equation for sediment volume or sediment balance (after taking dx and dt to zero):

$$\alpha \frac{\partial z}{\partial t} + \frac{\partial \phi a}{\partial t} + \frac{\partial \phi a u}{\partial x} = 0 \qquad \text{(A3)}$$

**** Relation of ϕ and ρ_m

To level the number of equations and variables (a, u, z, ϕ) one more equation is required. That is the relation of the concentration and specific mass (density) of the water/sediment mixture. It can be described in different ways but here it is supported by a sediment transport formula which relates the transport to the flow velocity and the depth.

$$\rho_m = (1-\phi)\rho + \phi\rho_s \qquad \text{(A4)}$$

in which ρ = density of water

ρ_s = density of sediment particles

If the concentration can be described by a sediment transport formula we find

$$\phi = \alpha \frac{s}{au}$$

in which $s = f(u,a)$ = the sediment transport formula per unit of width

α = the porosity of the sediment in the bed

Then

$$\rho_m = \rho + \frac{\alpha s}{au}(\rho_s - \rho) = \rho\left(1 + \frac{\alpha \Delta s}{au}\right) \qquad \text{(A5)}$$

in which $\Delta = \frac{\rho_s - \rho}{\rho}$

4. Final set of basic equations

The set of equations derived can be simplified by eliminating terms from the momentum equation which yields:

eq. (A1) - $(u/a)\cdot$ eq. (A2) gives the following

Equation of motion (momentum balance)

$$\frac{\partial u}{\partial t} + u\frac{\partial u}{\partial x} + g\cos(\zeta)\left(\frac{\partial z_w}{\partial x} - i_b\right) + \frac{1}{2}g\cos(\zeta)\frac{a}{\rho_m}\frac{\partial \rho_m}{\partial x} + \frac{gu^2}{C^2 a}\cos(\zeta) = 0 \qquad \text{(A6)}$$

Equation of continuity of mass (mass balance)

$$\frac{\partial a}{\partial t} + a\frac{\partial u}{\partial x} + u\frac{\partial a}{\partial x} + \frac{a}{\rho_m}\left(\frac{\partial \rho_m}{\partial t} + u\frac{\partial \rho_m}{\partial x}\right) = 0 \qquad \text{(A7)}$$

Equation of continuity of sediment volume (Sediment balance)

$$\alpha\frac{\partial z}{\partial t} + \frac{\partial \phi a}{\partial t} + \frac{\partial \phi a u}{\partial x} = 0 \qquad \text{(A8)}$$

Concentration-density relation

$$\rho_m = (1-\phi)\rho + \phi\rho_s \qquad \text{(A9)}$$

$$\rho_m = \rho\left(1+\frac{\alpha\Delta s}{au}\right) \quad with \quad s = f(u,a) \qquad \text{(A10)}$$

In the following these equations are rewritten for the first approach of flow with high sediment transport rates.

5. Basic equations for flow with high sediment concentrations: first approach

The general basic equations for the mountain river flow (section 3.2) can be rewritten if the concentration rate of the flow is due to high sediment transport, without including the adaptation of the suspended load to the flow situation. For the derivation of the new basic equations the concentration of sediment in the flow is predicted with a sediment transport formula which relates the transport to the local hydraulic conditions.

In general the transport formulas are a function of the flow velocity (not the depth). Hence,

$$\frac{\partial s}{\partial x} = f_u \frac{\partial u}{\partial x} \quad \text{and} \quad \frac{\partial s}{\partial t} = f_u \frac{\partial u}{\partial t}$$

The equations are rewritten as follows:

$$\rho_m = \rho + \frac{\alpha \rho \Delta s}{ua}$$

$$\frac{\partial \rho_m}{\partial x} = \frac{\alpha \rho \Delta}{ua}\left[\frac{\partial s}{\partial x} - \frac{s_b}{u} \frac{\partial u}{\partial x} \right]$$

$$\frac{\partial \rho_m}{\partial t} = \frac{\alpha \rho \Delta}{ua}\left[\frac{\partial s}{\partial t} - \frac{s_b}{u} \frac{\partial u}{\partial t} \right]$$

$$\phi = \alpha \frac{s}{ua}$$

$$\frac{\partial \phi a}{\partial t} = \alpha \frac{\partial (s/u)}{\partial t} = \frac{\alpha}{u} \frac{\partial s}{\partial t} - \frac{\alpha s}{u^2} \frac{\partial u}{\partial t}$$

$$\frac{\partial \phi a u}{\partial x} = \alpha \frac{\partial s}{\partial x}$$

Substitution of these components in the general basic equations gives

$$\frac{\partial u}{\partial t} + \left[u + \frac{\alpha \Delta g a (u f_u - s)}{2u(\alpha \Delta s + ua)}\right] \frac{\partial u}{\partial x} + g\left[1 + \frac{\alpha \Delta (a f_a - s)}{2(\alpha \Delta s + ua)}\right] \frac{\partial a}{\partial x} + g \frac{\partial z}{\partial x} + \frac{g u^2}{C^2 a} = 0 \qquad \text{(A11)}$$

$$\frac{\partial u}{\partial t} + u\left[1 + \frac{1}{2} Fr^{-2} V_c \cos(\zeta) \left(\frac{u}{s} f_u - 1\right)\right] \frac{\partial u}{\partial x} + g\cos(\zeta) \frac{\partial z_b}{\partial x} + g\cos(\zeta)\left[1 - \frac{1}{2} V_c\right] \frac{\partial a}{\partial x} + \frac{g u^2}{C^2 a} \cos(\zeta) - g\sin(\zeta) = 0 \qquad \text{(A12)}$$

$$\left[\frac{\alpha\Delta}{au}(uf_u - s)\right]\frac{\partial u}{\partial t} + u\left[1+\alpha\Delta\frac{f_u}{a}\right]\frac{\partial u}{\partial x} + \frac{u}{a}\frac{\partial a}{\partial t} + \frac{u^2}{a}\frac{\partial a}{\partial x} = 0 \qquad \text{(A13)}$$

$$\frac{\partial z}{\partial t} + \frac{a}{u}\left[\frac{uf_u - s}{au}\right]\frac{\partial u}{\partial t} + f_u\frac{\partial u}{\partial x} = 0 \qquad \text{(A14)}$$

In which $f_u = \frac{\partial s}{\partial u}$ and $s = f(u)$

$$Fr = \frac{u}{\sqrt{ga}} \quad \text{and} \quad V_c = \frac{\alpha\Delta s}{ua + \alpha\Delta s}$$

6. Basic equations for flow with high sediment concentrations: second approach

The concentration of sediment is determined by the sediment transport rate. The following assumptions apply:

- The influence of sediment on the water movement is supposed to be dependent on the concentration of suspended load only. This assumption holds for the fact that bed load only occurs in a small layer near the bottom, and therefore does not appreciably contribute to the concentration gradients averaged over the vertical.
- The adaptation of the suspended load concentration to the local hydraulic conditions is described with an additional basic equation for the depth integrated suspended load concentration (Galappatti, 1983).

The basic equations (6), (7) and (8) are rewritten after

substituting the relation (derived from eq. (9))

$$\rho_m = \rho + \phi(\rho_s - \rho)$$

and considering $\frac{\partial \rho}{\partial x} = \frac{\partial \rho}{\partial t} = \frac{\partial \rho_s}{\partial x} = \frac{\partial \rho_s}{\partial t} = 0$

For the redistribution process of concentration of suspended sediment in case of net erosion and sedimentation an additional equation is introduced. This is equation for the depth-integrated suspended-load concentration has been developed by Galappatti (1983) (Ribberink, 1986). For large velocities the validity of the equation increases for larger deviations of the concentration profile from the equilibrium profile (Wang 1990). This first order form of the equation for the depth averaged concentration Cs can be derived by assuming an asymptotic solution for the 2-dimensional convection-diffusion equation (in the vertical plane).

The boundary condition applied is that the vertical concentration gradient at $z=z_b$ is equal to the gradient of the equilibrium concentration (Ribberink, 1986). This implies that the pick-up rate of the sediment at the bed ($=-\varepsilon_s \partial Cs/\partial z$) is determined directly by the instantaneous flow conditions. The deposition rate ($= W_s \cdot Cs$) then depends on the actual concentration near the bed.

This equation can be written as

$$T_a \frac{\partial Cs}{\partial t} + L_a \frac{\partial Cs}{\partial x} + Cs - Cse = 0$$

In which T_a represents the adaptation time and L_a is the adaptation length: $L_a \approx u \cdot T_a$

$T_a = \frac{\gamma_{21}+1}{\gamma_0} \frac{a}{W_s}$ for which the coefficient $(\gamma_{21}+1)/\gamma_0$ can be computed depending on the diffusion coefficient for sediment ε_s
If the expression for the diffusion coefficient is used deri-

ved by van Rijn (1987) then the following relation is found for the adaption time

$$L_a \approx uT_a$$

$$U = \frac{u_*}{u}$$

$$T_a \approx \frac{\tau a}{W_s}$$

$$x_\tau = \frac{W_s/u_*}{1+2(W_s/u_*)^2}$$

$$\tau = \exp[(4.287-22.453U)x_\tau^3 + (24.827U-6.412)x_\tau^2 + (3.2U-1.568)x_\tau]$$

Sediment transport and equilibrium concentration are computed using the van Rijn transport formulas for bedload and suspended load (van Rijn, 1984).

The following system of basic equations is derived:

$$\frac{\partial u}{\partial t} + u\frac{\partial u}{\partial x} + g\cos(\zeta)\frac{\partial a}{\partial x} + \frac{1}{2}R_1 g\cos(\zeta)\frac{\partial Cs}{\partial x} + g\cos(\zeta)\frac{\partial z_b}{\partial x} - g\sin(\zeta) + \frac{gu^2}{C^2 a}\cos(\zeta) = 0 \qquad \text{(A15)}$$

$$\frac{\partial a}{\partial t} + u\frac{\partial a}{\partial x} + a\frac{\partial u}{\partial x} + R_1\left(\frac{\partial Cs}{\partial t} + u\frac{\partial Cs}{\partial x}\right) = 0 \qquad \text{(A16)}$$

$$\alpha\frac{\partial z}{\partial t} + \alpha f_u\frac{\partial u}{\partial x} + \frac{R_1}{\Delta}\left(\frac{\partial Cs}{\partial t} + u\frac{\partial Cs}{\partial x}\right) = 0 \qquad \text{(A17)}$$

$$T_a \frac{\partial Cs}{\partial t} + L_a \frac{\partial Cs}{\partial x} + Cs - Cse = 0 \qquad \text{(A18)}$$

In which Cs = Concentration of suspended material

$R_1 = (a\Delta)/(1+\Delta Cs)$

$Cse = s_s/ua$ (s_s=suspended load rate from van Rijn)

= equilibrium concentration (capacity)

7. Characteristic celerities for basic equations for high concentrated flow

Celerities for flow with large concentration: first approach

The general matrix approach is used to determine the characteristic celerities of the system of basic equations. Therefore the basic equations (11), (12), (13) are rewritten

$$\frac{\partial u}{\partial t} + uR_A\frac{\partial u}{\partial x} + gR_B\frac{\partial a}{\partial x} + g\cos(\zeta)\frac{\partial z_b}{\partial x} - g\sin(\zeta) + \frac{gu^2}{C^2a}\cos(\zeta) = 0$$

$$R_C\frac{\partial u}{\partial t} + uR_D\frac{\partial u}{\partial x} + \frac{u}{a}\frac{\partial a}{\partial t} + \frac{u^2}{a}\frac{\partial a}{\partial x} = 0$$

$$\frac{\partial z}{\partial t} + \frac{a}{u}R_G\frac{\partial u}{\partial t} + f_u\frac{\partial u}{\partial x} = 0$$

In which

$$R_A = 1 + \frac{1}{2} Fr^{-2} V_c \left(\frac{u}{s} f_u - 1\right) \cos(\zeta)$$

$$R_B = \cos(\zeta)\left[1 - \frac{V_c}{2}\right]$$

$$R_C = \frac{\alpha \Delta}{ua} (u f_u - s)$$

$$R_D = 1 + \alpha \Delta \frac{f_u}{a}$$

$$(R_E = 1)$$

$$(R_F = 1)$$

$$R_G = \frac{u f_u - s}{ua}$$

$$V_c = \frac{\alpha \Delta s}{ua + \alpha \Delta s}$$

To a function $F(x, t)$ applies

$$F(x+\Delta x, t+\Delta t) \approx F(x, t) + \Delta x \frac{\partial F(x, t)}{\partial x} + \Delta t \frac{\partial F(x, t)}{\partial t}$$

assuming $c = \frac{\Delta x}{\Delta t}$ and $F(x+\Delta x, t+\Delta t) - F(x, t) = \Delta F$

gives

$$\frac{\Delta F}{\Delta t} = \left(\frac{\partial F}{\partial t} + c \frac{\partial F}{\partial x}\right) \quad \text{or} \quad \left(\frac{dF}{dt}\right)_c = \frac{\partial F}{\partial t} + c \frac{\partial F}{\partial x}$$

In which $(dF/dt)_c$ is the derative of the function F in the direction $dx/dt = c$. This relation can be formed for the three variables u, a, z. Together with the basic equations we have six equations. The six partial deratives are supposed the unknowns in the equations. The coefficient matrix of the system can now be formed. Determinant of coefficients is equal

to zero yields (for $s=f(u)$):

$$c^3 + \left[-uR_A + \frac{ga}{u}\cos(\zeta)R_G - u + \frac{ga}{u}R_BR_C\right]c^2 + \tag{A19}$$
$$+ \left[u^2R_A - ga(R_DR_B + \cos(\zeta)R_G) - g\cos(\zeta)f_u\right]c + guf_u\cos(\zeta) = 0$$

The relative celerities ($\varphi=c/u$) now can be represented as

$$\varphi^3 + \left[-R_A - Fr^{-2}R_G\cos(\zeta) - 1 + Fr^{-2}R_BR_C\right]\varphi^2 +$$
$$+ \left[R_A - \frac{gf_u\cos(\zeta)}{u^2} - Fr^{-2}R_G\cos(\zeta) - Fr^{-2}R_DR_B\right]\varphi + Fr^{-2}\cos(\zeta)\frac{f_u}{a} = 0$$

(A20)

The three roots of the system can be found using the goniometrical solution method. If

$$A_2 = \left[-R_A + Fr^{-2}R_G\cos(\zeta) - 1 + Fr^{-2}R_BR_C\right]$$

$$A_1 = \left[-\frac{gf_u\cos(\zeta)}{u^2} - Fr^{-2}R_G\cos(\zeta) + R_A - Fr^{-2}R_DR_B\right]$$

$$A_0 = Fr^{-2}\cos(\zeta)\frac{f_u}{a}$$

Then $q = \frac{A_2^2}{3} - A_1$; $r = \frac{A_1A_2}{3} - A_0 - \frac{2}{27}A_2^3$

if ($27r^2 < 4q^3$) then $\cos(\xi) = \left(\frac{3}{q}\right)^{\frac{3}{2}}\frac{r}{2}$ and

$$\varphi_1 = \frac{2}{\sqrt{3}}\sqrt{q}\,\cos\left(\frac{\xi}{3}\right) + \frac{A_2}{3}$$

$$\varphi_2 = -\frac{2}{\sqrt{3}}\sqrt{q}\cos\left(\frac{\pi-\xi}{3}\right) + \frac{A_2}{3}$$

$$\varphi_3 = -\frac{2}{\sqrt{3}}\sqrt{q}\cos\left(\frac{\pi+\xi}{3}\right) + \frac{A_2}{3}$$

The roots of the system have been investigated for two sediment transport formulas: The Meyer Peter Müller formula (Meyer-Peter & Müller 1984) and the Engelund Hansen formula (Engelund & Hansen 1967).

Meyer Peter Müller formula (bedload)

$$s_b = 13.3\left[\frac{u^2}{\sqrt{CC_{90}^3}\Delta d_m} - 0.047\right]^{\frac{3}{2}} d_m^{\frac{3}{2}}\sqrt{g\Delta}$$

$$C_{90} = 18\log\left(\frac{12a}{D_{90}}\right)$$

$$f_u = \frac{39.3u}{\sqrt{CC_{90}^3}\Delta d_m}\sqrt{\frac{u^2}{\sqrt{CC_{90}^3}\Delta d_m} - 0.047}\; d_m^{\frac{3}{2}}\sqrt{g\Delta}$$

Engelund Hansen formula (bedload and suspended load)

$$s_t = \frac{0.084\,u^5}{C^3\Delta^2 d_m\sqrt{g}}$$

$$f_u = \frac{0.42\,u^4}{C^3\Delta^2 d_m\sqrt{g}}$$

Incorporating these formulas in the solution method gives the numerical values of the celerities. The celerities have been determined as a function of the flow velocity for a fixed water depth. The relative celerities are plotted in fig. 1 as a function of the Froude number for various values of $\psi = f_u/a$.

In fig. 2 the celerities are plotted as a function of the flow velocity for flow in the Kali Thermas Lama in Indonesia (see section 4.3). In fig. 3 the celerities are plotted for a flow over a horizontal bed. In these figures the celerities are also plotted, with dashed lines, for the basic equations for flow without the influence of the concentration (section 3.4).

Celerities for flow with large sediment concentrations: second approach

Equal to the celerities for the equations with high bed-load concentrations the matrix approach is used to determine the characteristic celerities of flow with high suspended load concentrations. The four basic equations (14), (15), (16) and (17) and the expressions for the derivatives of a, u, Cs, z in the characteristic direction $dx/dt = c$ can be again represented in a coefficient matrix.

Determinant of coefficients equal to zero yields The quartic equation that represents the four celerities of the system (for $L_a = uT_a$):

$$c^4 - 3uc^3 + \left[3u^2 - gf_u\cos(\zeta) - ga\cos(\zeta)\right]c^2 + \\ + \left[2guf_u\cos(\zeta) + gau\cos(\zeta) - u^3\right]c - gu^2f_u\cos(\zeta) = 0 \qquad \text{(A21)}$$

which can be rewritten as

$$(c-u)\left(c^3 - 2uc^2 + \left[u^2 - ga\cos(\zeta) - gf_u\cos(\zeta)\right]c + guf_u\cos(\zeta)\right) = 0$$

The first celerity is equal to the flow velocity. The remaining cubic equation can be solved analytically using a goniometric solution method. The equation is equal to that for the celerities of the equations for flow with low sediment concentrations (see section 3.4.2).

For several cases the celerities are determined and evaluated. Three cases are presented here. The conditions are

based on data from the Thermas Lama river in Indonesia, section 4.3.

Case 1 Subcritical flow

Data: $Fr = 0.1$ $\Delta = 1.91$

$d_{50} = 0.3$ mm $C = 50$ $m^{1/2}/s$

$u = 0.5$ m/s $a = 2.548$ m

The van Rijn transport formula gives:

$s_b = 6.791 \cdot 10^{-7}$ m^2/s

$s_s = 13.151 \cdot 10^{-7}$ m^2/s

$fu_b = 1.125 \cdot 10^{-6}$ m

$$c^4 - 1.5c^3 + 24.246c^2 + 12.37c - 2.7587 = 0$$

Solution:

$c_1 =$	5.5 m/s	(water)
$c_2 =$	-4.5 m/s	(water)
$c_3 =$	$2.23 \cdot 10^{-6}$ m/s	(bottom)
$c_4 =$	0.5 m/s	(concentration)

Case 2 Critical flow

Data: $Fr = 1$ $\Delta = 1.91$

$d_{50} = 0.3$ mm $C = 50$ $m^{1/2}/s$

$u = 3.14$ m/s $a = 1.00506$ m

The van Rijn transport formula gives:

$s_b = 9.47 \cdot 10^{-3}$ m^2/s

$s_s = 21.84 \cdot 10^{-3}$ m^2/s

$fu_b = 12.8 \cdot 10^{-3}$ m

$$c^4 - 9.42c^3 + 19.59c^2 + 0.805c - 1.2378 = 0$$

Solution:

$c_1 =$	6.29 m/s	(water)
$c_2 =$	-0.2454 m/s	(water)
$c_3 =$	0.24539 m/s	(bottom)
$c_4 =$	3.14 m/s	(concentration)

Case 3 Supercritical flow

Data: $Fr = 4$ $\Delta = 1.91$

$d_{50} = 0.3$ mm $C = 50$ m$^{\frac{1}{2}}$/s

$u = 10$ m/s $a = 0.637$ m

The van Rijn transport formula gives:

$s_b = 1.56577$ m^2/s

$s_s = 2.306116$ m^2/s

$fu_b = 0.65822$ m

$$c^4 - 30c^3 + 287.294c^2 + 808.367c - 645.7144 = 0$$

Solution:

$c_1 =$	12.7657 m/s	(water)
$c_2 =$	7.8766 m/s	(water)
$c_3 =$	-0.6423 m/s	(bottom)
$c_4 =$	10 m/s	

From these cases it follows that the differences in the celerities for the flow with and the flow without the influence of sediment concentration is negligible. The velocity of propagation of small disturbances is therefore equal for both cases. For the applications however it follows that the influence of the sediment concentration appears in the shape alterations of bed irregularities during time.

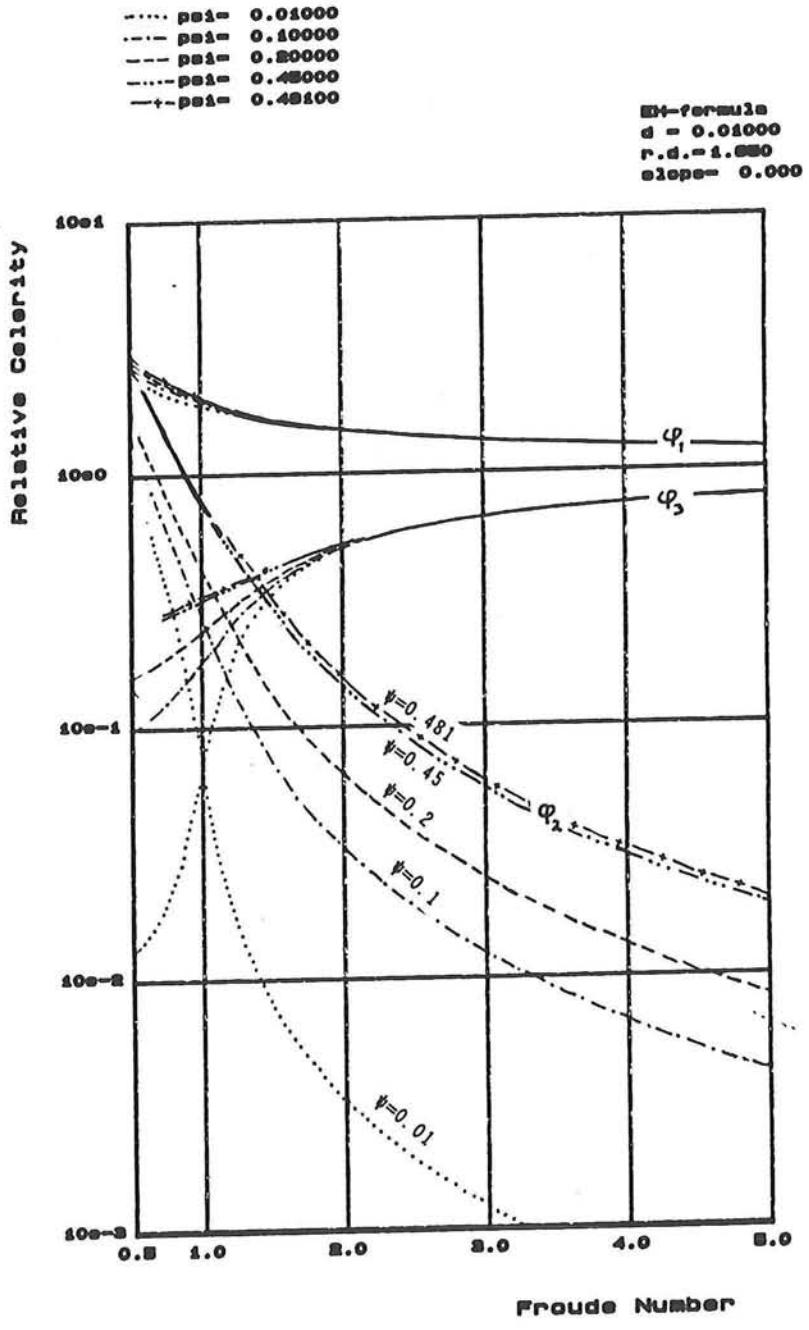

fig. 1 Relative celerities for various ψ-values

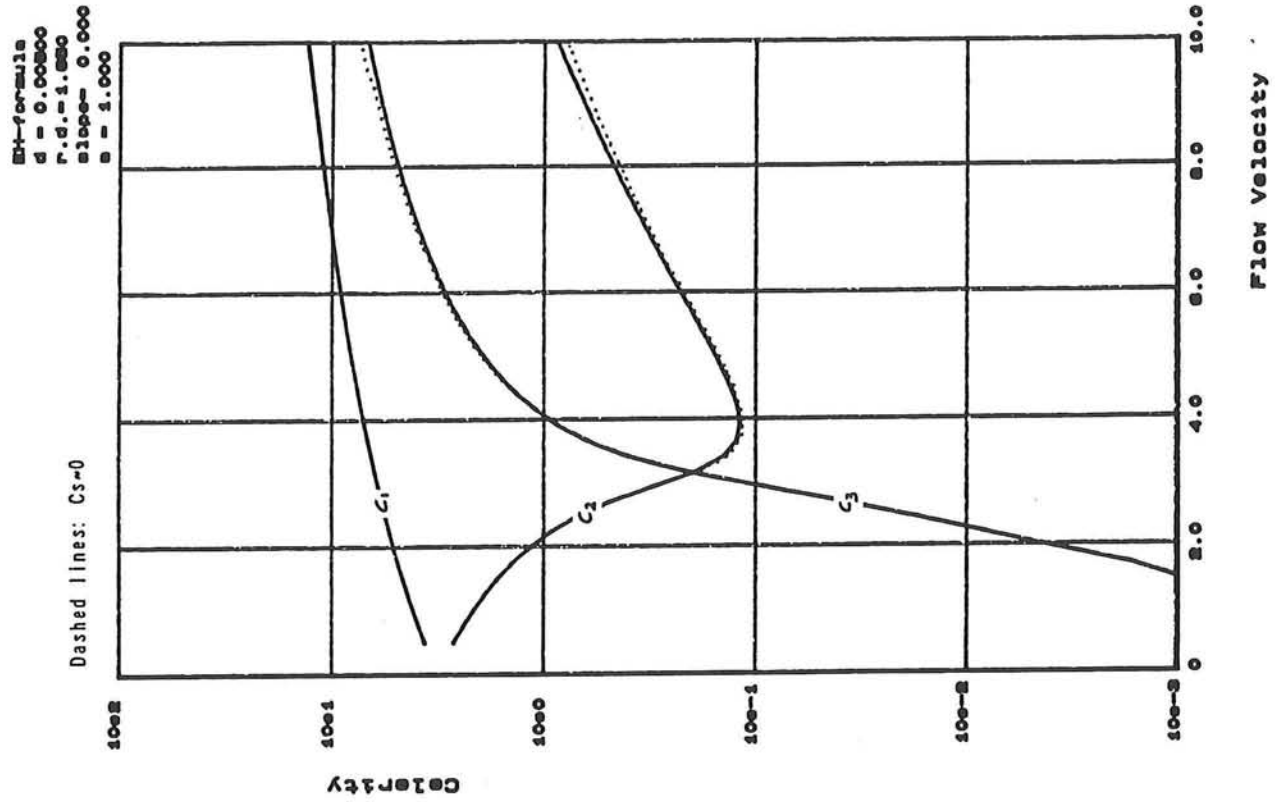

fig. 3 Celerities as a function of the flow velocity

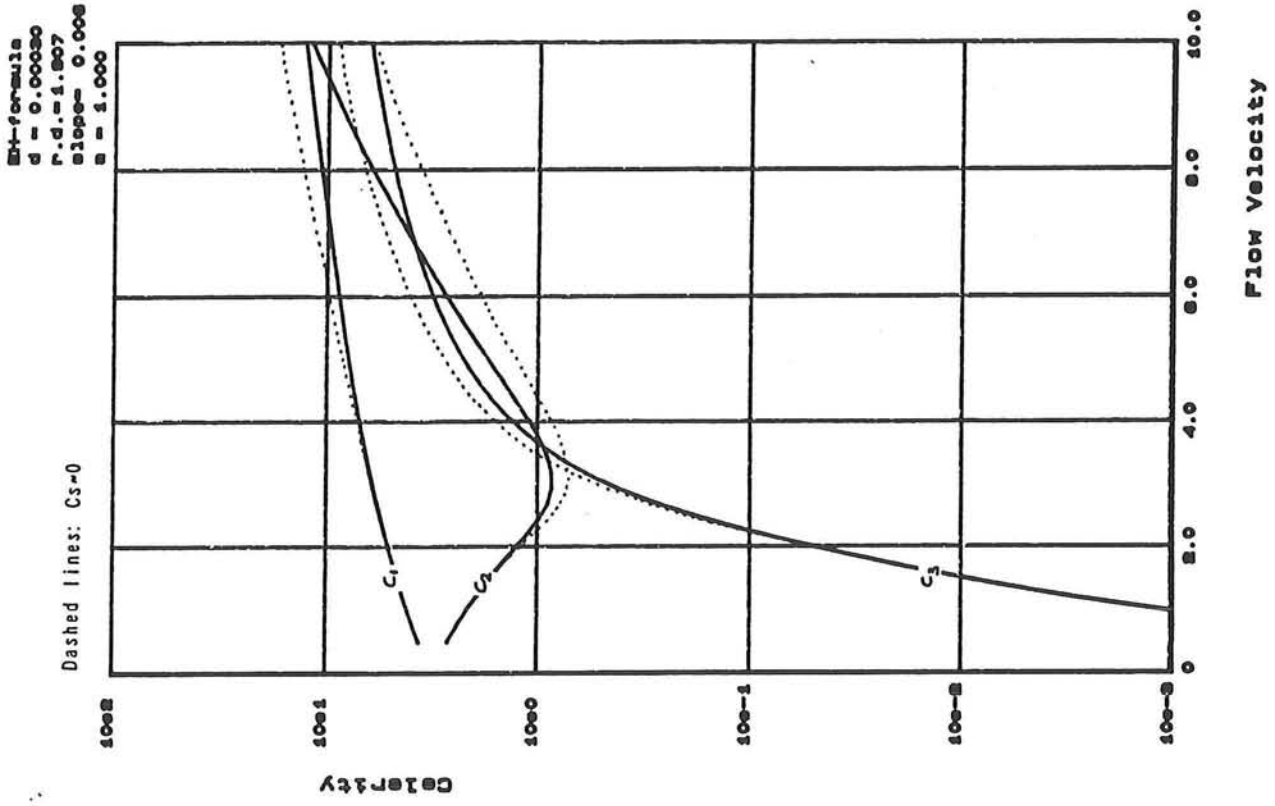

fig. 2 Celerities for Kali Thermas Lama conditions

Appendix 2

Model for steady non-uniform flow on a fixed bed

1. Introduction

The steady non-uniform flow is described in section 3.3. In addition to the description of the solution of the gradually varied flow equations in that section, the theory behind these subjects will be treated in this appendix. First the classification of flow is described in part 2. Then three numerical and two analytical methods are described to solve the equations. In part 4. the method of locating a hydraulic jump is described. Finally the computer program STUWK, which has been developed to apply the solution methods for steady non-uniform flow, is discussed.

2. Classification of flow profiles

It is necessary to distinguish different types of flow for ease of survey and for comprehensibility of the results from gradually varied flow computations. The conditions of the flow determine this classification. In section 3.3.2 the subdivision of the flow into three regions (*1, 2, 3*) and the subdivision of bed slopes into *H, M, C, S, A* is described. Here a representation of this classification of surface profiles is given in the following table.

Channel	Condition (Flow)	Type
Mild Slope	$a > a_n > a_c$ (subcr.)	*M1*
($a_n > a_c$)	$a_n > a > a_c$ (subcr.)	*M2*
	$a_n > a_c > a$ (supercr.)	*M3*

Steep Slope	$a>a_c>a_n$ (subcr.)	*S1*
($a_n<a_c$)	$a_c>a>a_n$ (supercr.)	*S2*
	$a_c>a_n>a$ (supercr.)	*S3*
Critical Slope	$a>a_n=a_c$ (subcr.)	*C1*
($a_n=a_c$)	$a<a_n=a_c$ (supercr.)	*C3*
Horizontal Bed	$a>a_c$ (subcr.)	*H2*
($a_n=\infty$)	$a<a_c$ (supercr.)	*H3*
Adverse Slope	$a>a_c$ (subcr.)	*A2*
($a_n<0$)	$a<a_c$ (supercr.)	*A3*

Examples of these flow types are shown in fig. 7, fig. 8 and fig. 9 (applications of the program STUWK).

3. Hydraulic jump computation

A hydraulic jump occurs when a supercritical stream meets a subcritical stream of sufficient depth. The supercritical stream jumps up to meet its alternate (downstream subcritical) depth. The empirical relations that are developed to describe the length of such a jump and its alternate depth are treated in section 3. 3. 5.

In this appendix a general method is described to determine the location of the hydraulic jump starting from the upstream supercritical surface profile and the downstream subcritical profile. First a classification of the jumps on a sloping floor is given.

Hydraulic jumps on a horizontal floor are of several distinctive types. According to Ven Te Chow (1959), these types can be conveniently classified dependent on the Froude Number

$$Fr_1 = q/\sqrt{ga_1^3}$$

of the incoming flow as follows:

$Fr_1 = 1.0$: No jump (Critical flow)
$Fr_1 = 1.0 - 1.7$: Undular jump (Energy dissipation practically zero)
$Fr_1 = 1.7 - 2.5$: Weak jump (Energy dissipation ~ 1.7%-18%)
$Fr_1 = 2.5 - 4.5$: Oscillating jump (Energy dissip. ~ 45%)
$Fr_1 = 4.5 - 9.0$: Steady jump (Energy dissipation ~ 45%-70%)
$Fr_1 > 9.0$: Strong jump (Energy dissipation ~ 85%)

This subdivision turns out to be visible in the size of the depth change: A small depth change gives a undular jump while a great depth change gives a stronger jump.

Classification of the hydraulic jumps is important for surveyability and distinction of various possible appearing jumps.

The location of the hydraulic jump can now be estimated using the upstream and downstream surface profiles, the sequent depths (eq. 3.3.20) belonging to the supercritical profile and the length of the jump (eq. 3.3.21). Theoretically speaking the jump occurs where the sequent depth curve (collective curve of depths y_t conjugate to the corresponding depths y_1 of the supercritical surface profile), intersects with the subcritical surface profile (downstream). This theoretical condition is generally used to locate the position of the jump on extensive longitudinal profiles.

For a closer estimation of the location of the jump, the length of the jump has to be considered also. The following will illustrate this procedure for locating the jump, represented in fig. 1.

Consider a sluice gate (point A) acting as an upstream control and the pool elevation (point B) acting as a downstream control, in a mild-slope channel.

depth at B = y_1

depth at B′ = Y_t
curve A′ B′ C = Curve of sequent depths
curve CDE = curve A′ B′ C displaced to the right by distance L_j

The algorithm for the location of the jump is as follows:

1- Starting from point A, compute the M3-profile ABC. Point C is the critical depth.

2- Calculate the sequent depth profile CB′ A′ in which every point B′ is sequent to a point B vertically below it on the curve ABC (conjugate values computed from eq.-(3.3.20).

3- Compute L_j with eq. (3.3.21) for each point on the curve CB′ A′ and shift this curve by horizontally displacing each point in the downstream direction by respective L_j values. The resulting curve is CDE.

4- Starting from point P, compute the M2-profile PDQ.

5- The intersection of the curve PDQ with CDE (point D) gives the downstream end of the jump. The toe of the jump, point B, is located by drawing a horizontal line from D to CB′ A′ at B′ and then a vertical line from B′ to cut the curve ABC at B.

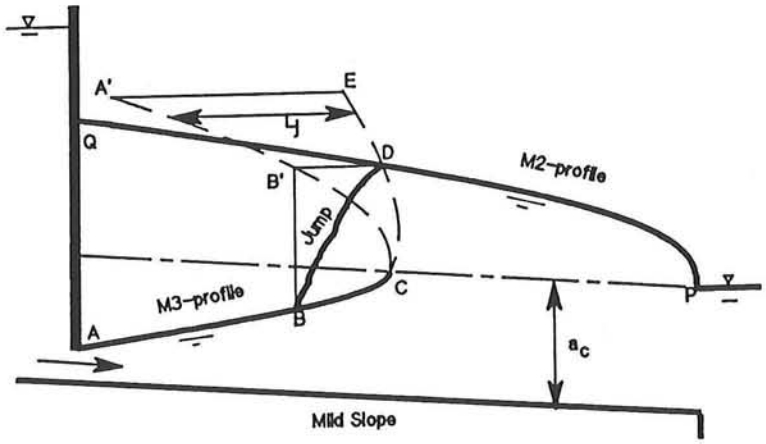

fig. 1 Locating the Jump

Note that this procedure gives direct determination of the end points of a jump and the method is general and can therefore be applied in a wide variety of jump situations.

This procedure for locating the jump has been generalized and adapted to be incorporated in a computer program. Therefore the supercritical and sequent depth curve are computed starting at the upstream boundary (The Runga Kutta Method is chosen because computation stepsizes in x-direction can be fixed in advance and can therefore be kept sufficiently small to increase the accuracy of the computed location of the intersection which represents the end of the jump). The subcritical curve is computed in upstream direction. The sequent depth curve is displaced over the distance L_j.

The intersection of the curves is found by computing the intersection of each line segment (from which the displaced sequent depth curve is made up) with the subcritical curve line segments until the desired point ($X=X_1$) has been found, see fig. 2.

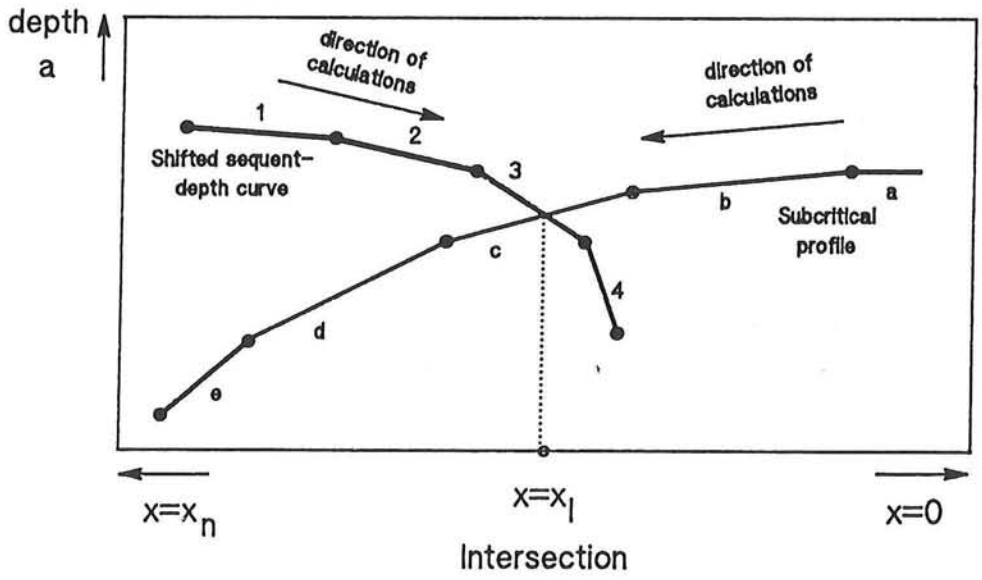

fig. 2 Intersection procedure for locating the end of the jump

The program reckons with four possible intersections so

that it can be applied in a wide variety of jump situations. The possible intersections as included in the model are shown in fig. 6.

4. Computer program STUWK

To compute the surface profiles and a hydraulic jump, the discussed computations and numerical methods are combined to one computer program, called STUWK. Before application of the program one has always to realize that these computations are only valid in wide prismatic channels with a constant discharge, a constant slope and a constant roughness. This program, therefore has a mainly instructive character to increase one's understanding in this field of study and to verify calculations made independently.

The structure of the computer program is briefly discussed, starting from the flow diagram.

Flow diagram

The sequence of the computations and the several possibilities of choosing a given computation method is clearly structured in the flow diagram in fig. 3 at the end of this appendix. Arrows indicate the direction of execution of the program.

The flow diagrams for the procedures that compute the surface profiles using the Heun Method (not described in this report) and the Runge Kutta Method are presented in fig. 4. In fig. 5 the flow diagram for the Simpson's Rule is presented. All methods start with calling the input data. Next the surface profiles are computed for a step size h.
A flow diagram for the hydraulic jump is showed in fig. 5.

The programming language that has been used to write the program is TURBO PASCAL.

Discussion of the program steps

After choosing a numerical method (see sections 3.3.3, 3.3.4) and inserting some data, the computations start automatically. The calculations proper start after the determination of the flow type or after the detection of the occurrence of a hydraulic jump.

The surface profile computations yield values of the distance x and the waterdepth a, which can be drawn on the screen for ease of survey.

An error determination is performed to every numerical surface profile computation. This error is estimated during execution, and practically corresponds with the difference between the numerical and the analytical solution of the final depth (a) or distance (x) (see also section 3.3.4).

When a hydraulic jump is detected, however, both upstream and downstream profiles are being computed and the location of the jump is being determined without an error estimation. The graphical results, drawn to the screen, include the sequent depth curve which can be useful for an evaluation if an expected jump cannot be computed.

Considerations on the program

1- Directions of curve computations

The supercritical profile is computed starting from the upstream boundary in downstream direction. The subcritical profile is computed starting at the downstream boundary x=0, proceeding in the upstream (negative) direction. In case of a hydraulic jump, the sequent depth curve and the displaced curve are deduced from the supercritical curve and their points are therefore also numbered increasing in the downstream direction.

2- Intersection procedure for hydraulic jumps

The intersection of the curves is found by computing the

intersection of every line segment, from which the shifted sequent depth curve is made up, with some subcritical curve line-segments, until the desired point has been found.

3- Negative x-values as a result

The upstream x values (distances) are negative with regard to x=0, the downstream boundary, because of the necessary compatibility with the used Runga Kutta Method algorithm. The positive x-direction is the downstream direction.

4- Graphical Output

Graphical output (results drawn on the screen) makes it possible to examine the flow profiles and the hydraulic jump.

Applications

Some results of the computations executed with STUWK are presented in fig. 7, fig. 8, fig. 9, fig. 10 and fig. 11. The surface profiles for distinctive flow types in the figures 7, 8 and 9 are computed for the bed slopes:

$i_b = 1 \cdot 10^{-4}$ (M-profiles)
$i_b = -1 \cdot 10^{-3}$ (A-profiles)
$i_b = 0$ (H-profiles)
$i_b = 5 \cdot 10^{-2}$ (S-profiles)

respectively, and a Chezy coefficient of C=50 $m^{\frac{1}{2}}/s$, a discharge q=2 m^2/s.

The vertical axis Y represents the elevation relative to the bedlevel at $X=0$. The horizontal axis X represents the location relative to the location of the downstream boundary.

The figures 10 and 11 represent computations of a hydraulic jump for a "steep slope" river section:

$i_b = 1 \cdot 10^{-2}$; C=50 $m^{\frac{1}{2}}/s$, q=0.07 m^2/s [fig. 10]
$i_b = 5 \cdot 10^{-2}$; C=50 $m^{\frac{1}{2}}/s$, q=2 m^2/s [fig. 11]

The locations of the jump as they are showed here, are in close agreement with measurements in flumes.

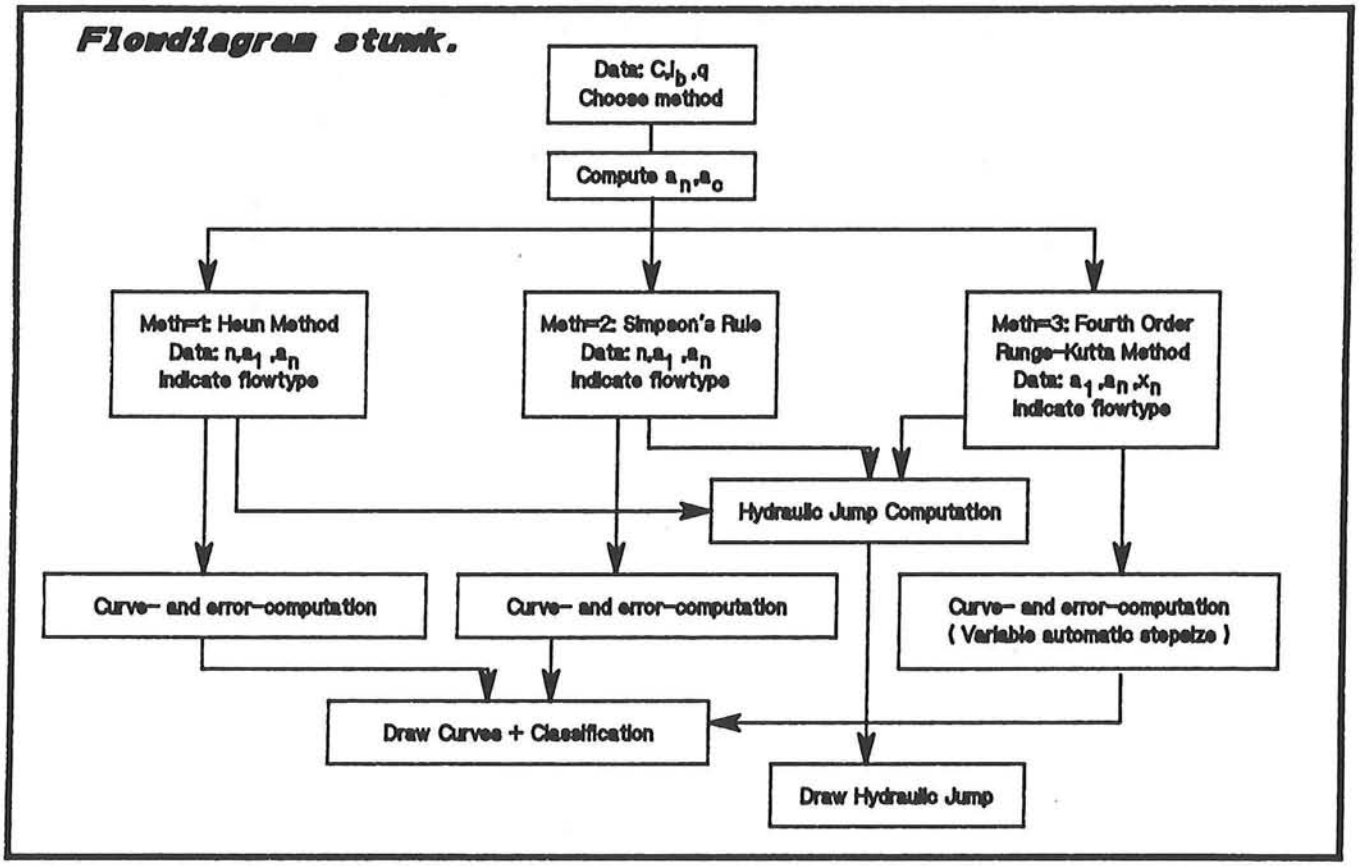
Flowdiagram stuwk.
Data: C,l_b,q
Choose method
Compute a_n,a_c
Meth=1: Heun Method
Data: n,a_1,a_n
Indicate flowtype
Meth=2: Simpson's Rule
Data: n,a_1,a_n
Indicate flowtype
Meth=3: Fourth Order
Runge-Kutta Method
Data: a_1,a_n,x_n
Indicate flowtype
Hydraulic Jump Computation
Curve- and error-computation
Curve- and error-computation
Curve- and error-computation
(Variable automatic stepsize)
Draw Curves + Classification
Draw Hydraulic Jump

fig. 3 STUWK

fig. 4 Heun/Runge-Kutta method

fig. 5 Simpson's Rule/hydraulic jump

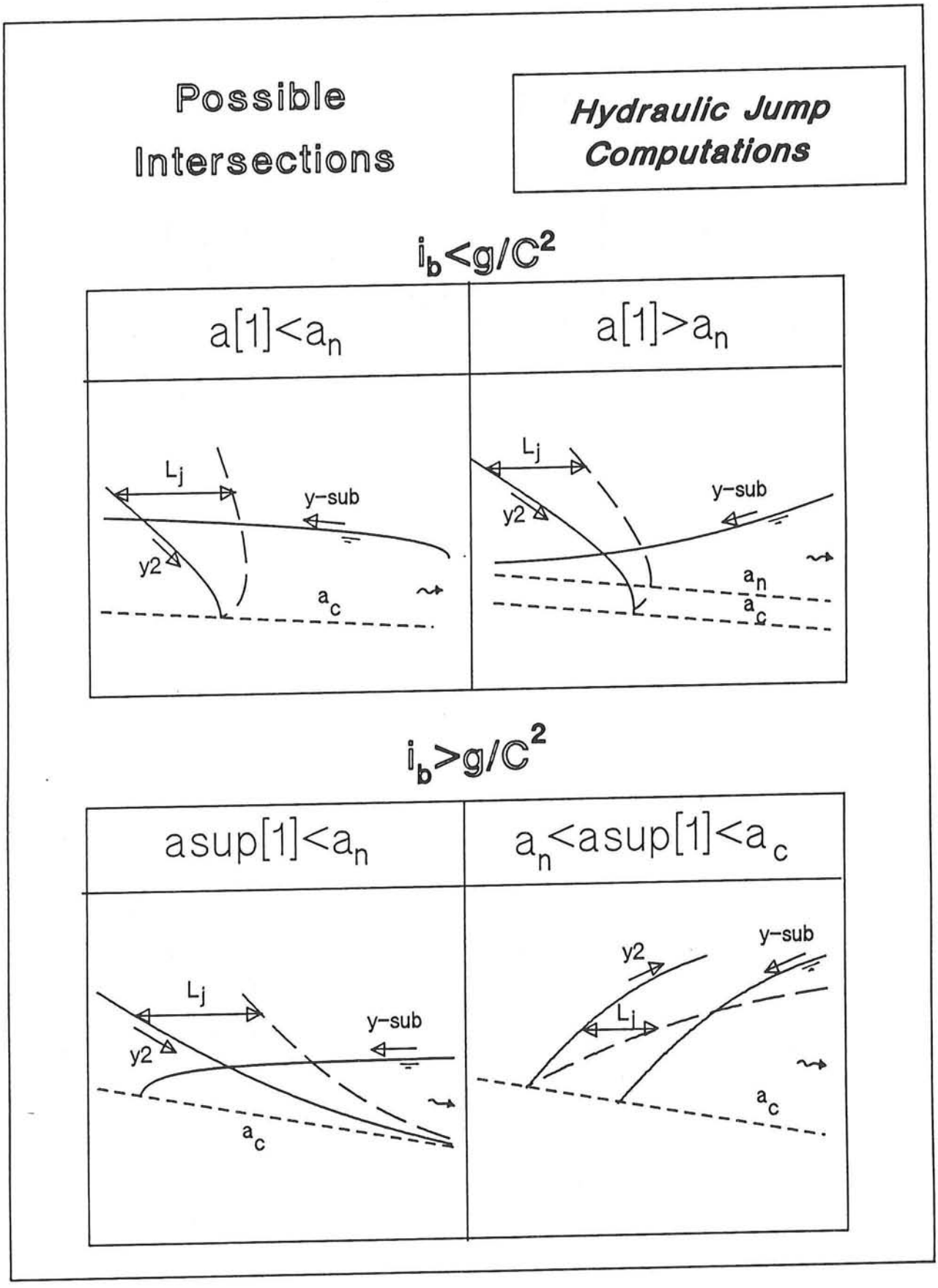

fig. 6 Intersection procedure

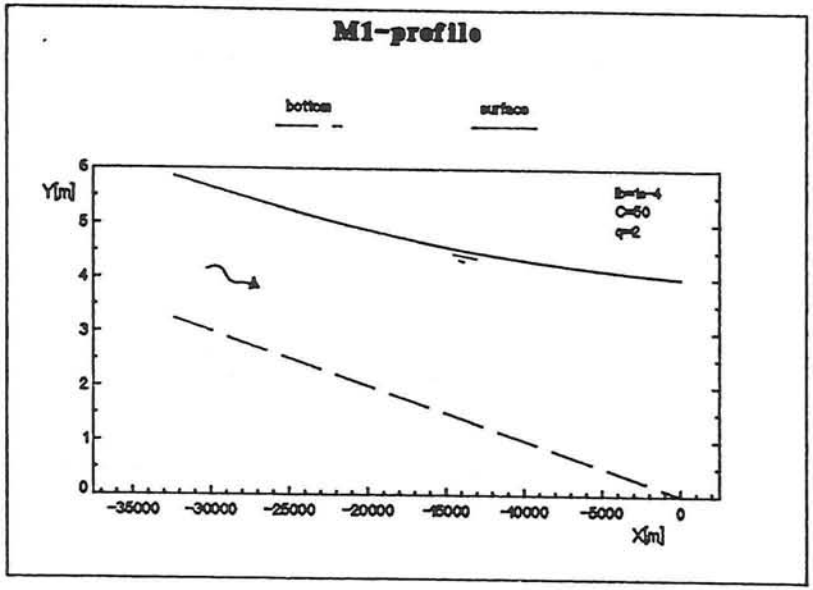

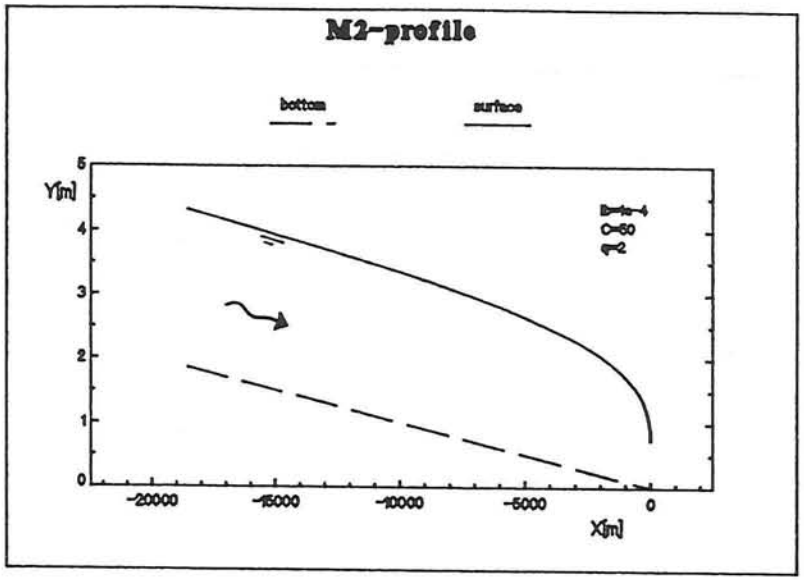

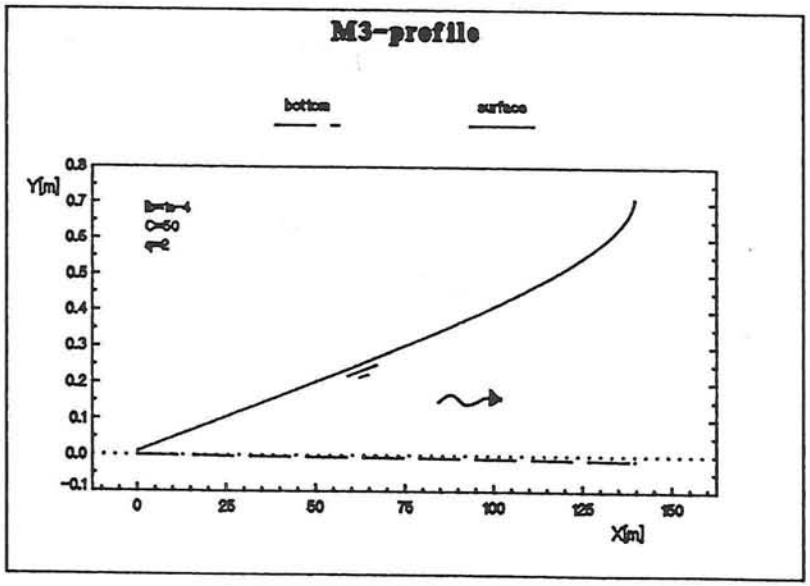

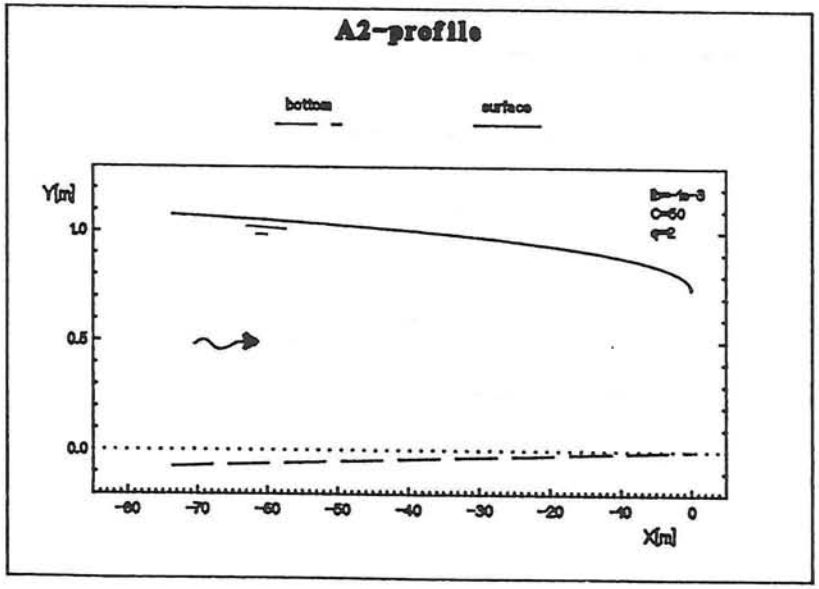

fig. 7 Applications of STUWK

fig. 8 Applications of STUWK

fig. 9 Applications of STUWK

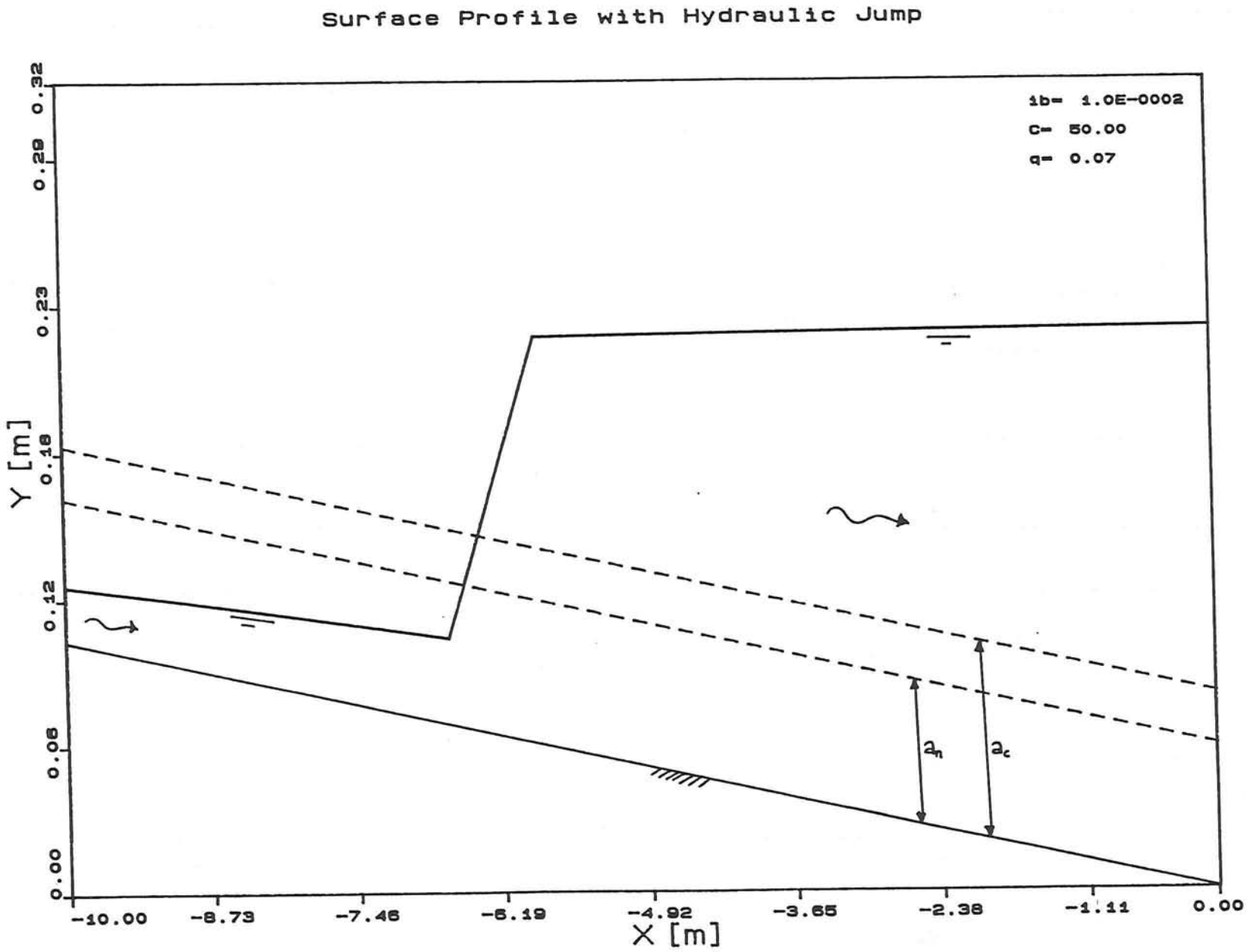

fig.10 Hydraulic jump

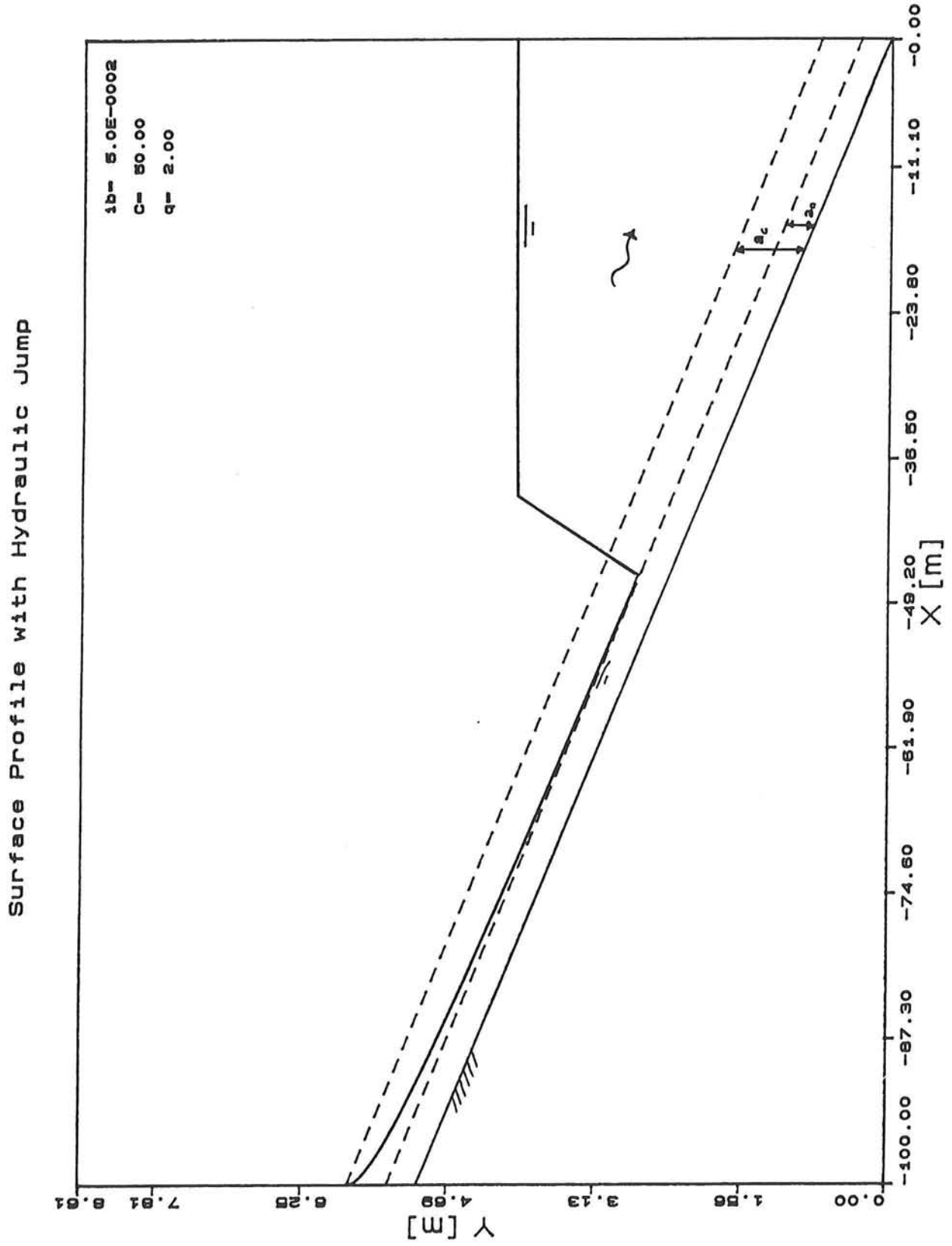

fig. 11 Hydraulic jump

Appendix 3

Numerical modelling of mountain river flow

1. Basic equations and discretization

The system of equations as given in section (3.7.1) for small bedslopes ($\cos(\zeta)\approx 1$ and $\sin(\zeta)\approx\zeta$) is:

$$\frac{\partial u}{\partial t} + u\frac{\partial u}{\partial x} + g\frac{\partial a}{\partial x} + \frac{1}{2}R_1 g\frac{\partial Cs}{\partial x} + g\frac{\partial z}{\partial x} + \frac{gu^2}{C^2 a} = 0 \qquad (3.18)$$

$$\frac{\partial a}{\partial t} + u\frac{\partial a}{\partial x} + a\frac{\partial u}{\partial x} + R_1\left[\frac{\partial Cs}{\partial t} + u\frac{\partial Cs}{\partial x}\right] = 0 \qquad (3.19)$$

$$\alpha\frac{\partial z}{\partial t} + \alpha f_u\frac{\partial u}{\partial x} + \frac{R_1}{\Delta}\left[\frac{\partial Cs}{\partial t} + u\frac{\partial Cs}{\partial x}\right] = 0 \qquad (3.20)$$

$$T_a\frac{\partial Cs}{\partial t} + L_a\frac{\partial Cs}{\partial x} + Cs - Cse = 0 \qquad (3.21)$$

The basic equations are discretized using the Preissmann implicit scheme (Preissmann, 1960).

$$f(x,t) = \frac{\theta}{2}\left[f_{j+1}^{n_t+1} + f_j^{n_t+1}\right] + f_0$$

$$\frac{\partial f}{\partial x} = \frac{\theta}{\Delta x}\left[f_{j+1}^{n_t+1} - f_j^{n_t+1}\right] + \frac{\partial f}{\partial x}_0$$

$$\frac{\partial f}{\partial t} = \frac{f_{j+1}^{n_t+1} + f_j^{n_t+1}}{2\Delta t} + \frac{\partial f}{\partial t}_0$$

In which the index zero denotes the components of the discretized variables and deratives on the (known) time level n_t. The solution of the algebraic equations is described in the following sections for three methods.

2. Newton's iteration method

The Newton's iteration method can be used to solve a system of non-linear equations. The four algebraic equations which follow from the discretization will be denoted by

$$f_{1j}(a_j^{n_t+1}, u_j^{n_t+1}, Cs_j^{n_t+1}, z_j^{n_t+1})$$
$$f_{2j}(a_j^{n_t+1}, u_j^{n_t+1}, Cs_j^{n_t+1}, z_j^{n_t+1})$$
$$f_{3j}(a_j^{n_t+1}, u_j^{n_t+1}, Cs_j^{n_t+1}, z_j^{n_t+1})$$
$$f_{4j}(a_j^{n_t+1}, u_j^{n_t+1}, Cs_j^{n_t+1}, z_j^{n_t+1})$$

If boundary conditions

$$E_0^A(a_0^{n_t+1}, u_0^{n_t+1}, Cs_0^{n_t+1}) = 0$$
$$E_0^B(a_0^{n_t+1}, u_o^{n_t+1}, Cs_0^{n_t+1}) = 0$$
$$E_o^C(a_0^{n_t+1}, u_0^{n_t+1}, Cs_0^{n_t+1}) = 0$$

are given at the upstream end, and $E_{nx}^{D}(z_{nx}^{nt+1})=0$ at the downstream end, then there exists a system of $4(n_x+1)$ equations for $4(n_x+1)$ unknowns (system $F(x)$).
Since this system is non linear in the unknown variables it cannot be represented with a matrix elimination method. Most commonly used is Newton's iteration method for systems (Mathews, 1987). Newton's iteration method begins with assigning trial values to the unknowns. Taylor's theorem for functions can be used to approximate the zero values (roots) of the system starting from their estimated values. (Higher order terms may be neglected if the trial values are close to the actual roots of the system).

Now a Jacobian Matrix can be defined as follows:

$$J_j = \begin{pmatrix} \frac{\partial F_j}{\partial u_1^1} & \frac{\partial F_j}{\partial a_1^1} & \frac{\partial F_j}{\partial Cs_1^1} & \frac{\partial F_j}{\partial z_1^1} \\ \frac{\partial F_{j+1}}{\partial u_1^1} & \frac{\partial F_{j+1}}{\partial a_1^1} & \frac{\partial F_{j+1}}{\partial Cs_1^1} & \frac{\partial F_{j+1}}{\partial z_1^1} \\ \frac{\partial F_{j+2}}{\partial u_1^1} & \frac{\partial F_{j+2}}{\partial a_1^1} & \frac{\partial F_{j+2}}{\partial Cs_1^1} & \frac{\partial F_{j+2}}{\partial z_1^1} \\ \frac{\partial F_{j+3}}{\partial u_1^1} & \frac{\partial F_{j+3}}{\partial a_1^1} & \frac{\partial F_{j+3}}{\partial Cs_1^1} & \frac{\partial F_{j+3}}{\partial z_1^1} \end{pmatrix}$$

in which F_j = j^{th} equation of the system $F(\vec{x})$ and if

$$\vec{x}^{[i]} = \begin{pmatrix} u_0^{n_t+1} \\ a_0^{n_t+1} \\ Cs_0^{n_t+1} \\ z_0^{n_t+1} \\ \cdot \\ \cdot \\ \cdot \\ \cdot \\ u_{n_x}^{n_t+1} \\ a_{n_x}^{n_t+1} \\ Cs_{n_x}^{n_t+1} \\ z_{n_x}^{n_t+1} \end{pmatrix} \quad \text{then } J(\vec{x}^{[i]}) = \begin{pmatrix} J_0 & & & \\ & J_1 & & 0 \\ & & \cdot & \\ & & & \cdot \\ & 0 & & \cdot \\ & & & & J_{n_x} \end{pmatrix}$$

where $\vec{x}^{[i]}$ = the i^{th} estimation of the roots

The iteration then proceeds as follows:

Step 1 Evaluate the function $F(\vec{x}^{[i]})$

Step 2 Evaluate the Jacobian $J(\vec{x}^{[i]})$

Step 3 Solve the linear system $J(\vec{x}^{[i]})\,\Delta\vec{x} = -F(\vec{x}^{[i]})$ for $\Delta\vec{x}$.

Step 4 Compute the next point $\vec{x}^{[i+1]} = \vec{x}^{[i]} + \Delta\vec{x}$

Repeat the process until satisfactory convergence.

Remarks

- To save computation time, the updating of the Jacobian (step 2) can be done every k^{th} step ($k \approx 3$) instead of every step.
- For the solution of the linear system (step 3), the system has to be presented in matrix form, i.e. a banded matrix. This matrix is solved by means of the Gauss elimination method (see matrix representation of the algebraic equations, section 4). Solution yields a new vector $\Delta\vec{x}$.

The conclusions of the application of this method are given in section 4.2.2.

3. Predictor-corrector iteration method

Step 1

The Preissmann representation of the three basic equations of motion, suspended sediment, and continuity of mass (eq. 3.18, 3.19, 3.21) can be solved for every successive space step in downstream direction on the advanced time level (celerities for a, u, Cs are positive for supercritical flow, section 3.6.2). The bed level gradient $\partial z/\partial x$ in the equation of motion (3.18) is taken at the known current time level. For each (space) step the computed values of the upstream section serve as the upstream boundary:

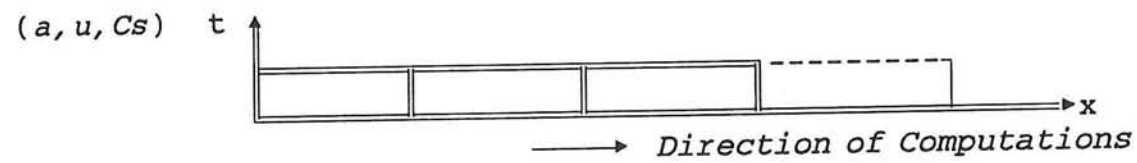

Step 2

The basic equation (3.20) for sediment is solved in upstream direction (the celerity of the bedlevels is negative). The concentration and velocity gradients are determined with values from iteration step 1. The equa-

tion has to be solved explicitly for the bed levels at the advanced time level, because the values from iteration step 1 are computed for bed levels at the current time level or

$$\frac{\partial z}{\partial t} + f_{a,u,Cs}(z_{t_0}) = 0$$

In which t_0= current time level

$f_{a,u,Cs}(z_{t0})$= function of u, a, Cs values determined in iteration step 1 for bedlevels at the current time level.

(Neumann's analysis of similar problems proved the occurrence of instability if an implicit scheme is applied, Stelling 1990). Discretization of $\partial z/\partial t$ with an explicit scheme with numerical damping gives:

$$\frac{\partial z}{\partial t} = \frac{0.25\overline{z}^0_{k-1} + 0.5\overline{z}^0_k + 0.25\overline{z}^0_{k+1} - \overline{z}^1_k}{\Delta t}$$

$$z_j^{n_t+1} = \frac{\overline{z}^1_{j-1} + \overline{z}^1_j}{2}$$

Step 3

Repeat iteration step 1 using the bedlevels computed in iteration step 2.

This process can be repeated until the result values converge. Conclusions on the application of this method are given in section 4. 2. 2.

4. Matrix solution method for linearised equations with predictor for flow variables

As both described methods don't work well a final method has been developed with a more simple numerical background but successful in solving the equations.

Again the basic equations are discretized using the Preissmann scheme. However, the coefficients of all deratives and all remaining non linear terms are predicted in advance

using an unsteady flow model for a fixed bed (bed variations assumed small compared to the water variations because of the small bed celerity). After substitution of the predicted values in the coefficients and terms (not in the deratives), a system of linear equations remains for the unknown variables at the advanced time level (The unknowns follow from the discretized deratives).

Predictor for flow variables

The values of a and u can be predicted at the advanced time level using the basic equations for water flow without sediment transport:

$$\frac{\partial u}{\partial t} + u_0\frac{\partial u}{\partial x} + g\frac{\partial a}{\partial x} + g\frac{\partial z}{\partial x} + \frac{gu_0^2}{C^2 a_0} = 0 \qquad \text{(I)}$$

$$\frac{\partial a}{\partial t} + u_0\frac{\partial a}{\partial x} + a_0\frac{\partial u}{\partial x} = 0 \qquad \text{(II)}$$

In which u_0, a_0 are the values at the current time level (for linearising)

The deratives are again discretized for the Preissmann scheme. Assuming supercritical flow the celerities become positive. This implies that the equations can be solved stepwise from the upstream boundary in downstream positive x-direction (single sweep). Rewriting the Preissmann discretized deratives for this case gives:

$$\frac{\partial u}{\partial x} = \frac{\theta}{\Delta x}u_{k+1}^{n_t+1} + \left[\frac{\partial u}{\partial x}\right]_p$$

$$\frac{\partial u}{\partial t} = \frac{u_{k+1}^{n_t+1}}{2\Delta t} + \left[\frac{\partial u}{\partial t}\right]_p$$

In which the components with index p represent the those parts of the discretized variables and deratives which are known in advance.

Substitution of these expressions for u and a in equations (I) and (II) and eliminating a_{k+1}^{nt+1} the following relation can be

found for the unknown velocity:

$$u_{k+1}^{n_t+1} = \frac{\alpha_1\alpha_3\Delta x^2 - g\theta\alpha_2\Delta x}{\alpha_3{}^2\Delta x^2 - \theta^2 g a_0}$$

with

$$\alpha_1 = -\frac{\partial U}{\partial t}_p - u_0\frac{\partial u}{\partial x}_p - g\frac{\partial a}{\partial x}_p - g\frac{\partial z}{\partial x}_p - \frac{gu_0^2}{C^2 a_0}$$

$$\alpha_2 = -\frac{\partial a}{\partial t}_p - u_0\frac{\partial a}{\partial x}_p - a_0\frac{\partial u}{\partial x}_p$$

$$\alpha_3 = \frac{1}{2\Delta t} + \frac{u_0\theta}{\Delta x}$$

For the depth then follows:

$$a_{k+1}^{n_t+1} = \frac{\alpha_2}{\alpha_3} - \frac{a_0\theta}{\alpha_3\Delta x}u_{k+1}^{n_t+1}$$

$Cs_{k+1}^{n_t+1}$ follows from the van Rijn transport formula.

Matrix Representation of the Algebraic Equations

After discretization and linearisation of the basic equations, a system of four linear algebraic equations for each Preissmann segment Δt is found. In the fourth equation, the depth-integrated suspended-sediment equation, the only unknown variables appeared to be the concentrations Cs_k^{nt+1} and Cs_{k+1}^{nt+1}. Therefore this equation can be solved independent of the other three equations. Since the celerity of the concentration is positive (section 3.6.2) the equation can be solved starting at the upstream boundary and computing stepwise in downstream direction. The following relation is used to find the solution of Cs_{k+1}^{nt+1} from the value of Cs from the upstream (solved) space step and the values of a, u, Cs from the predictor:

$$Cs_{k+1}^{n_t+1} = \frac{(\alpha_1 + \alpha_2 - \alpha_3 - \alpha_4 + Cse_0)}{\left(\frac{T_a}{2\Delta t} + \frac{L_a\theta}{\Delta x} + \frac{\theta}{2}\right)}$$

In which

$$\alpha_1 = \frac{T_{a_0}}{2\Delta t}\left(Cs_{k+1}^{n_t} + Cs_k^{n_t}\right)$$

$$\alpha_2 = \frac{L_a(1-\theta)}{\Delta x}\left(Cs_{k+1}^{n_t} - Cs_k^{n_t}\right)$$

$$\alpha_3 = \frac{(1-\theta)}{2}\left(Cs_{k+1}^{n_t} + Cs_k^{n_t}\right)$$

$$\alpha_4 = Cs_k^{n_t+1}\left(\frac{T_a}{2\Delta t} - \frac{L_a\theta}{\Delta x} + \frac{\theta}{2}\right)$$

The three remaining equations (momentum, mass, volume) now form a matrix for the six unknown values for a, u, z on the advanced time level for each space step (Preissmann box). The matrix $ELEM(n\_t, k)$ is:

$$\begin{pmatrix} \left(\frac{1}{2\Delta} - \frac{u_0\theta}{\Delta x}\right) & \frac{-g\theta}{\Delta x} & \frac{-g\theta}{\Delta x} & \left(\frac{1}{2\Delta t} + \frac{u_0\theta}{\Delta x}\right) & \frac{g\theta}{\Delta x} & \frac{g\theta}{\Delta x} \\ \frac{-a_0\theta}{\Delta x} & 0 & \left(\frac{1}{2\Delta t} - \frac{u_0\theta}{\Delta x}\right) & \frac{a_0}{\Delta x} & 0 & \left(\frac{1}{2\Delta t} + \frac{u_0\theta}{\Delta x}\right) \\ -f_{u_b}\frac{\theta}{\Delta x} & \frac{1}{2\Delta t} & 0 & f_{u_b}\frac{\theta}{\Delta x} & \frac{1}{2\Delta t} & 0 \end{pmatrix}$$

if vector $\vec{R} = \left(u_k^{n_t+1}, z_k^{n_t+1}, a_k^{n_t+1}, u_{k+1}^{n_t+1}, z_{k+1}^{n_t+1}, a_{k+1}^{n_t+1}\right)$

and

$$FUNCT = \begin{pmatrix} -\frac{\partial u}{\partial t_0} - u_0\frac{\partial u}{\partial x_0} - g\frac{\partial a}{\partial x_0} - g\frac{\partial z}{\partial x_0} - \frac{gu_0^2}{C^2 a_0} - \frac{1}{2}R_{1_0}g\frac{\partial Cs}{\partial x} \\ -\frac{\partial a}{\partial t_0} - u_0\frac{\partial a}{\partial x_0} - a_0\frac{\partial u}{\partial x_0} - R_{1_0}\left[\frac{\partial Cs}{\partial t} + u_0\frac{\partial Cs}{\partial x}\right] \\ -\frac{\partial z}{\partial t_0} - f_{u_{b0}}\frac{\partial u}{\partial x_0} - \frac{R_{1_0}}{\Delta}\left[\frac{\partial Cs}{\partial t} + u_0\frac{\partial Cs}{\partial x}\right] \end{pmatrix}$$

then $ELEM(n_t, k)\cdot\vec{R} = FUNCT$

If the length of one Preissmann box is Δx and the length of the river section under consideration is $n_x\Delta x$, then the total number of equations is $3\cdot n_x$.

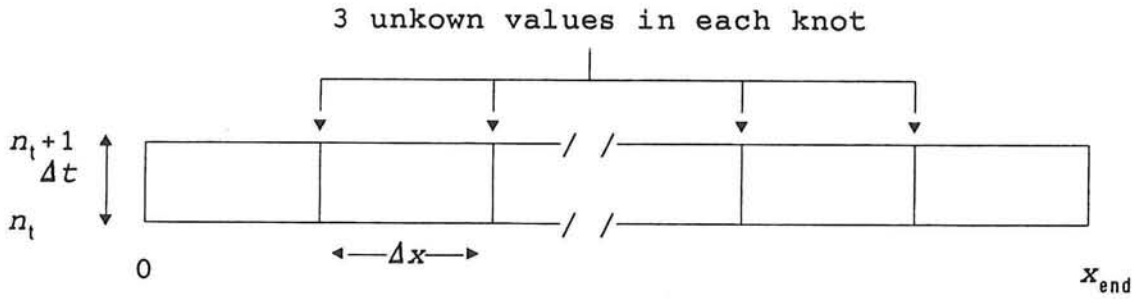

The number of knots on the advanced time level is n_x+1, and because each knot holds 3 unknown variables, this yields $3 \cdot n_x+3$ unknown variables. To equalize the amount of equations to the number of unknown variables it is necessary to derive three more relations for *a, u* and *z*. These are the **Boundary Conditions**.

The system of $m=3 \cdot n_x+3$ equations can be represented by a banded matrix with length m and width of the band = 8:

$$\begin{pmatrix} ELEM(n_t,0) & & & & 0 \\ 0 & ELEM(n_t,1) & 0 & & \\ & \cdot & & & \\ & & \cdot & & \\ & & & \cdot & \\ & 0 & & & ELEM(n_t,n_x-1) \end{pmatrix} \vec{R} = \begin{pmatrix} FUNCT_0 \\ FUNCT_1 \\ \cdot \\ \cdot \\ FUNCT_{n_x-1} \end{pmatrix}$$

Solution of this matrix is done by means of a Gauss elimination for which the matrix and the composed vector *FUNCT* is first transformed working from the top of the matrix to the tail.

$$m_{ji} = \frac{e_{ji}^{(i-1)}}{e_{1i}^{(i-1)}} \Rightarrow e_{jk}^{(i)} = e_{jk}^{(i-1)} - m_{ji} e_{ik}^{(i_1)}$$

$$f_j^{(i)} = f_j^{(i-1)} - m_{ji} f_i^{(i-1)}$$

In which m_{ji} = multiplicator
e_{jk} = element of the matrix: j^{th} row, k^{th} column
f_j = j^{th} element of the vector *FUNCT*

Next the solution of the matrix is found by calculating the

values starting at the tail of the matrix (lit).

Initial Condition at t=0

In section 4.2.3 of this report the boundary conditions and inital condition are described. In addition to that description the base flow initial condition is treated in this appendix.

The flow at t=0 is assumed to be small and quasi-steady. Influence of sediment concentration on the water movement is neglected. The equations that apply to these assumptions are the basic equations for steady non-uniform flow on a fixed bed (section 3.3):

$$u\frac{\partial u}{\partial x} + g\frac{\partial a}{\partial x} + g\frac{\partial z}{\partial x} + \frac{gu^2}{C^2 a} = 0$$

$$a\frac{\partial u}{\partial x} + u\frac{\partial a}{\partial x} - \frac{\partial q}{\partial x} = 0$$

The solution of the steady non-uniform flow as presented in section 3.3 does not hold because of the variation in the bedslope. Therefore, in conformity with the numerical solution for the full equations, an implicit method has been developed. The values of a, u are determined using the values of the upstream given or computed values of a, u. The variables a, u and their derratives are rewritten as

$$u_p = \frac{u^0_{k+1}}{2} + \frac{u^0_k}{2}$$

$$\frac{\partial u}{\partial x}_p = \frac{u^0_{k+1}}{\Delta x} - \frac{u^0_k}{\Delta x}$$

Because of the steady properties of the flow the variables on an advanced time level do not differ from those on the current time level. Therefore only the variables on the time level "0" have to be included in the scheme.

Inserting the scheme in the differential equations and eliminating a_{k+1}^0 gives

$$(u_{k+1}^0)^4\left[\frac{1}{2\Delta x}+\frac{1}{2}\alpha_1\right] + (u_{k+1}^0)^3\left[\frac{1}{2\Delta x}+\alpha_1\right] +$$

$$+ (u_{k+1}^0)^2\left[\alpha_2-\frac{ga_k^0}{\Delta x}+\frac{1}{2}(u_k^0)^2\alpha_1\right] + (u_{k+1}^0)\left[u_k^0\alpha_2\right] + \frac{gu_k^0a_k^0}{\Delta x} = 0$$

Where

$$\alpha_1 = \frac{g}{C^2a_k^0}$$

$$\alpha_2 = g\frac{\partial z}{\partial x} - \frac{(u_n^0)^2}{2\Delta x}$$

This quartic equation in u_{k+1}^0 can be solved numerically using the Newton Raphson method with u_k^0 as the first approximation for u_{k+1}^0 and with all values at location "k". The computations proceed downstream because of the positive celerities for the water in supercritical flow. The depth follows from $q=u\cdot a=$constant. The concentration of suspended load is assumed to be equal to the suspended transport equilibrium capacity (Cse) and can be determined using the Van Rijn Transport formula.

5. Program SABOFLOW and applications

For the computations of the unsteady sediment-laden flow in volcanic rivers the computer program SABOFLOW has been developed. The program consists of several units, incorporating the numerical method (section 4.2.3) and the supporting procedures. The full structure is outlined in fig. 4. Another program which shows the graphic results of the computations is called SABOPLOT. The structure of this program is outlined in fig. 5.

Comments on the flow chart of SABOFLOW (fig. 4):

- "Are You Sure" refers to the repetition of the input of the required values.
- One can choose whether the computations are executed with or without the influence of the suspended load concentration *Cs*.
- Maximum and minimum values of a, u, z are determined for the output scaling of the graphical representation (SABOPLOT).

Comments on the flow chart of SABOPLOT (fig. 5):

- Bed levels are plotted relative to a straight line from level z at $t=0, x=0$ to level z at $t=0, x=x_n$, so that bed levels deviating from this line can be plotted more clearly.

In the following a few applications of the model are described . The computations are limited in the time period and the length of the channel section when using a personal computer. Therefore the initial condition is not taken as a small discharge in all the computations (e.g. computation of the morphology during the period of maximum discharge, instead of computing during the full time period of the flood wave). However, the results clearly illustrate the properties of the model. A discussion of the various applications is given in section 4.3.

Flow over a small shoal

In fig. 1 the initial bed level (t=0) is given for a small 5 cm high shoal on a river bed with a 1% sloping bottom.

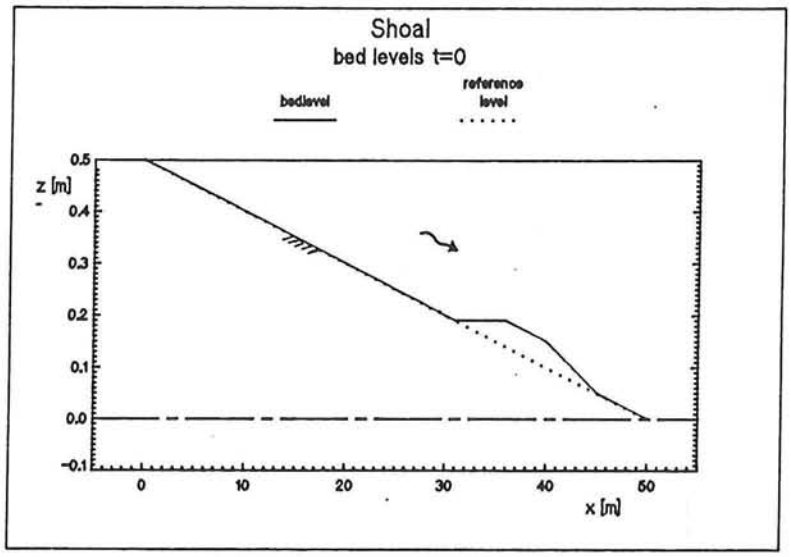

fig. 1 Bed levels shoal

The computations are executed for a time interval of 200 s, imposing normal depth and equilibrium concentration at x=0.
In fig. 6 the bed levels are shown relative to the bed level at t=0. This graphic shows the upstream propagation of the shoal.
In fig. 7 the computed flow velocities (u) and waterdepths (a) are shown. Note that an increased depth and a decreased depth exist at the top of the shoal. The gradient of the velocity ($\partial u/\partial x$) at the top of the shoal can cause local erosion. In fig. 8 the flow velocities and suspended transport concentration (Cs) are given. Because of the phase lag between bed level and concentration variations, a gradient of the concentration ($\partial Cs/\partial x$) at the top of the shoal can cause local sedimentation. The growth of the shoal during the time is therefore dependent on the magnitude of the gradients of u and Cs at the top of the shoal (local erosion or sedimentation).

In fig. 9 and fig. 10 the results are given for the same case if the concentration of suspended material is neglected. The bed levels in fig. 9 show a decrease of the height of the shoal caused by the local erosion at the top of the shoal. Fig. 10 shows the computed velocities and depths for this case. The results are compared to the computations with concentration and discussed in section 4. 3.

Flow over a small trench

The same conditions apply as for the small shoal, but the river bed is lowered over 5 cm instead of being raised. The initial bed levels are shown in figure 2.

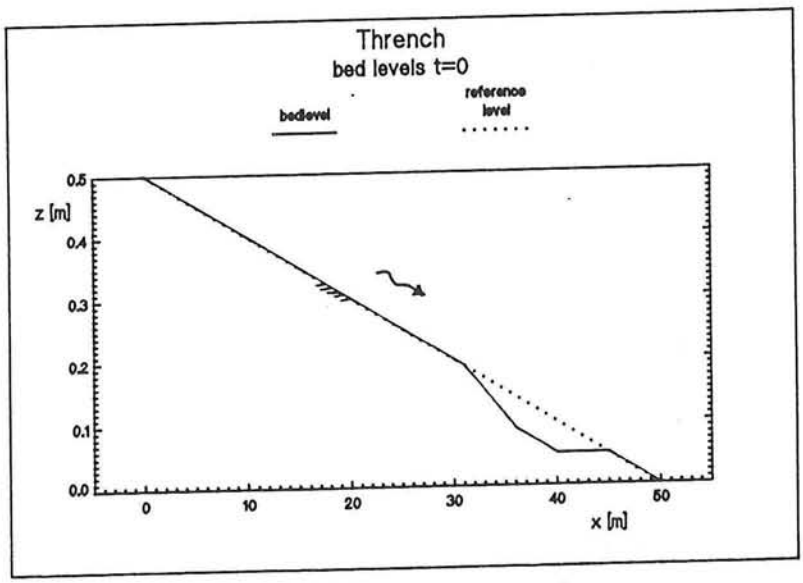

fig. 2 Bed levels trench

The results are presented in fig. 11 and fig. 12. Again upstream propagation of the trench can be noticed.

Kali Thermas Lama - Indonesia

The data for the Kali Thermas Lama are discussed in section 4. 3. Two simplified cases are considered. In the

following a description of these cases is given.

Case 1, accumulation

The severe accumulation in the river bed clearly manifests itself in the substantial rise of the river bed near the Karanggondang bridge. This phenomenon can be caused by sedimentation upstream of the bridge (the bridge obstructs the flow and can cause a hydraulic jump), and by the upstream propagation of bed level elevations from the downstream reach (mild slopes cause sedimentation). It has been investigated whether these downstream elavations can affect the river bed near the bridge. The initial bed levels for this case are presented in fig. 3a.

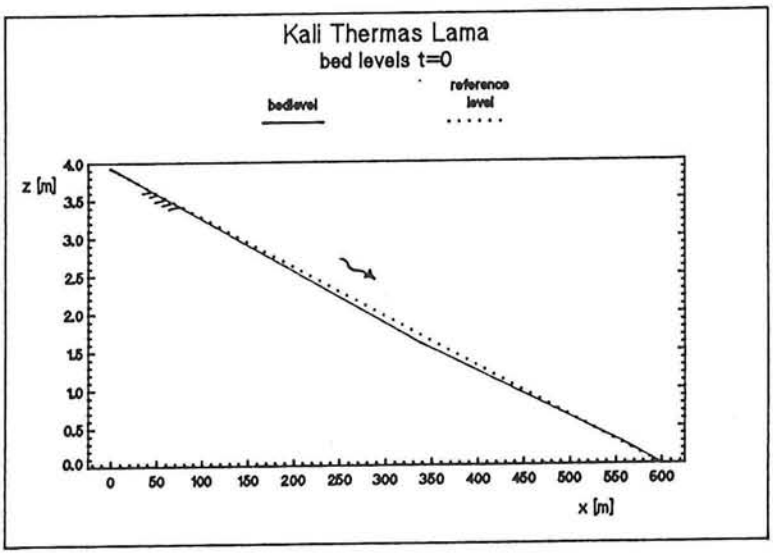

fig. 3a Bed levels Kali Thermas Lama - Case 1

At the upstream boundary (the bridge) normal depth and equilibrium concentration are imposed. The computation is seperated into three parts, respectively 1.a, 1.b, 1.c ,for computational reasons (economical use of time and memory). The first part of the discharge curve (fig. 3b) is introduced in the computations (1h to 4.5h). Results of the are shown in fig. 13a, fig. 13b and fig. 13c. The upstream propagation of the bed

variation finally causes a net bed elavation at the bridge (case 1.c).

Case 2. Degradation

The upper channel section of the Kali Thermas Lama appears to be eroding. This degradation can be caused by detention of suspended sediment upstream of the Sumbersari dam. In these computations the top of the discharge curve (fig. 3b) and the normal depth are imposed at the upstream boundary. The sediment concentration is assumed to be a part of the equilibrium concentration. The bed slope is approximately 6%. Results of the computations are given in fig. 14. Degradation occurred already for this small period.

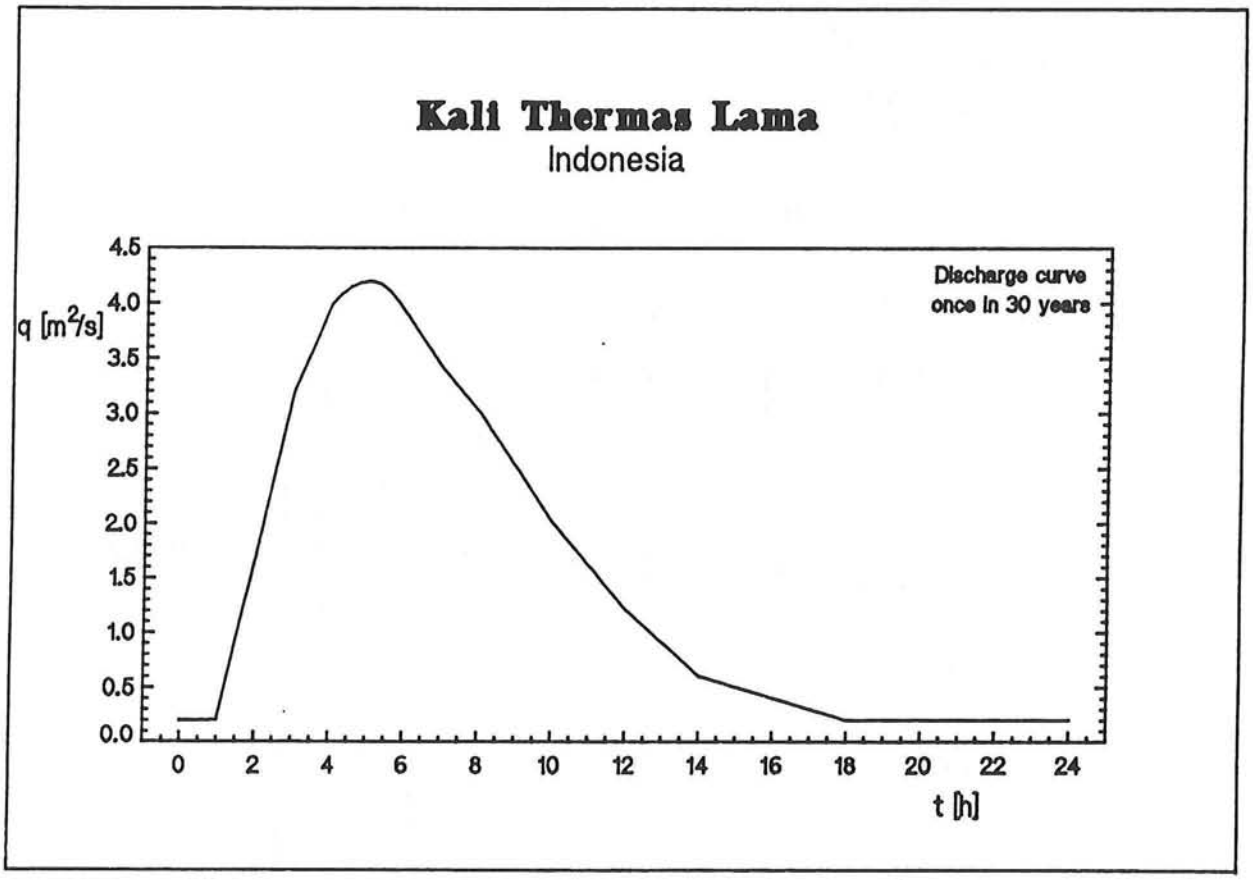

fig. 3b Discharge curve

Flow Chart program SABOFLOW

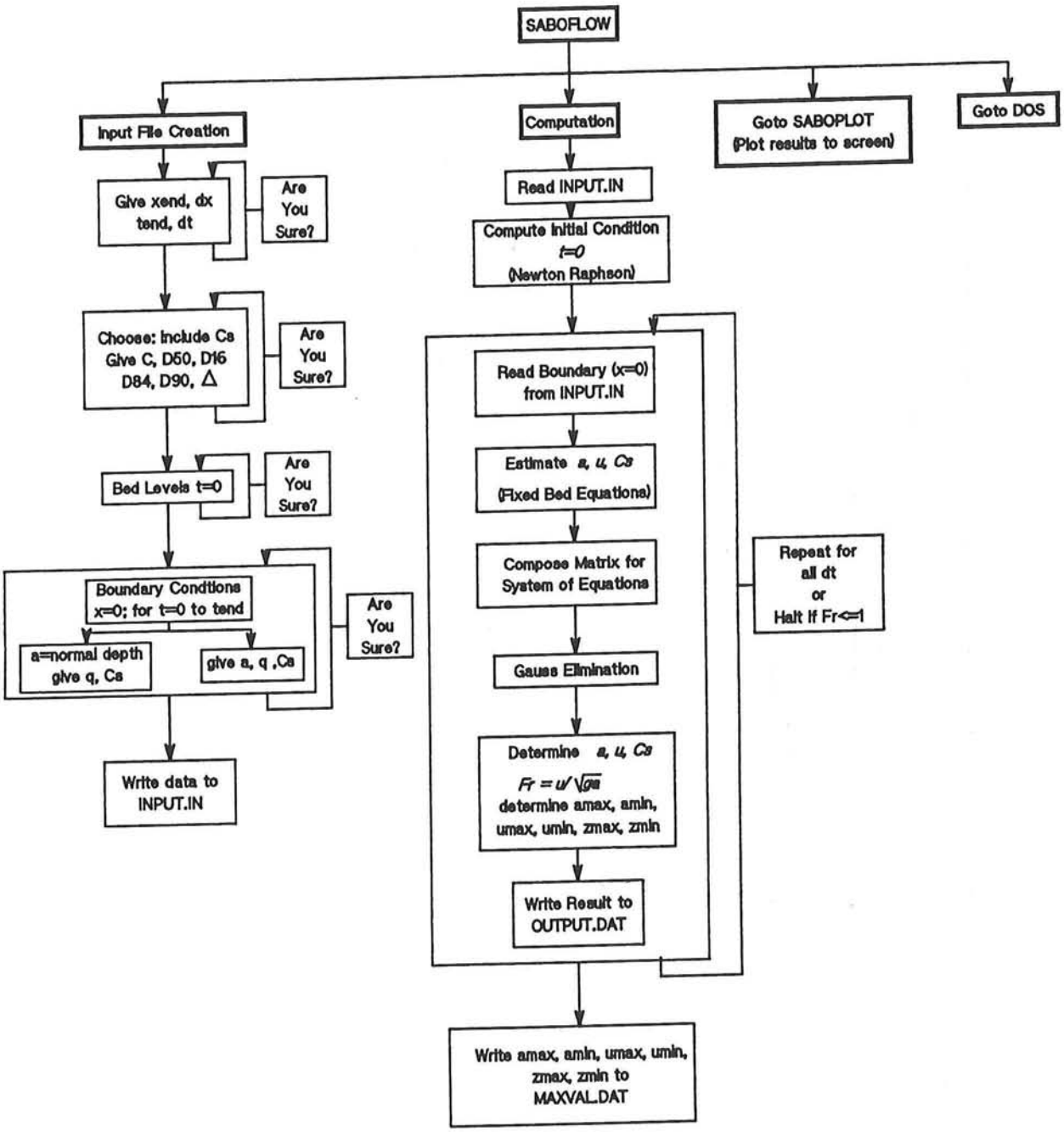

fig. 4 SABOFLOW

Flow Chart program SABOPLOT

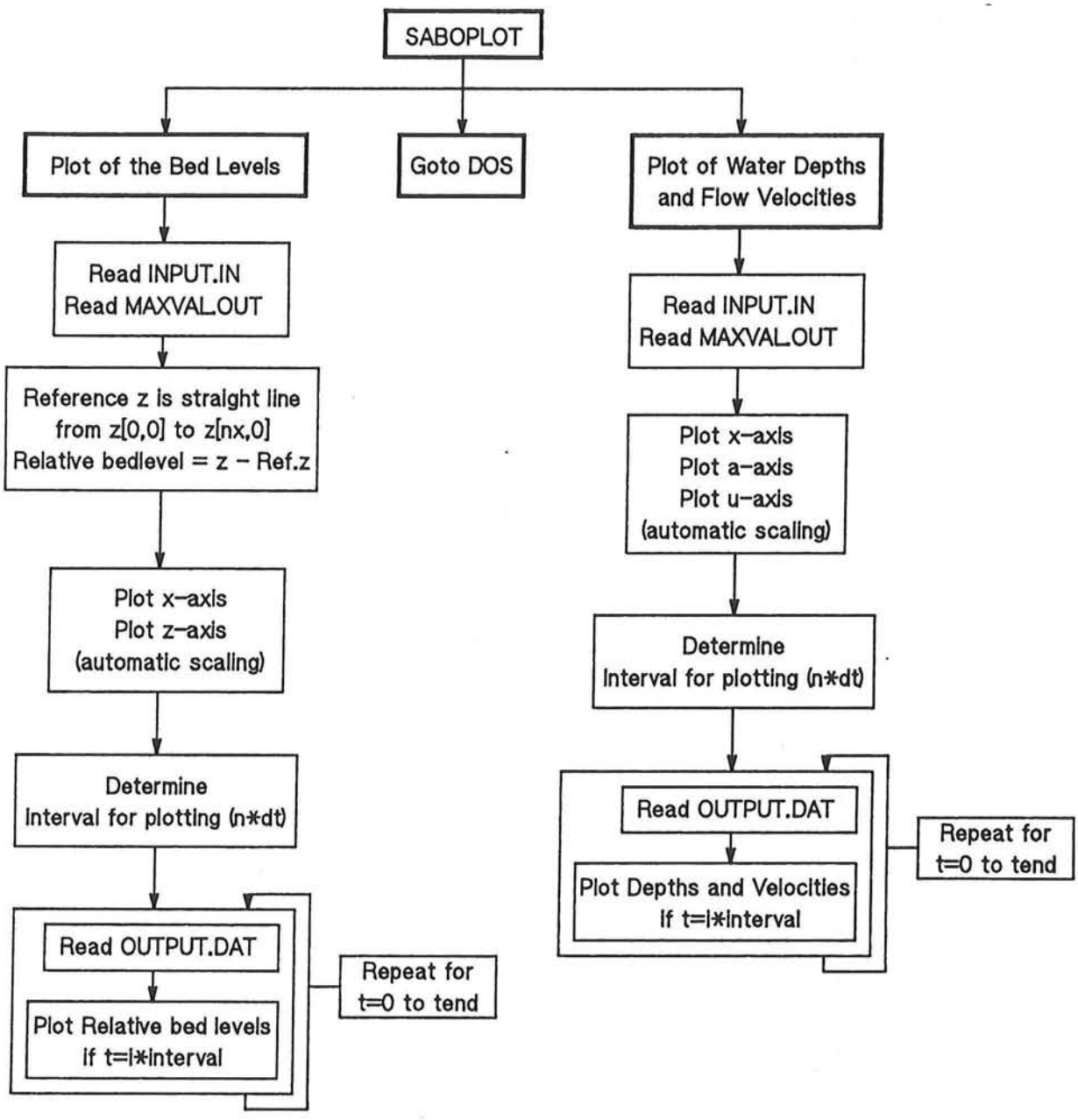

fig. 5 SABOPLOT

fig. 6 Bedlevels (shoal)

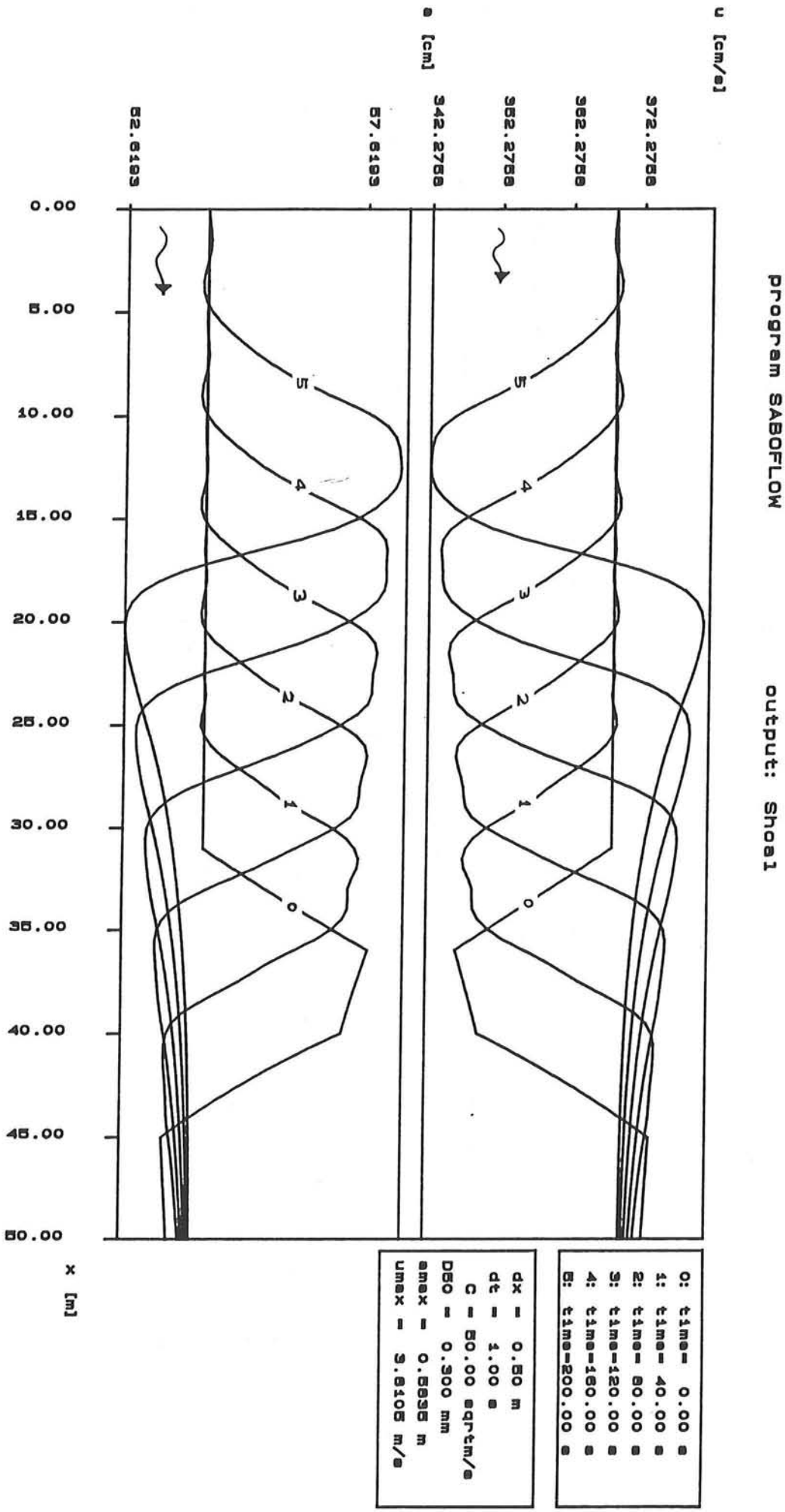

fig. 7 Velocities, depths (shoal)

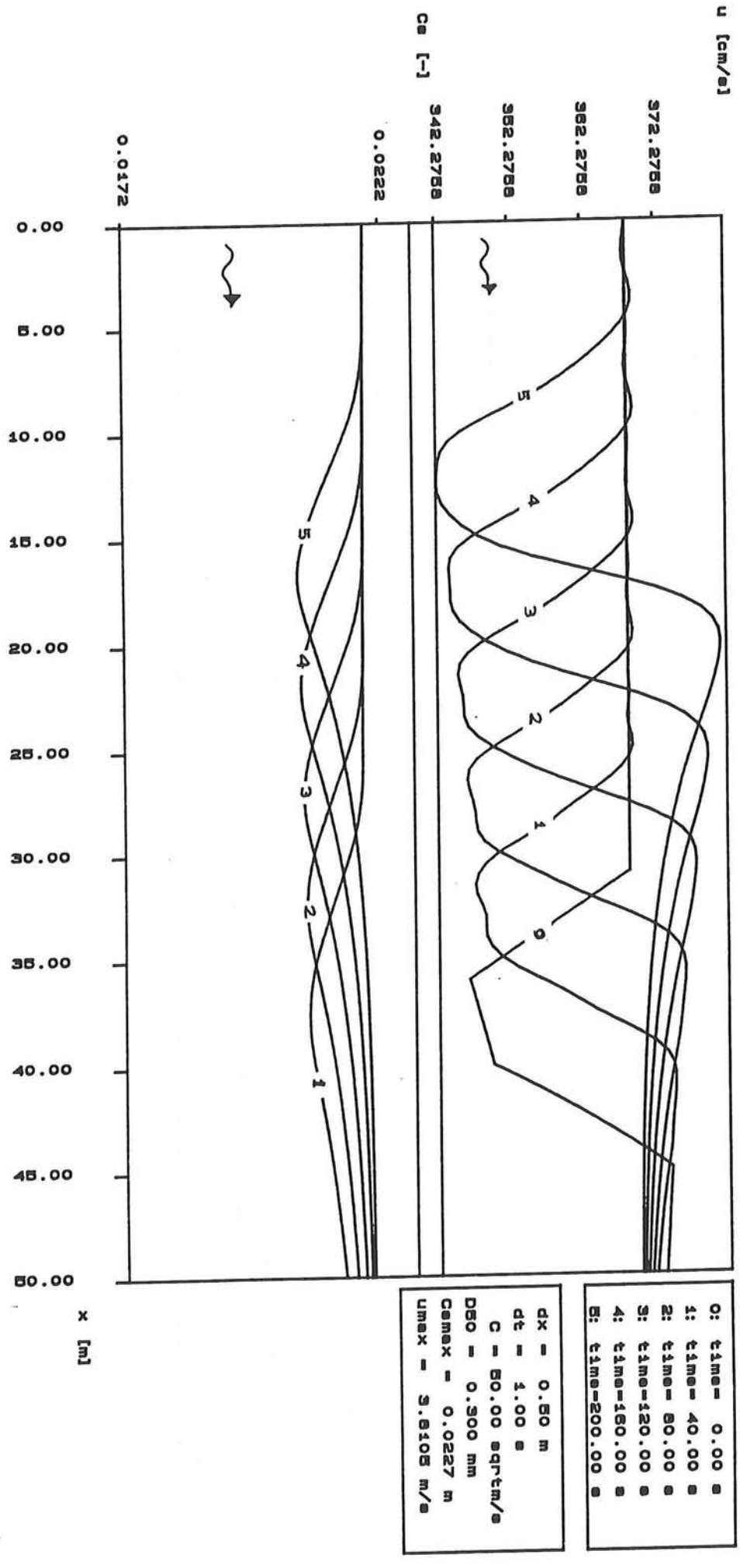

fig. 8 Velocities, concentrations (shoal)

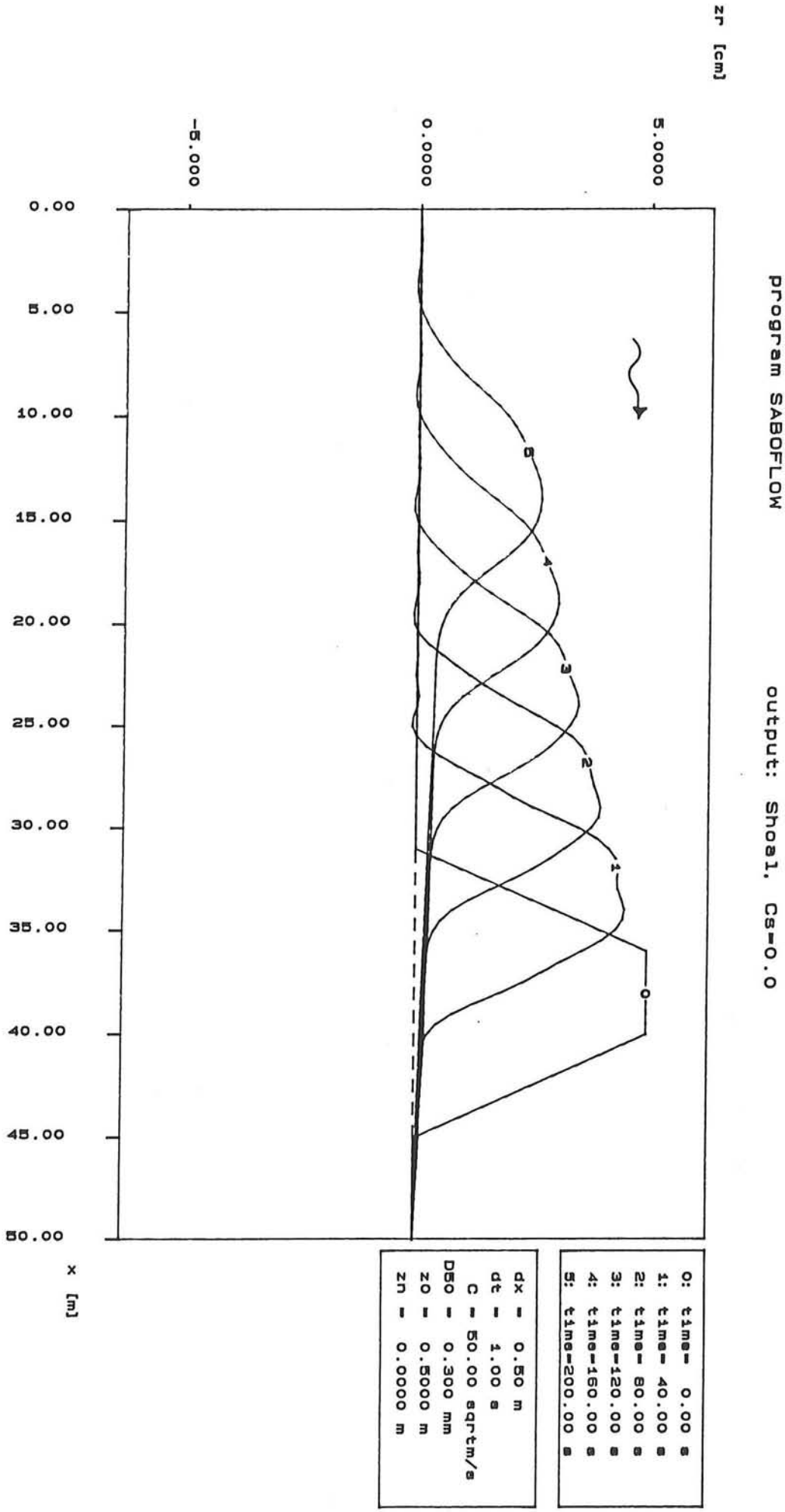

fig. 9 Bedlevels shoal with Cs≈0

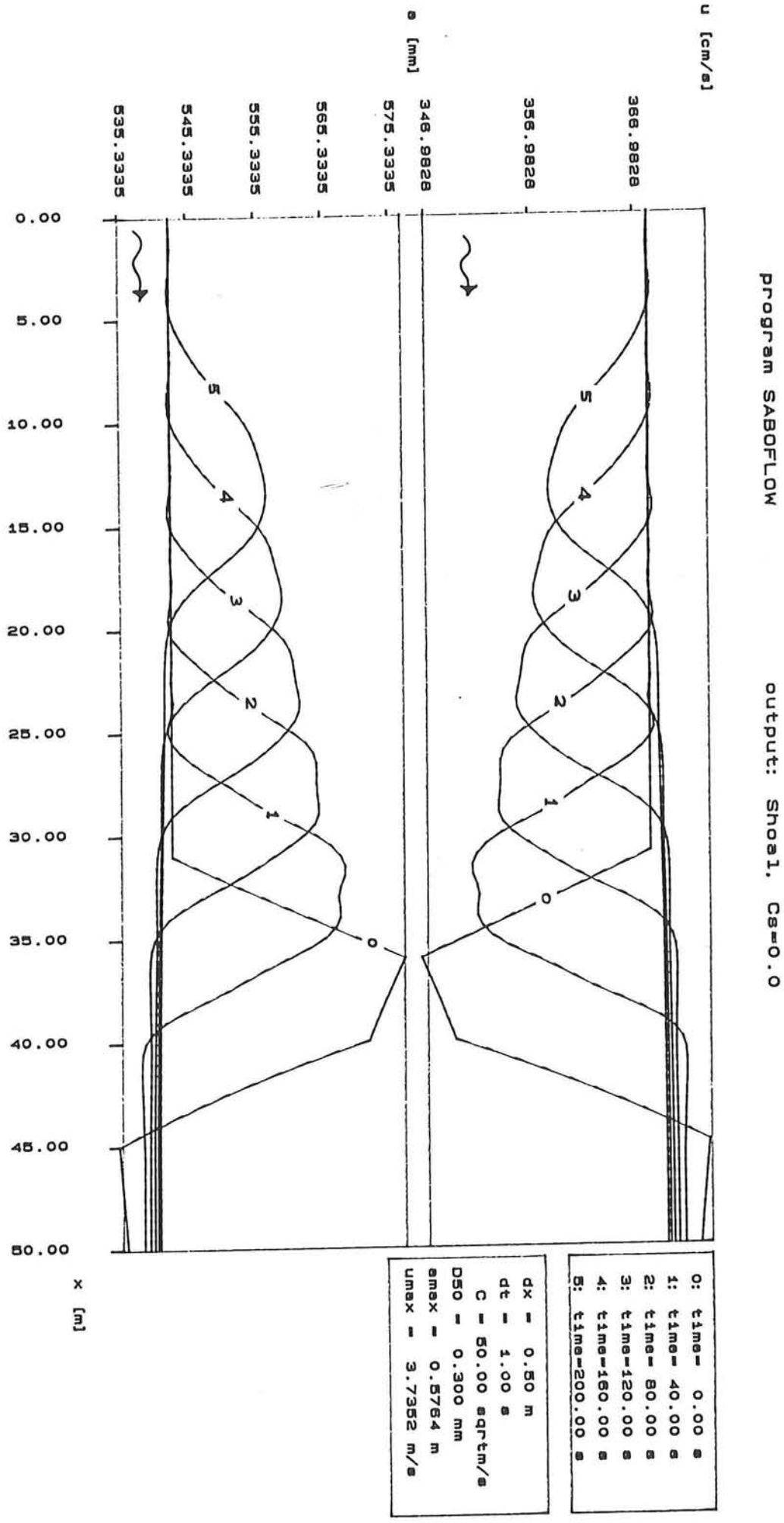

fig. 10 Velocities, depths shoal with Cs≈0

fig. 11 Bedlevels (trench)

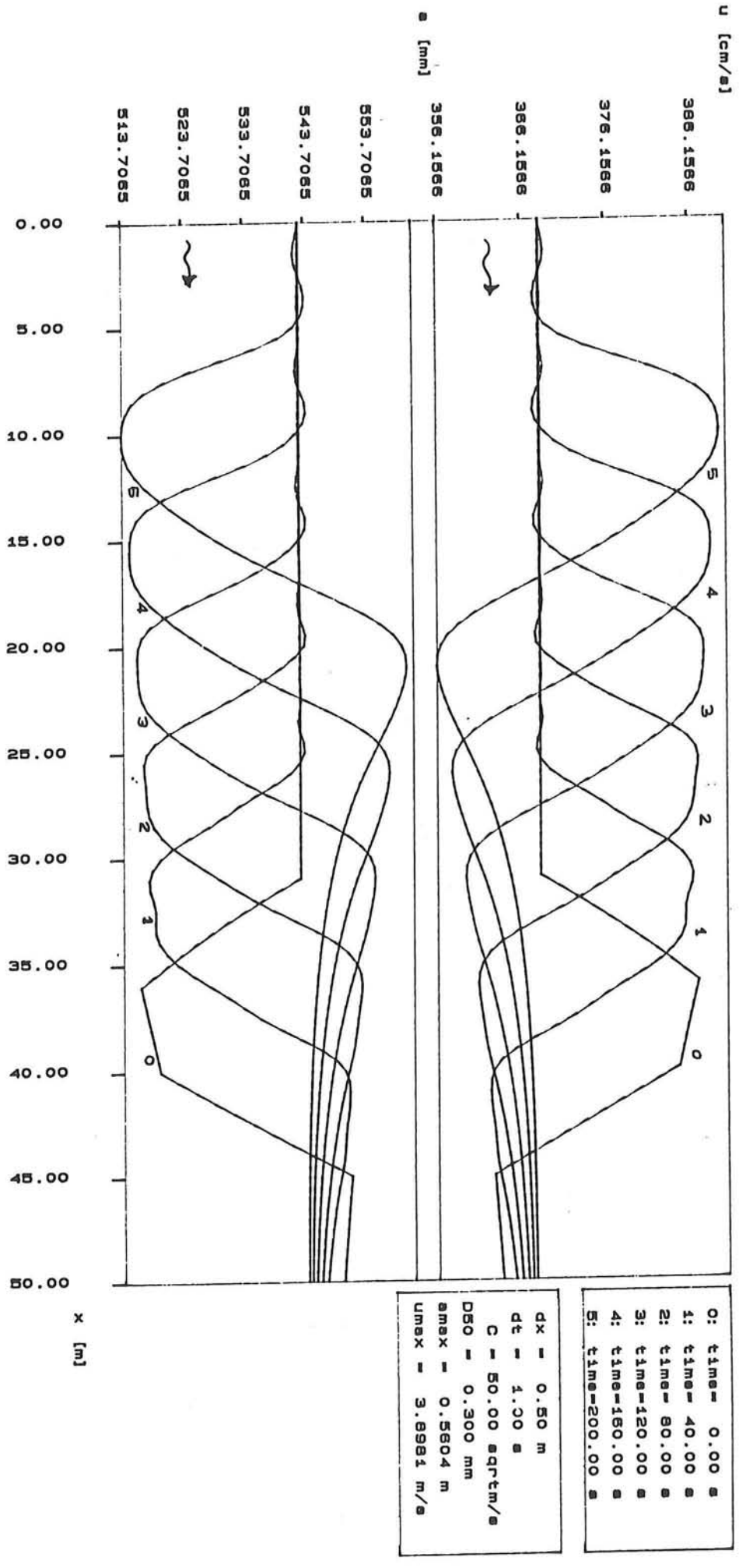

fig. 12 Velocities, depths (trench)

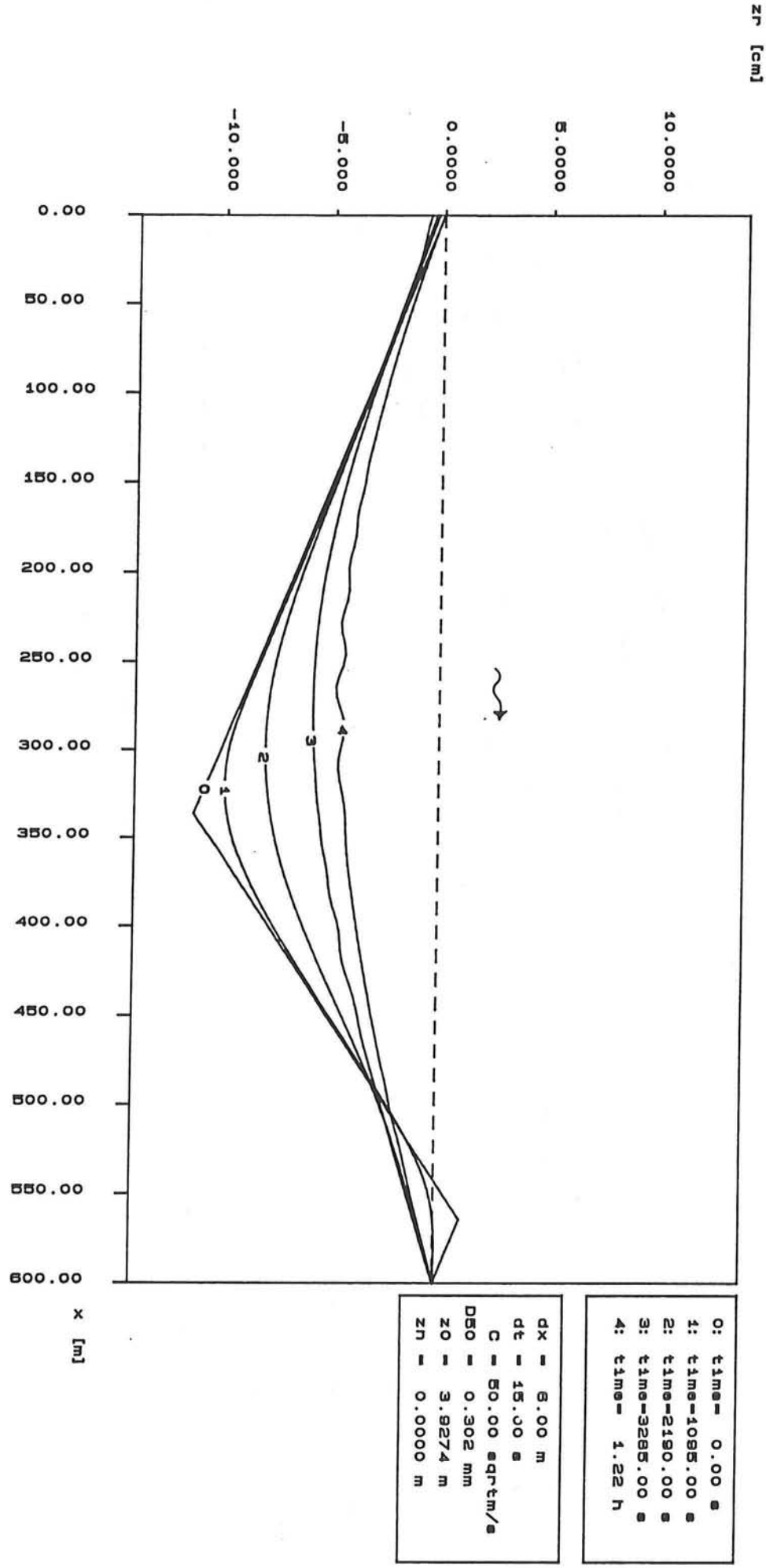

fig. 13a Bedlevels Kali Thermas Lama: part 1.a

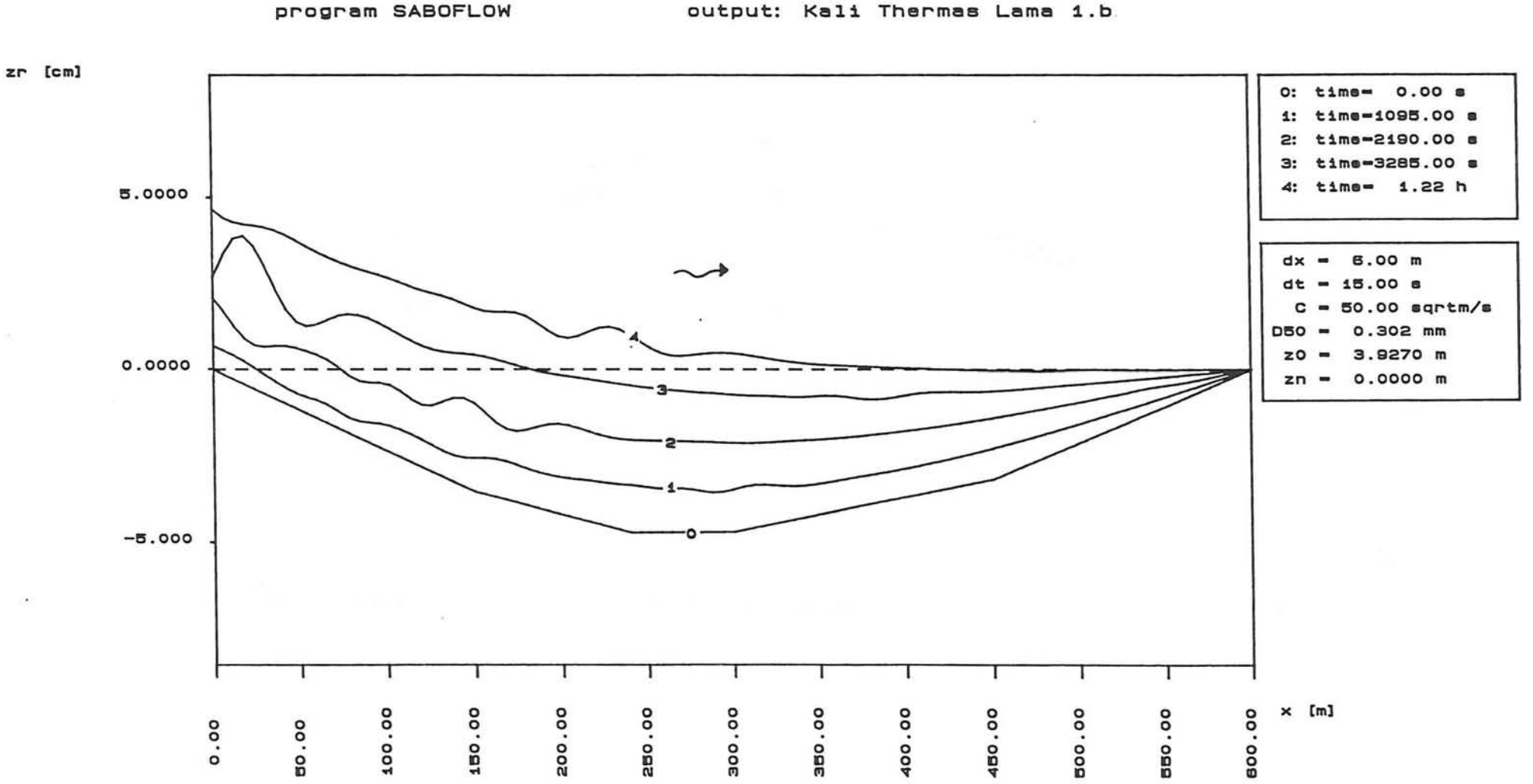

fig. 13b Bedlevels Kali Thermas Lama: part 1.b

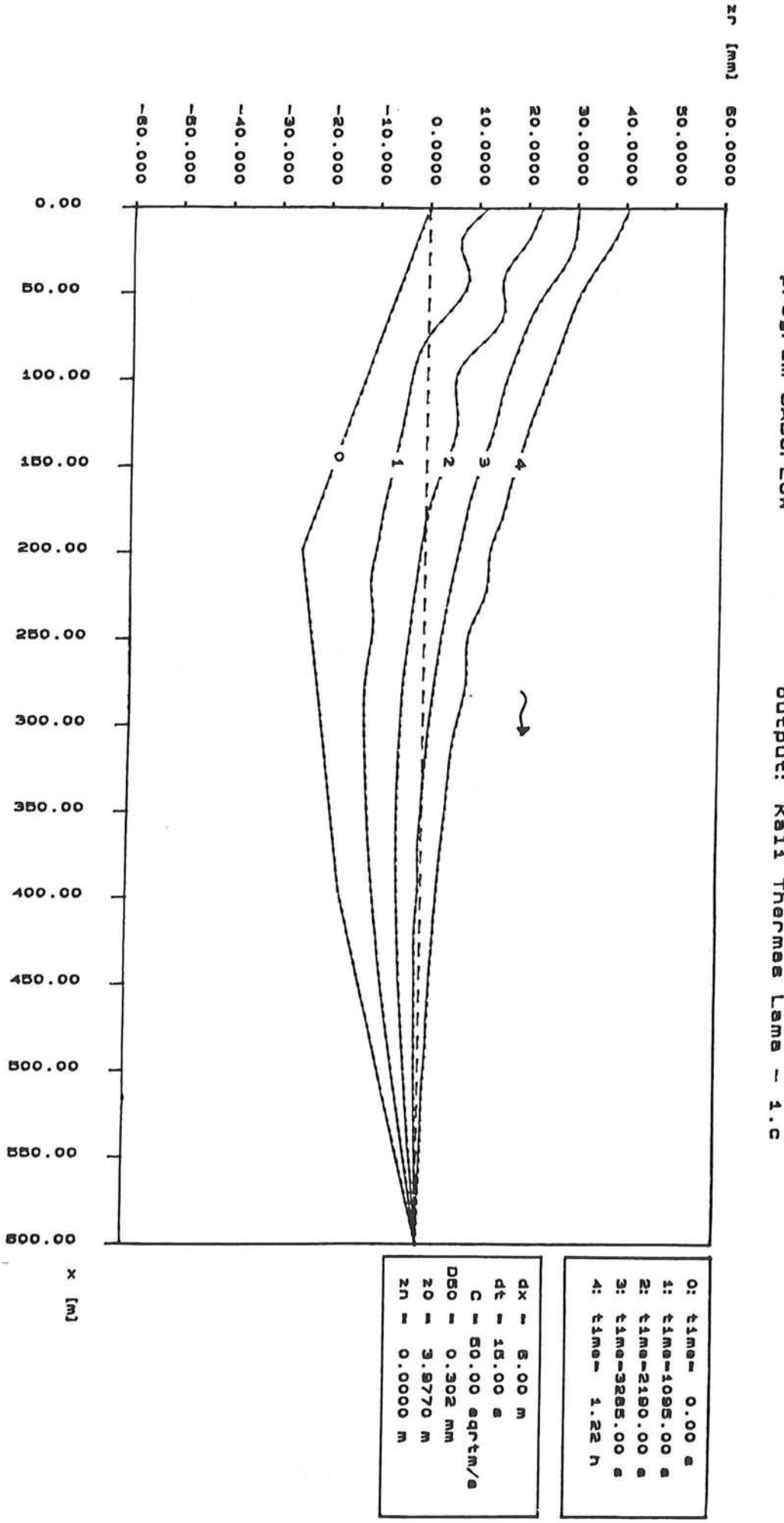

fig. 13c Bedlevels Kali Thermas Lama: part 1.c

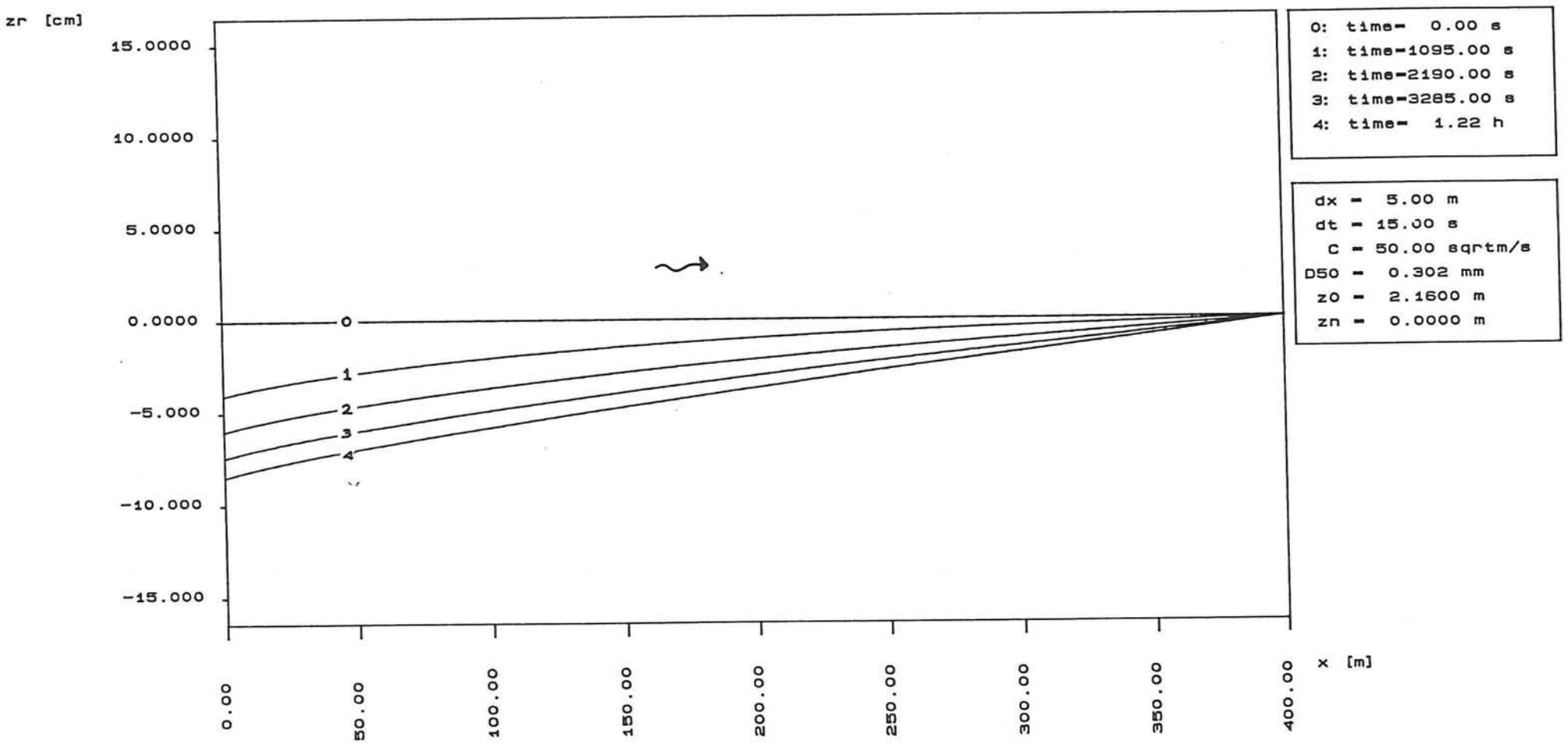

fig. 14 Bedlevels Kali Thermas Lama: degradation